

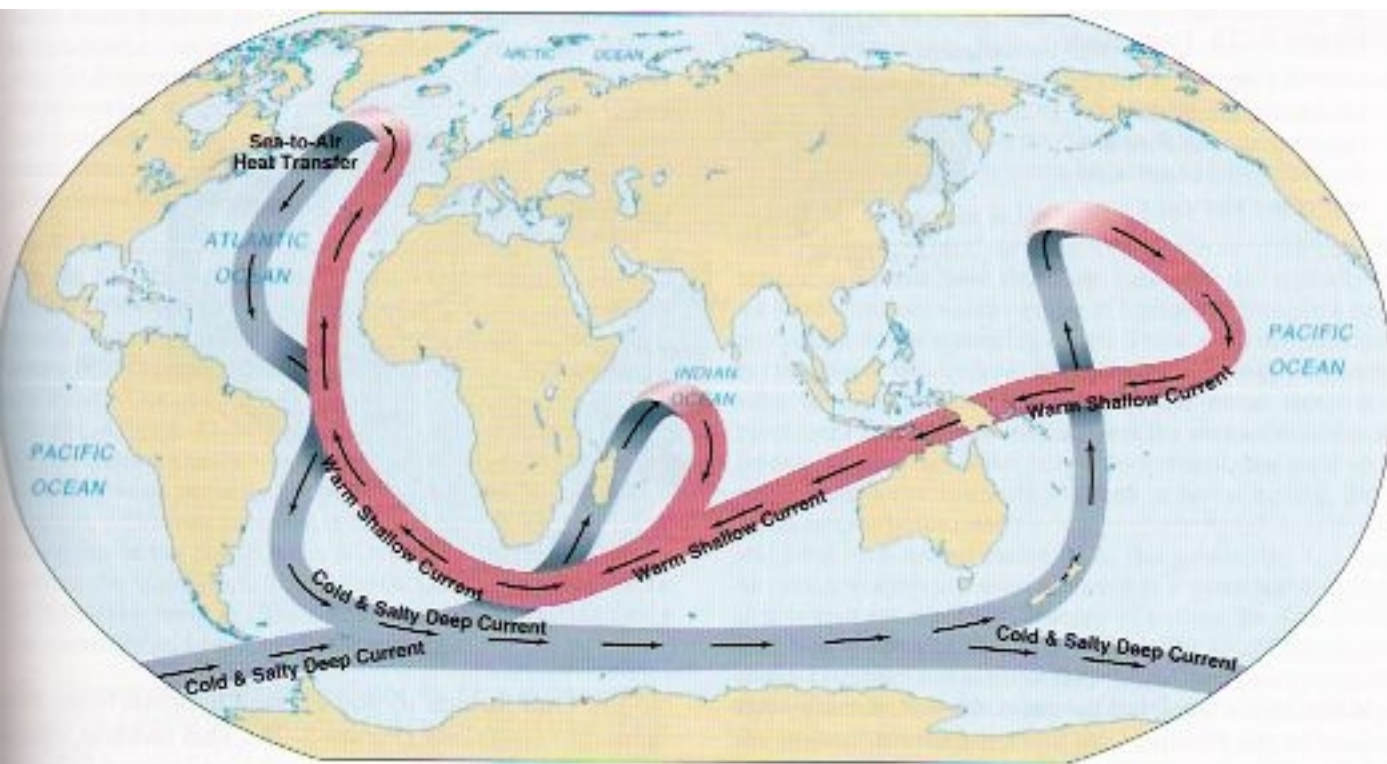
# AMOC

EPS 131 intro to physical oceanography

EPS 231 Climate dynamics

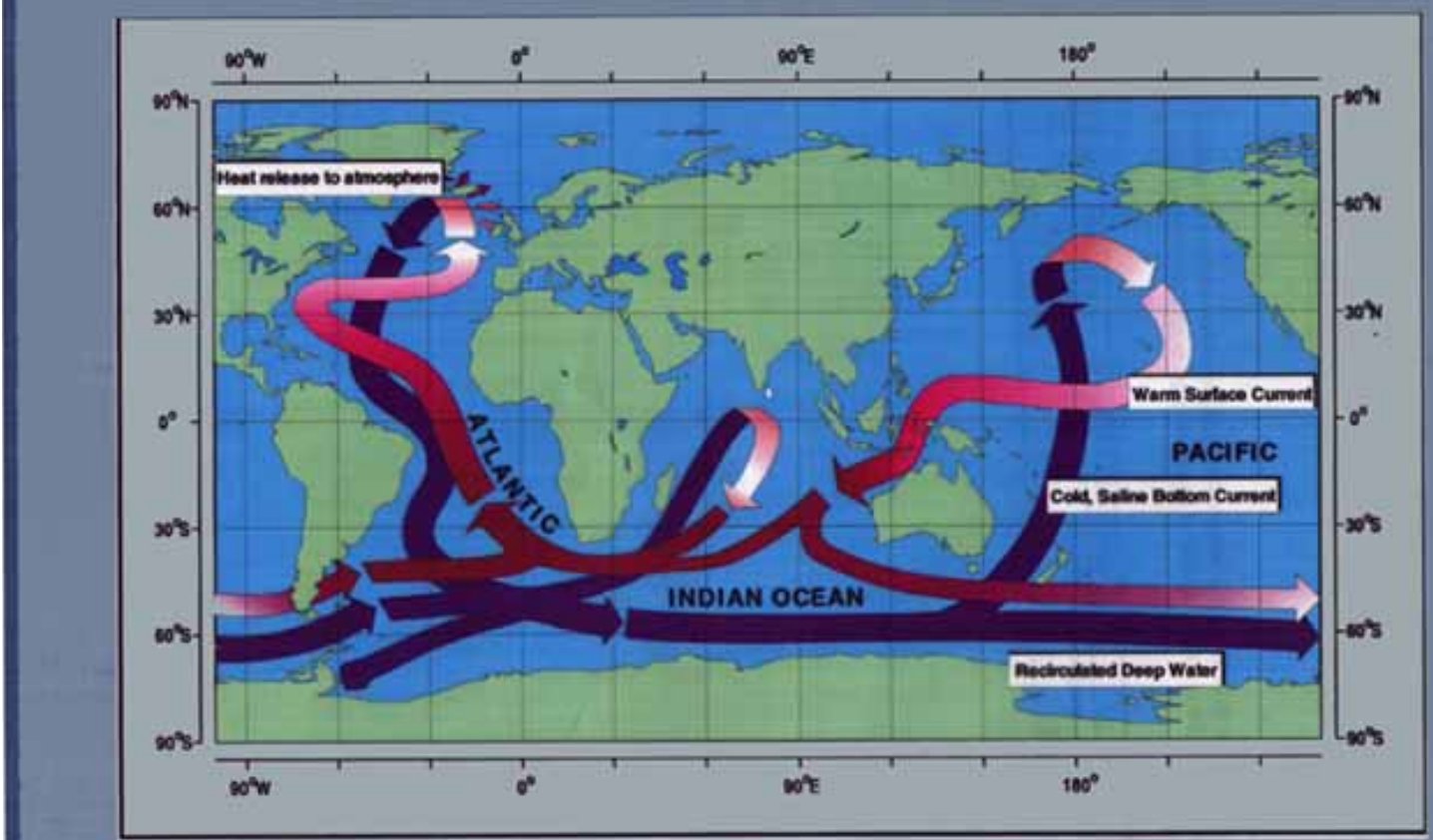
Eli Tziperman

# The Atlantic Meridional Overturning Circulation (AMOC)



**AMOC schematics:** the sinking occurs over very small high-latitude areas in the ocean. the upwelling back to the surface is very broad, over entire ocean basins, not as depicted.

## The Atlantic Thermohaline Circulation - A key Element of the Global Oceanic Circulation -



Schematic diagram of the global ocean circulation pathways, the 'conveyer' belt (after W. Broecker, modified by E. Maier-Reimer).

# The Atlantic Meridional Overturning Circulation (AMOC)

Plate 9. A 2-layer thermohaline conveyor belt. Blue: abyssal water (deep & bottom layers), red: uppermost layer flow (thermocline & intermediate water); transports in Sverdrup circled.

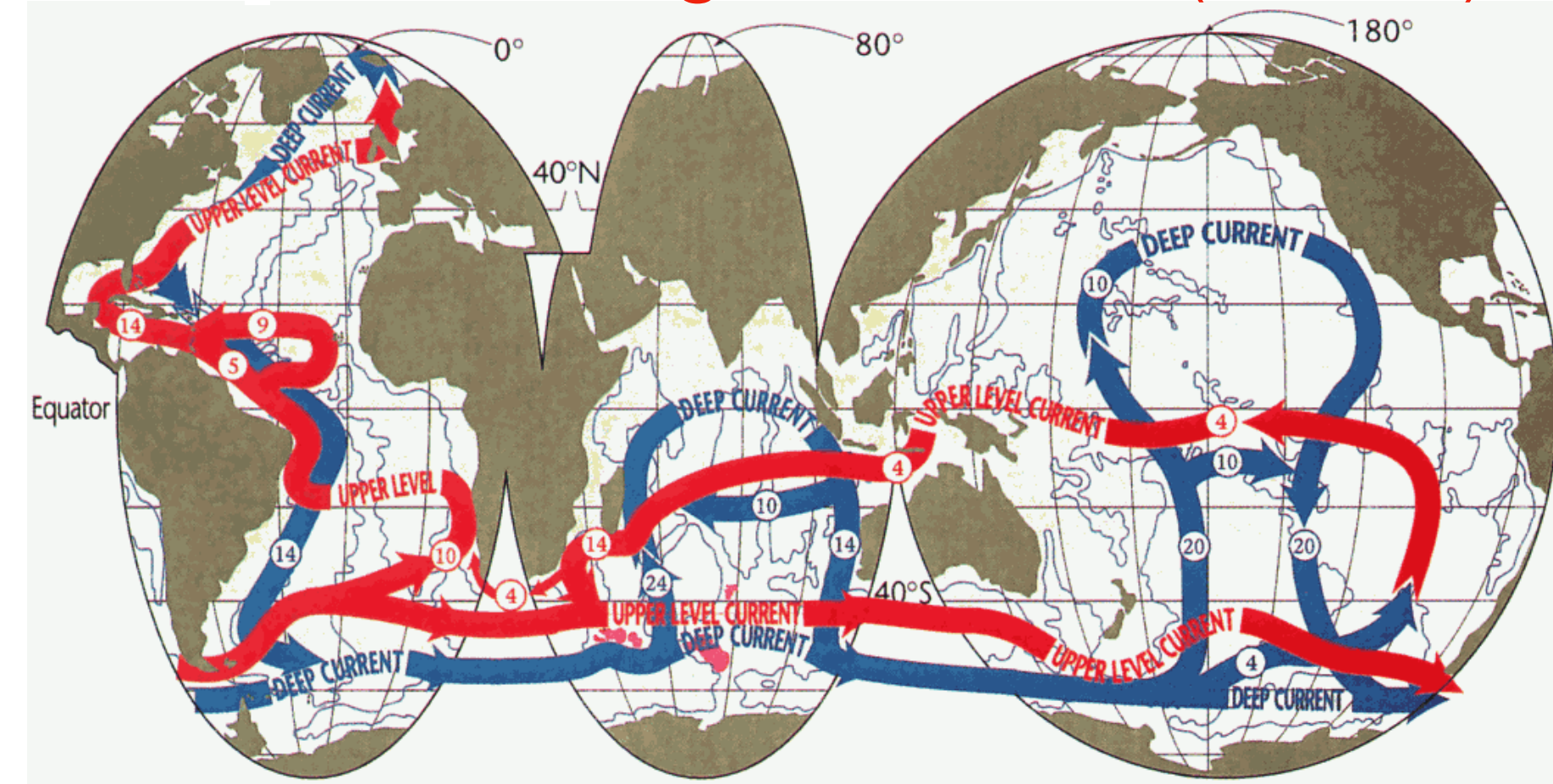
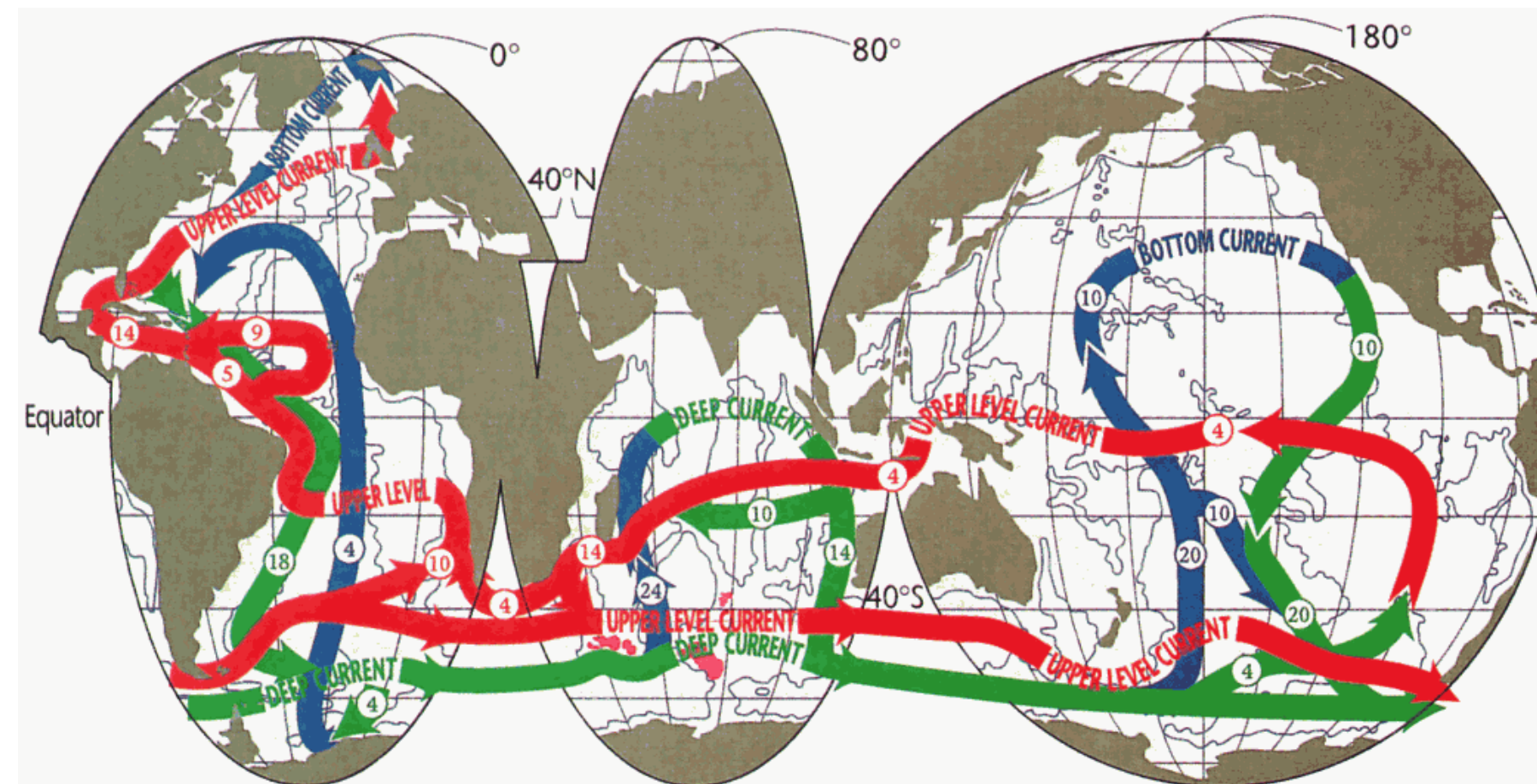
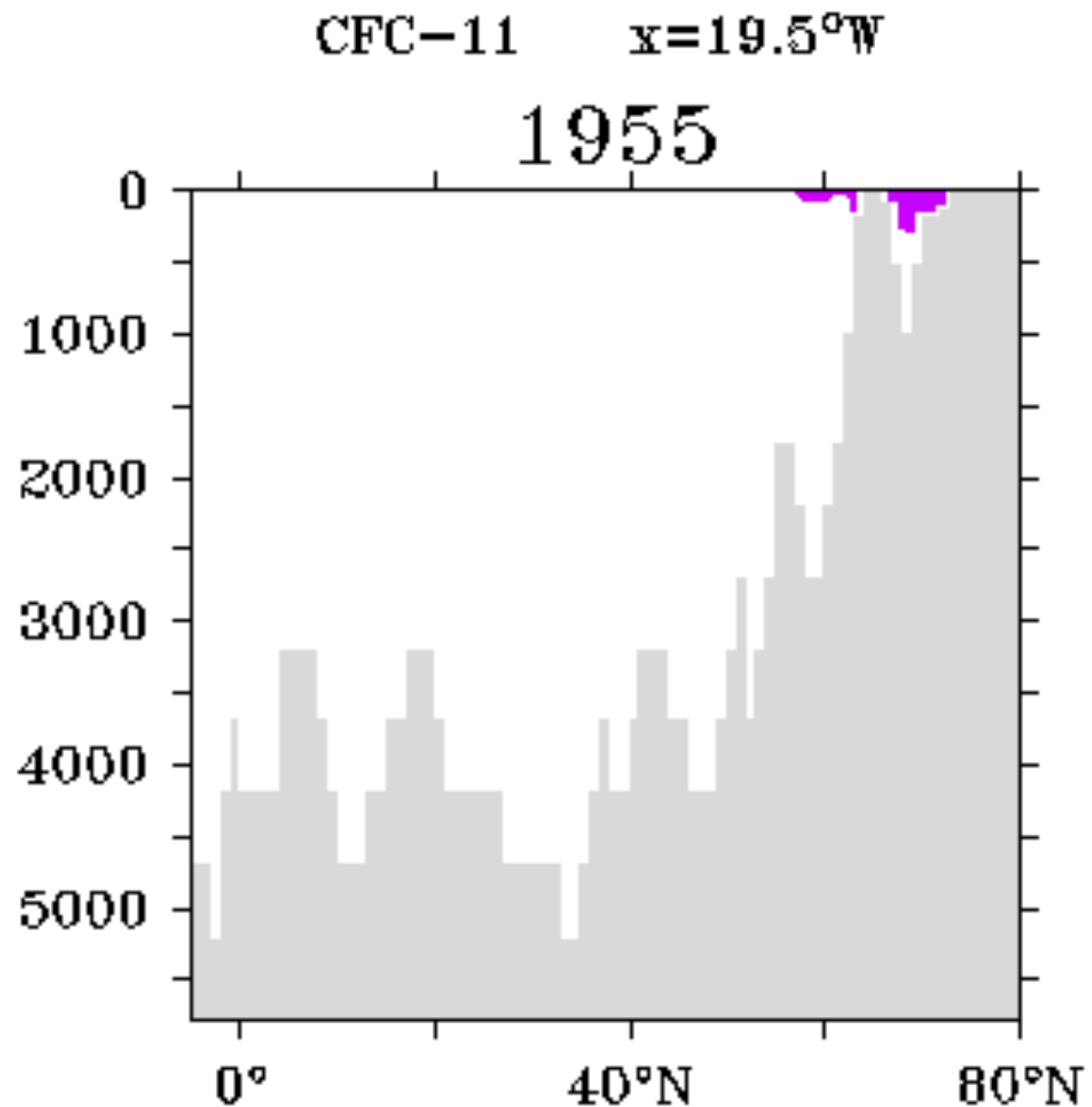


Plate 10. A 3-layer thermohaline conveyor belt. red: thermocline & intermediate layers, green: deep flow, blue: bottom circulation.



**Schmitz 1995**

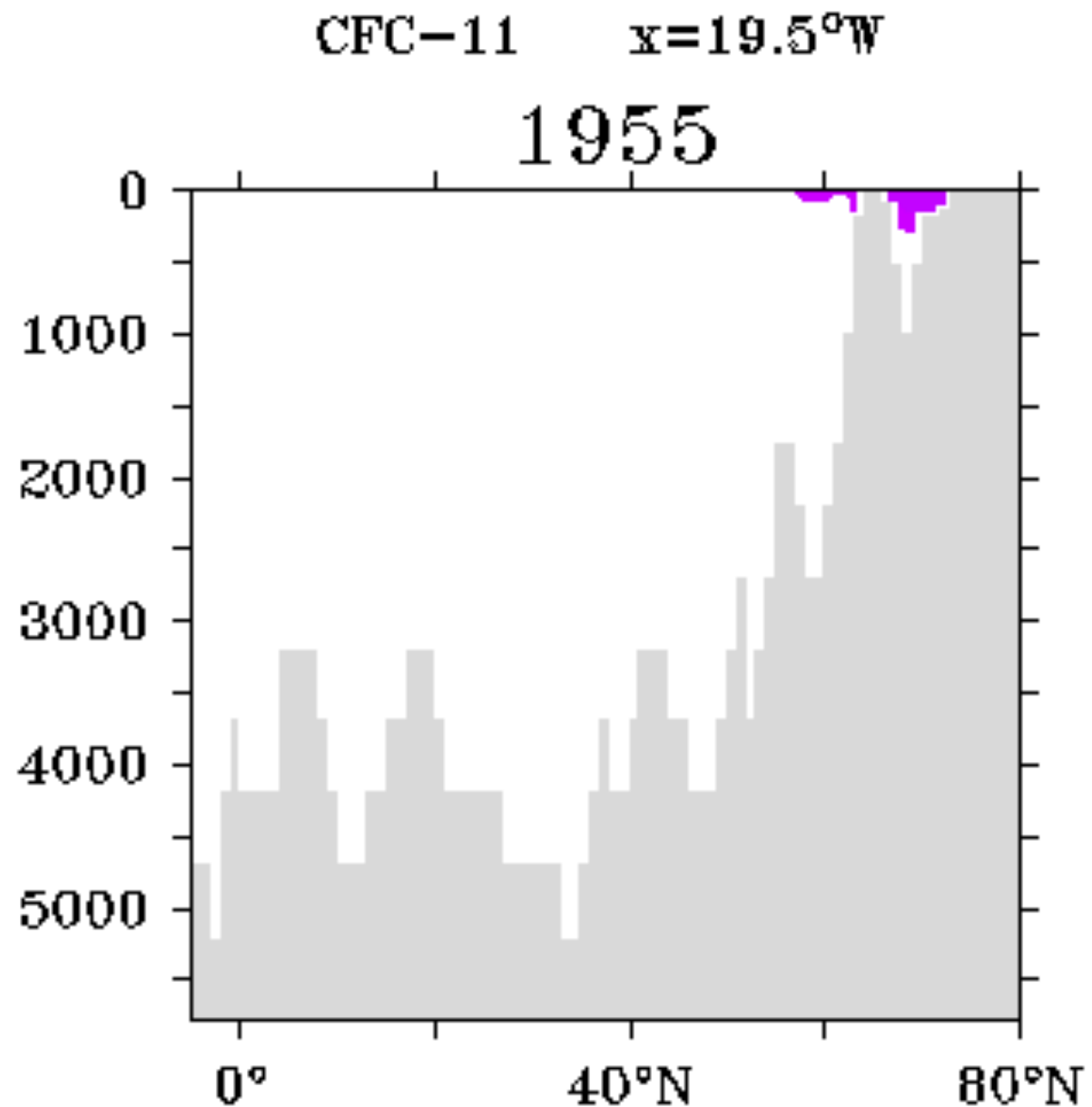
# The Atlantic Meridional Overturning Circulation (AMOC)



Observations of CFC spreading in the North Atlantic Ocean, showing the sinking of deep water there.

<http://puddle.mit.edu/~mick/cfcsec.html>  
(link does not work anymore?)

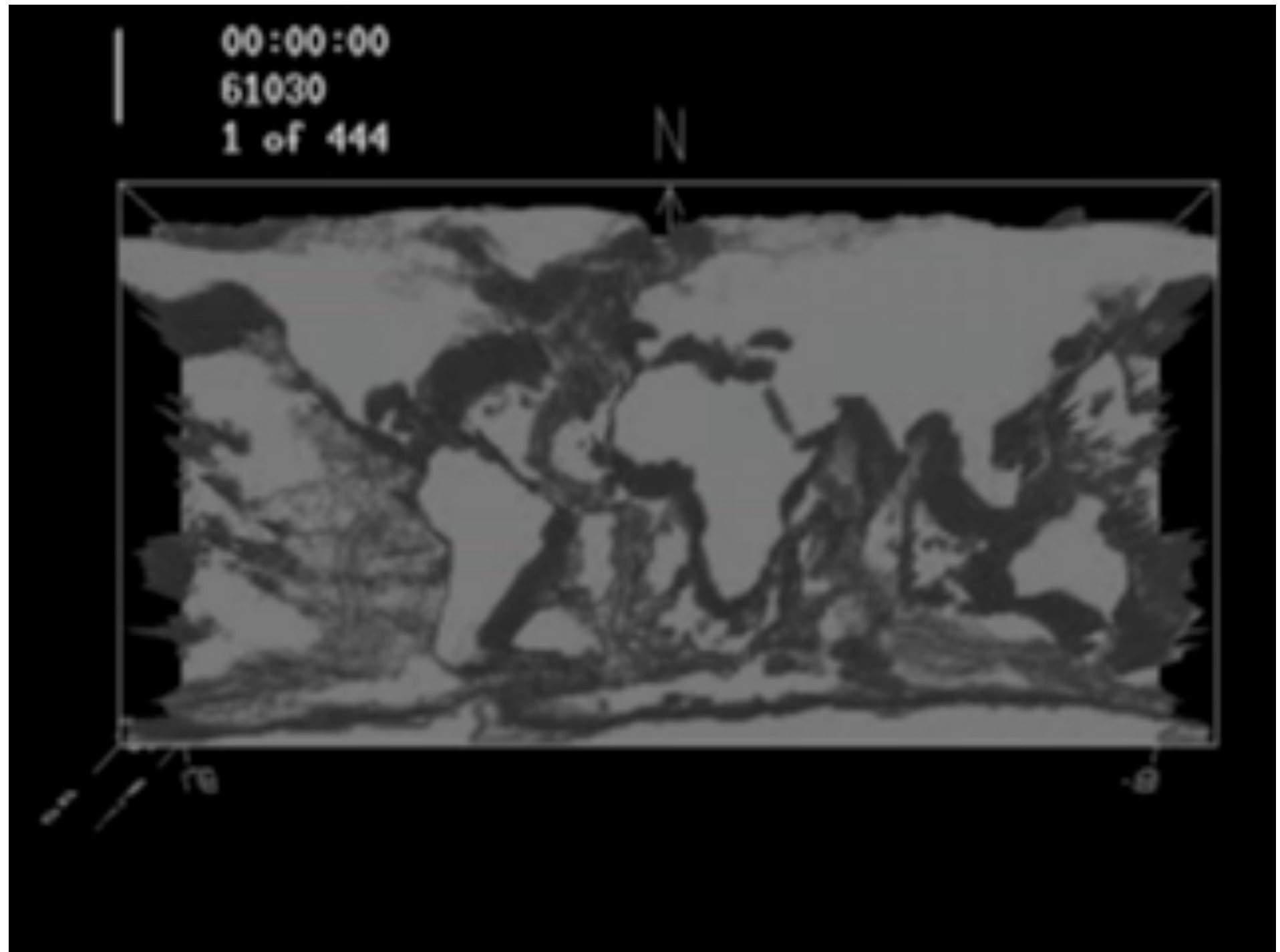
# The Atlantic Meridional Overturning Circulation (AMOC)



Observations of CFC spreading in the North Atlantic Ocean, showing the sinking of deep water there.

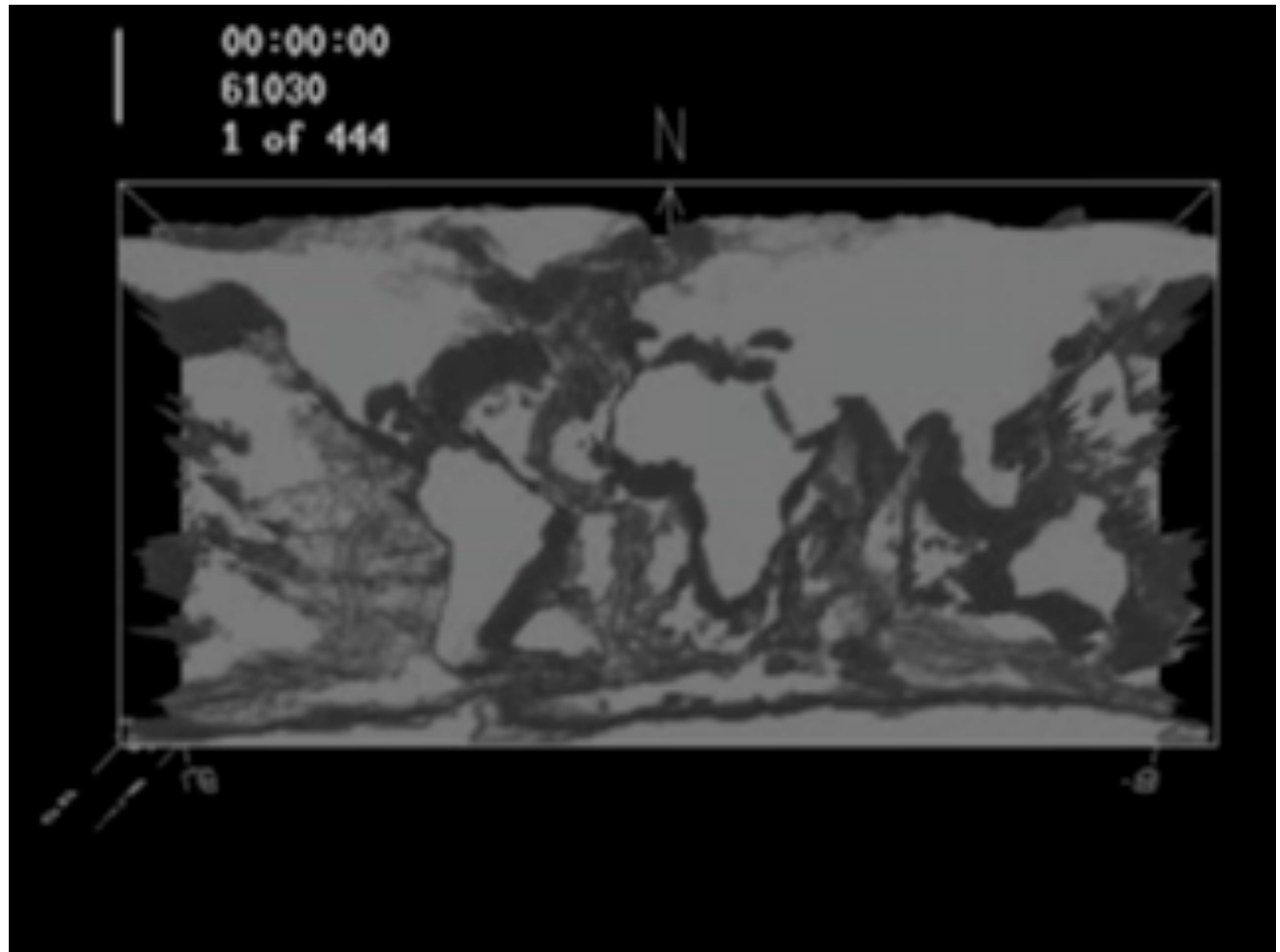
<http://puddle.mit.edu/~mick/cfcsec.html>  
(link does not work anymore?)

# The Atlantic Meridional Overturning Circulation (AMOC)



Simulation of tracer spreading in deep ocean

# The Atlantic Meridional Overturning Circulation (AMOC)



Simulation of tracer spreading in deep ocean

# The Atlantic Meridional Overturning Circulation in the news

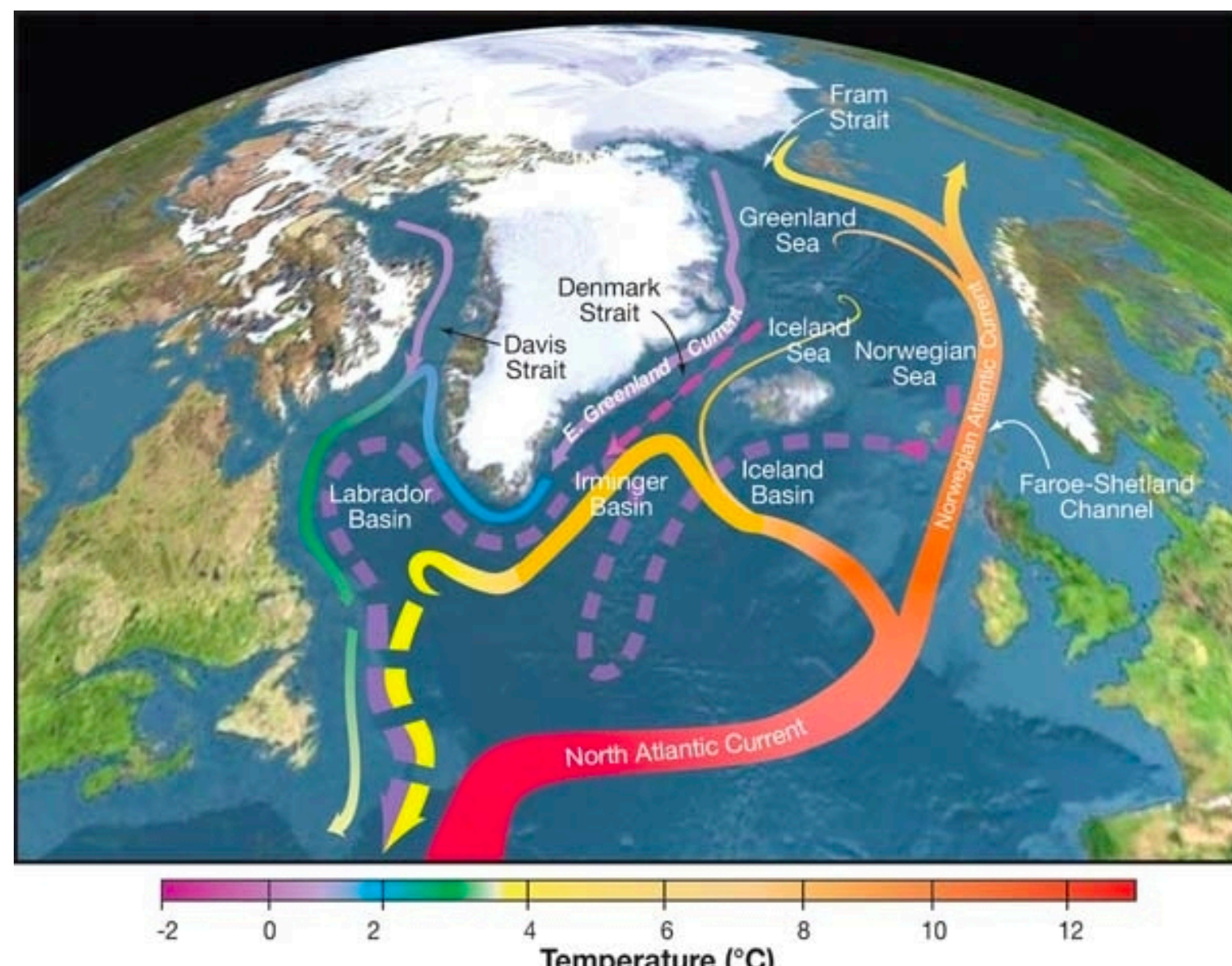
The New York Times

## Atlantic Ocean current shows weakening signs

By Andrew C. Revkin

Nov. 30, 2005

NEW YORK — Atlantic Ocean currents that make Northern Europe warmer than it would otherwise be have weakened by about a third over the last 50 years, British oceanographers are reporting.



# The day after tomorrow

[https://www.youtube.com/watch?v=Ku\\_IseK3xTc](https://www.youtube.com/watch?v=Ku_IseK3xTc)

# The day after tomorrow

[https://www.youtube.com/watch?v=Ku\\_IseK3xTc](https://www.youtube.com/watch?v=Ku_IseK3xTc)

# A news update about AMOC

The New York Times

## *Atlantic Ocean current shows weakening signs*

By Andrew C. Revkin

Nov. 30, 2005



**NEW YORK** — Atlantic Ocean currents that make Northern Europe warmer than it would otherwise be have weakened by about a third over the last 50 years, British oceanographers are reporting.

# A news update about AMOC

The New York Times

## *Atlantic Ocean current shows weakening signs*

By Andrew C. Revkin

Nov. 30, 2005



**NEW YORK** — Atlantic Ocean currents that make Northern Europe warmer than it would otherwise be have weakened by about a third over the last 50 years, British oceanographers are reporting.

The New York Times

## *Scientists Back Off Theory of a Colder Europe in a Warming World*

May 15, 2007



Gradual melting of the Greenland ice sheet, above left, might weaken the North Atlantic Current, which bathes parts of Europe with equatorial water. But any cooling effect in Europe would be overwhelmed by a general warming of the atmosphere.

# Trying to estimate the warming effect of the Atlantic Meridional Overturning Circulation (AMOC)

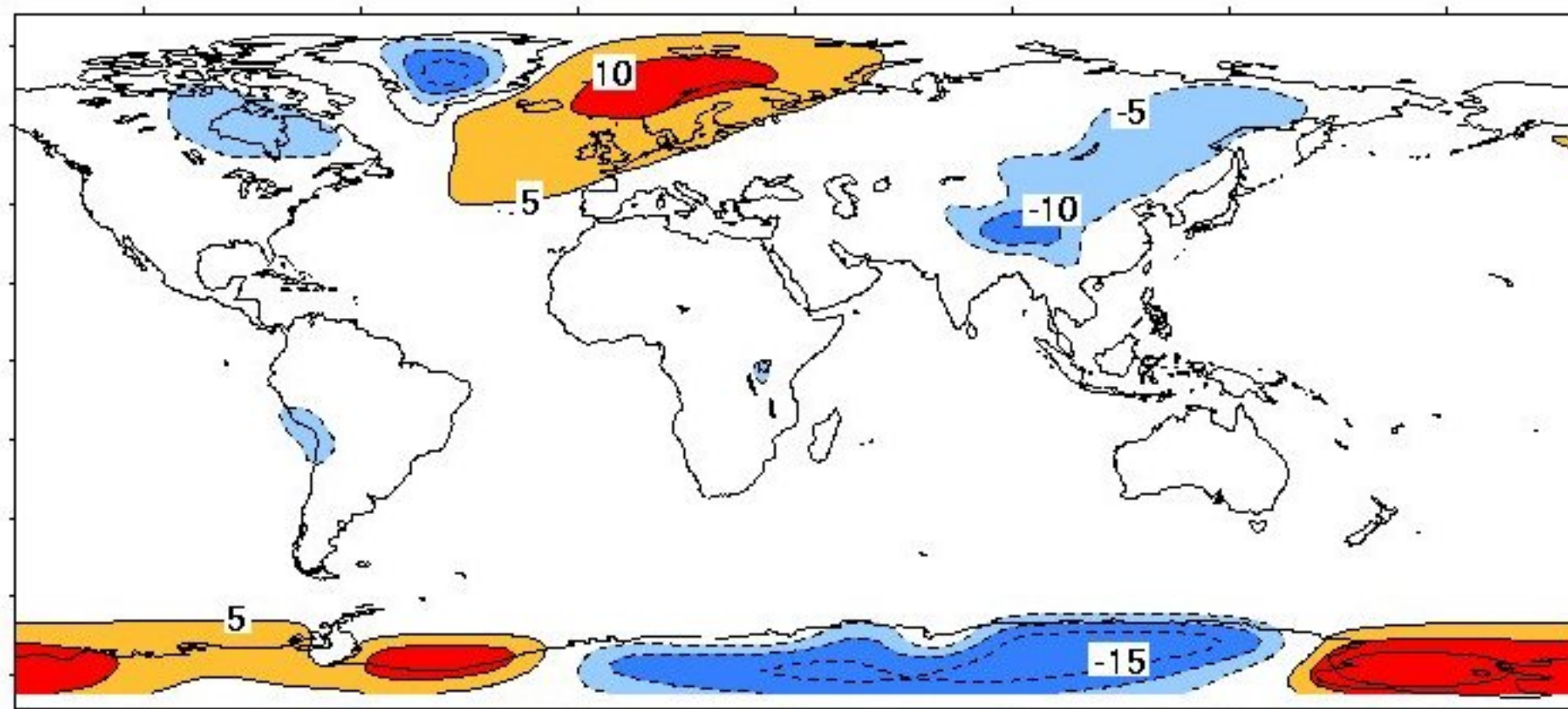


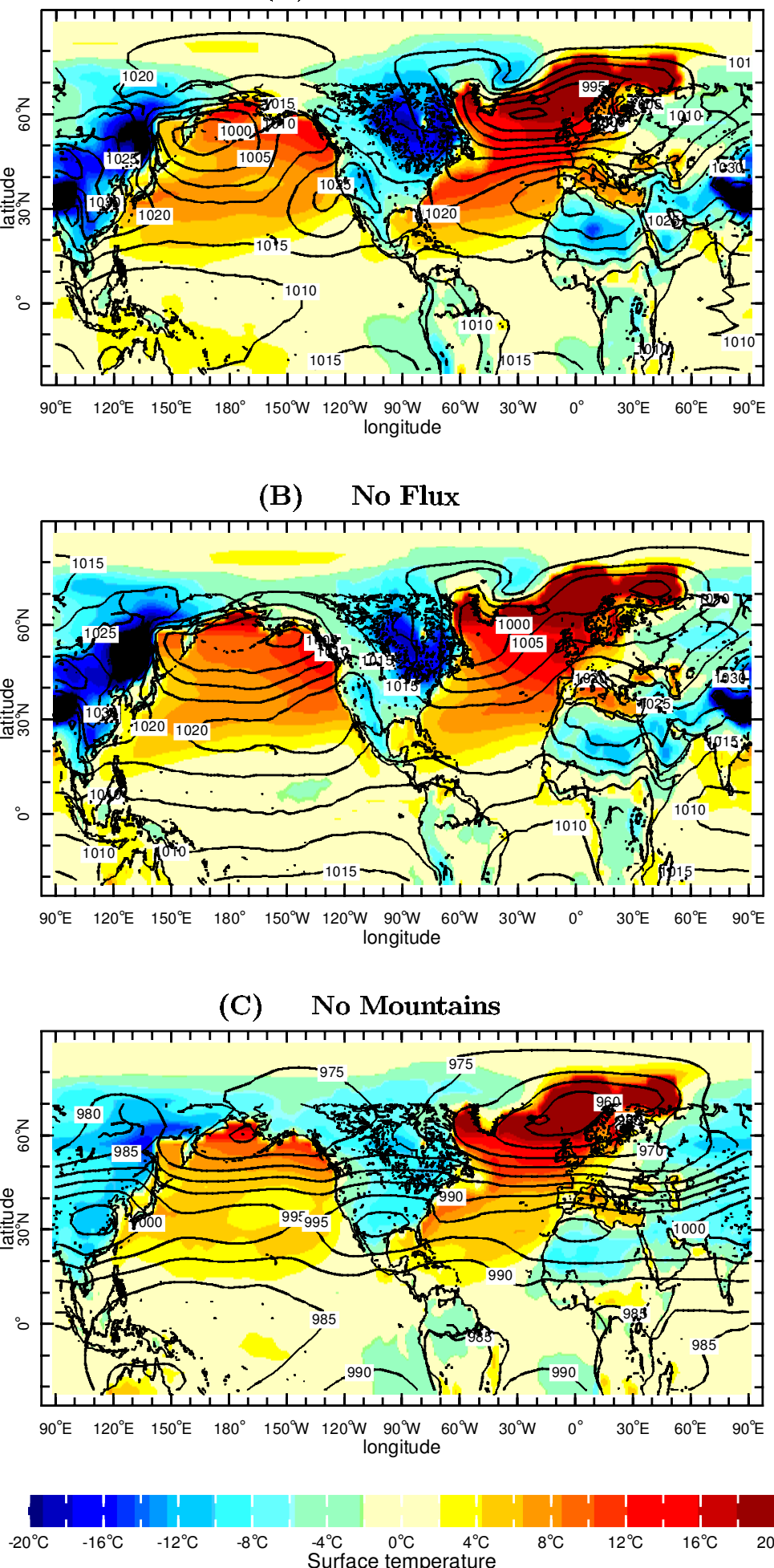
**Figure 1.** Deviation of the annual-mean surface air temperature from its zonal average, computed from the NCAR air temperature climatology. Anomalously cold areas are found over some continental regions, anomalously warm areas over ocean deep water formation regions.

[Whether this pattern should be attributed to the AMOC is debatable, see next slide.]

# Is the Gulf Stream responsible for Europe's mild winters?

SEAGER, BATTISTI, YIN, GORDON, NAIK, CLEMENT & CANE, 2002

Figure 14. Sea-level pressure (mb) and zonal eddy surface temperature in degC (colours) for January for (a) the case with mountains and q-flux, (b) the case with mountains and the q-flux set to zero, and (c) the case without mountains but with the q-flux.



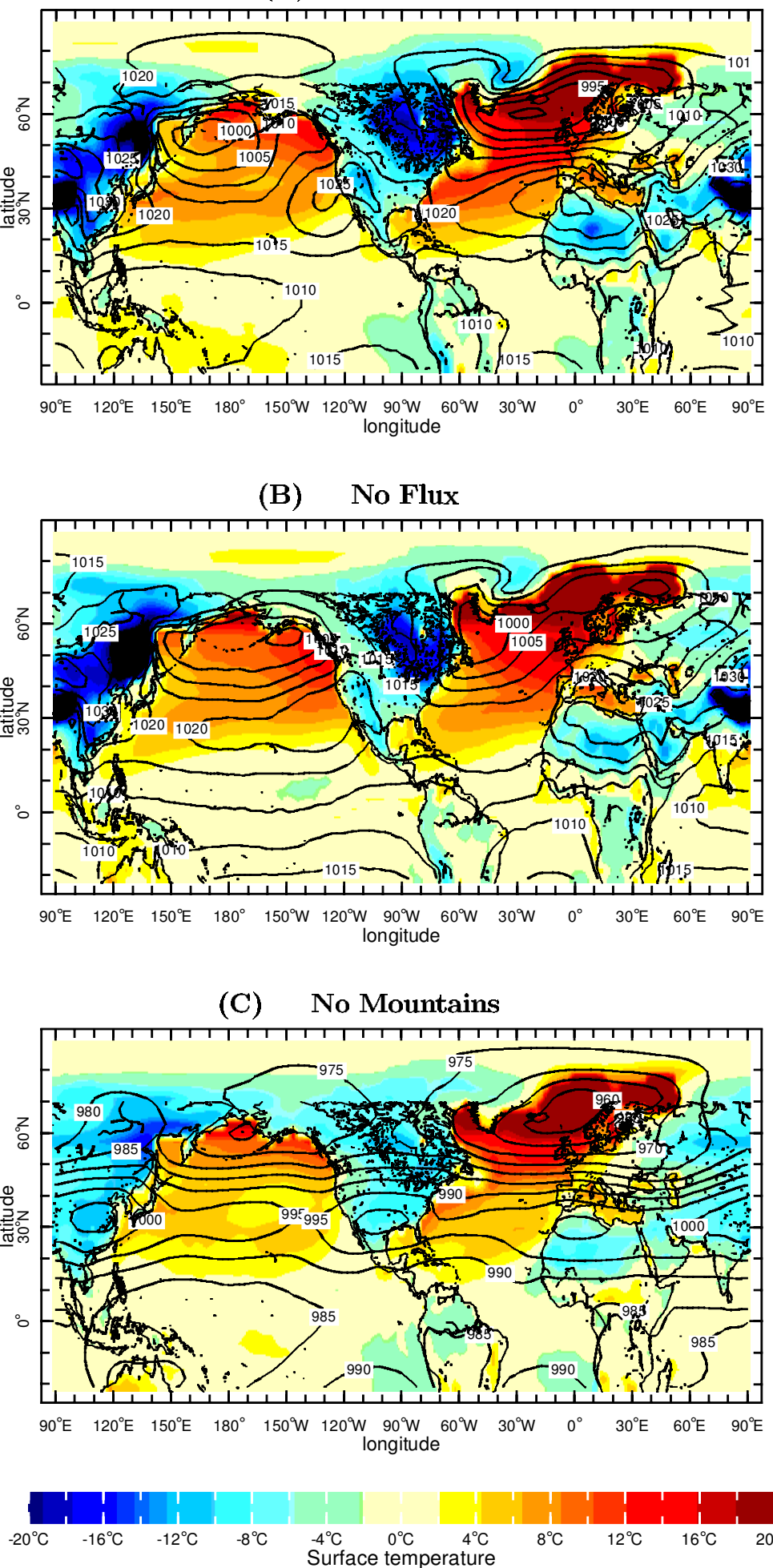
# Is the Gulf Stream responsible for Europe's mild winters?

SEAGER, BATTISTI, YIN, GORDON, NAIK, CLEMENT & CANE, 2002

Figure 14. Sea-level pressure (mb) and zonal eddy surface temperature in degC (colours) for January for (a) the case with mountains and q-flux, (b) the case with mountains and the q-flux set to zero, and (c) the case without mountains but with the q-flux.



→ (some of) Europe's warmth relative to same latitude in North America is attributed to the position of the atmospheric jet stream, which is, in turn, affected by the Rocky mountains.



# Observing the Atlantic Meridional Overturning Circulation

# Is the Atlantic Meridional Overturning Circulation collapsing already due to global warming??

**Table 1 | Meridional transport in depth classes across 25° N**

	1957	1981	1992	1998	2004
Shallower than 1,000 m depth					
Gulf Stream and Ekman	+35.6	+35.6	+35.6	+37.6	+37.6
Mid-ocean geostrophic	-12.7	-16.9	-16.2	-21.5	-22.8
<b>Total shallower than 1,000 m</b>	<b>+22.9</b>	<b>+18.7</b>	<b>+19.4</b>	<b>+16.1</b>	<b>+14.8</b>
1,000-3,000 m	-10.5	-9.0	-10.2	-12.2	-10.4
3,000-5,000 m	-14.8	-11.8	-10.4	-6.1	-6.9
Deeper than 5,000 m	+2.4	+2.1	+1.2	+2.2	+2.5

Values of meridional transport are given in Sverdrups. Positive transports are northward.

(Bryden et al 2005)

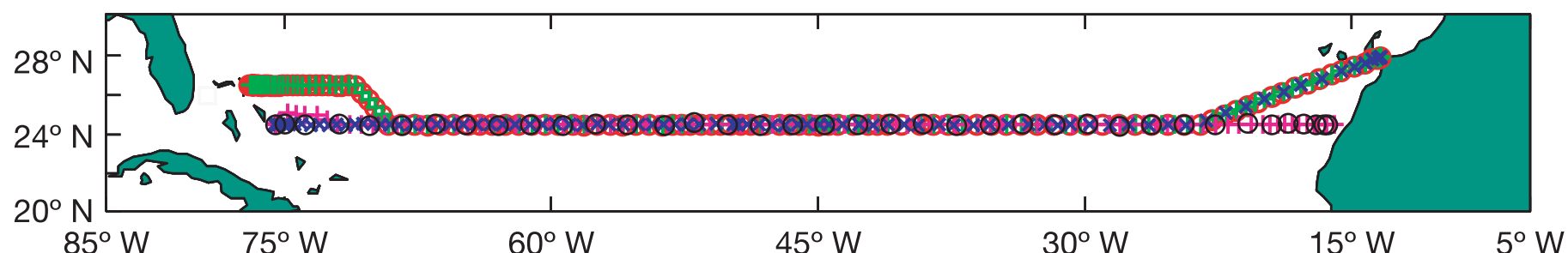


Figure 1 | Station positions for transatlantic hydrographic sections taken in 1957, 1981, 1992, 1998 and 2004. The 1957 and 1992 sections each went zonally along 24.58 N from the African coast to the Bahama Islands. Because of diplomatic clearance issues, the 1981, 1998 and 2004 sections angled southwestward from the African coast at about 288 N to join the 24.58 N section at about 238 W. The 1998 and 2004 sections angled northwestward at about 738 W to finish the section along 26.58 N.

# RAPID: monitoring the Atlantic Meridional Overturning Circulation at 26.5°N

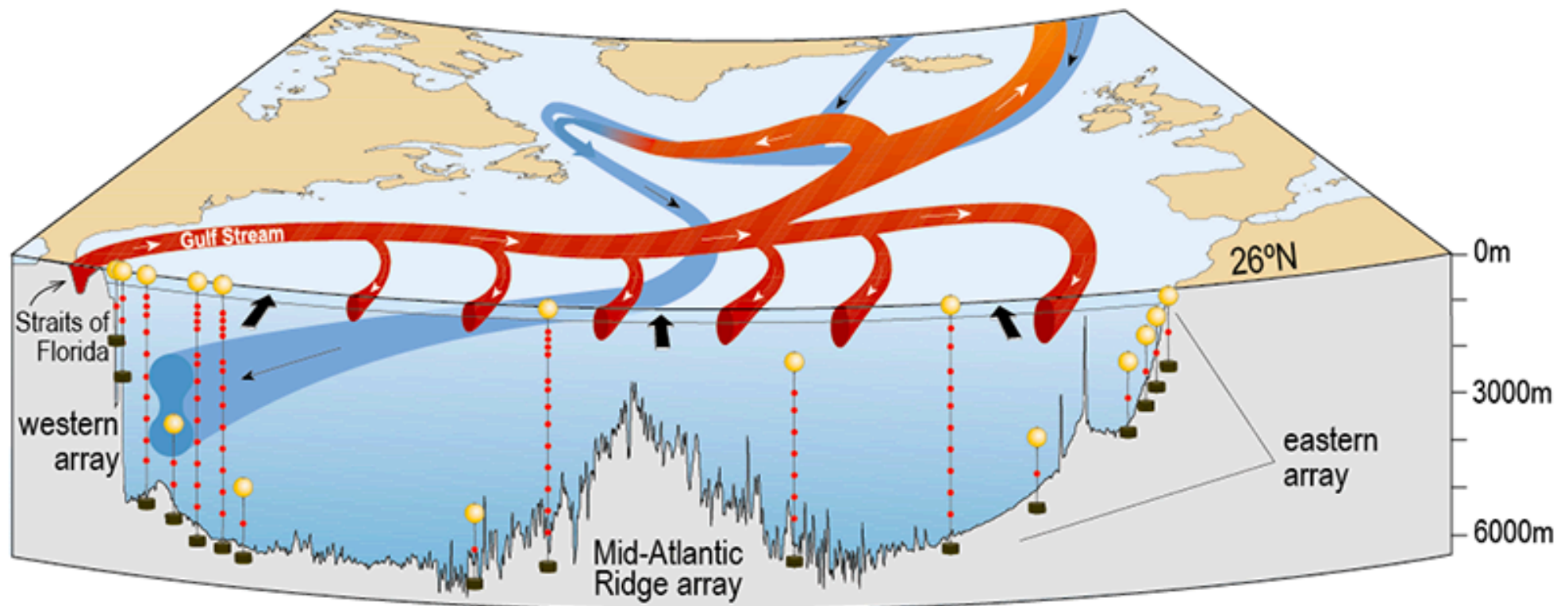
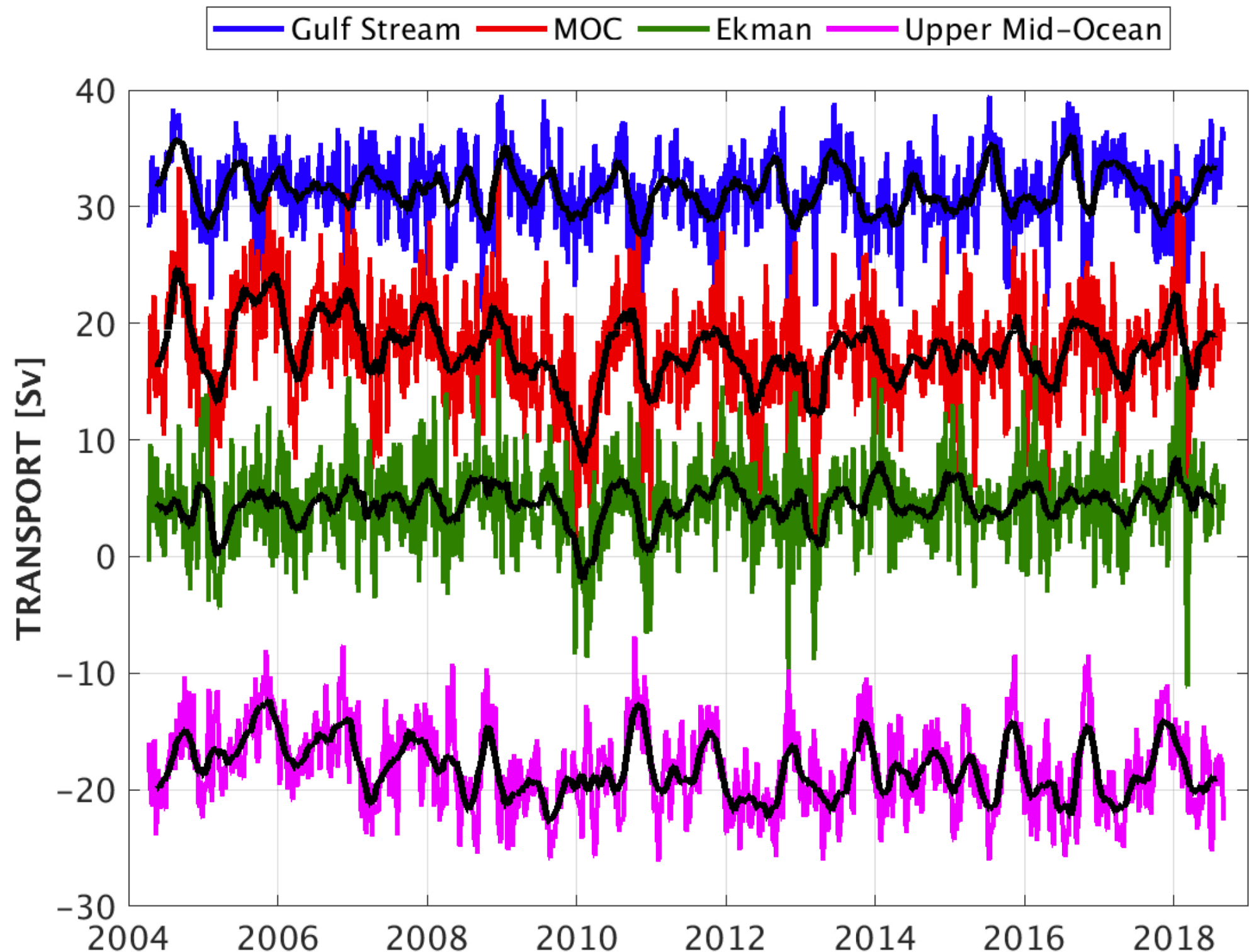


Figure 5. The North Atlantic overturning circulation with the location of the RAPID array moorings along 26°N. Modified from Church, 2007.

A view of the back deck of the RRS James Cook during the RAPID cruise in April 2014.



# RAPID: monitoring the Atlantic Meridional Overturning Circulation at 26.5°N

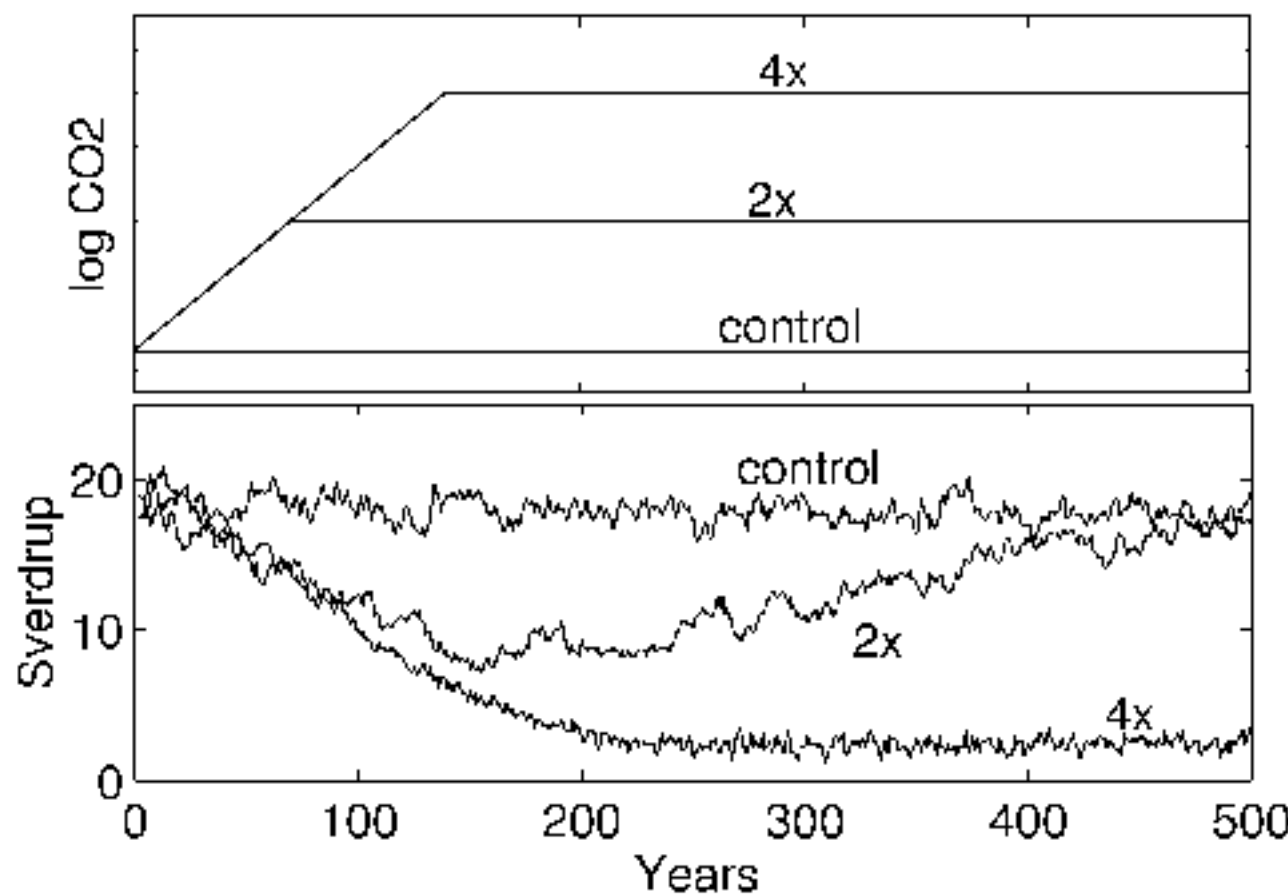


# Ocean diapycnal mixing: Brazil basin tracer release experiment

# The Atlantic Meridional Overturning Circulation Under a future climate change

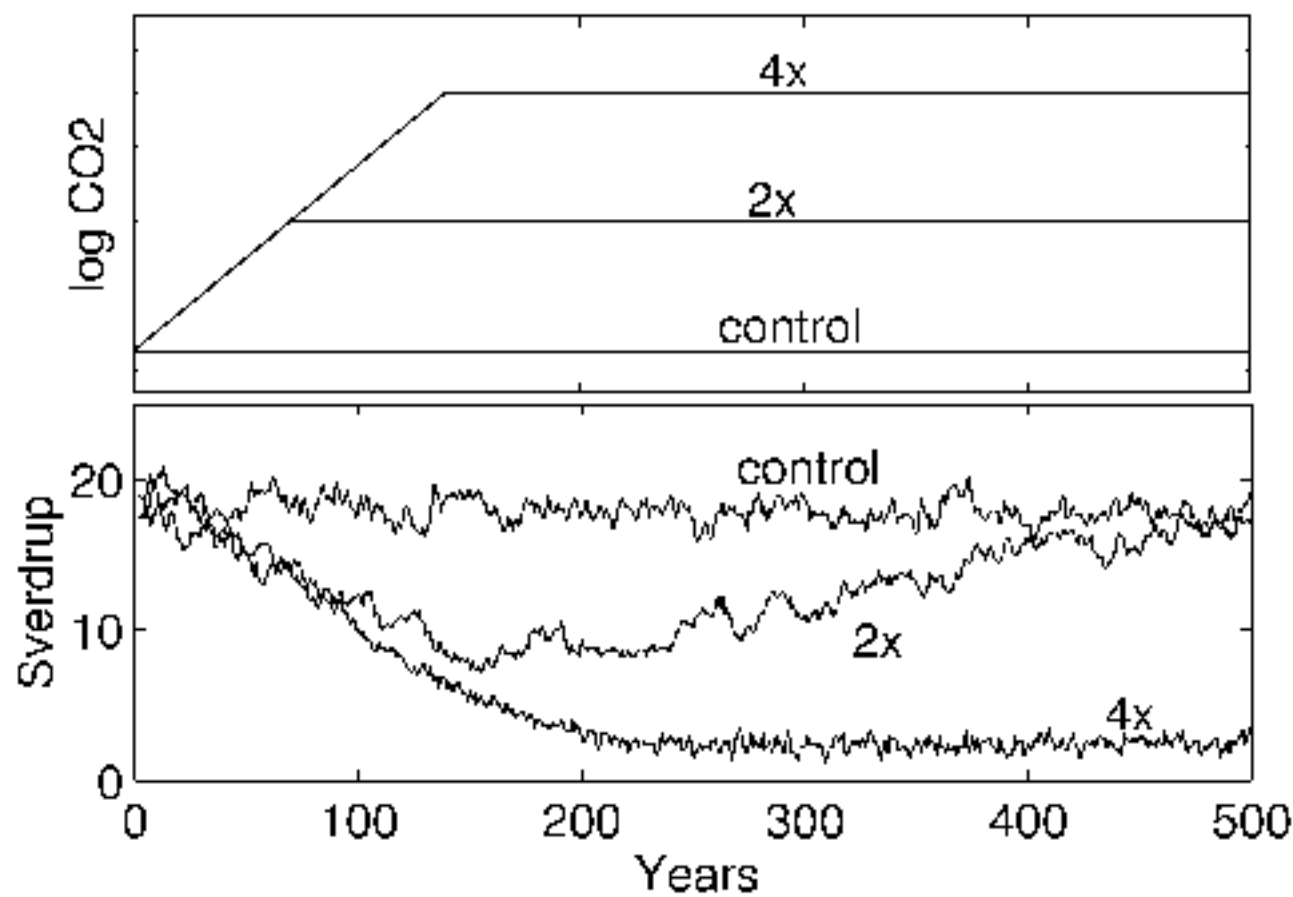
# Collapse of the Atlantic Meridional Overturning Circulation (AMOC) in a global warming scenario

Manabe and Stouffer 1993



# Collapse of the Atlantic Meridional Overturning Circulation (AMOC) in a global warming scenario

Manabe and Stouffer 1993



VELLINGA and WOOD 2002

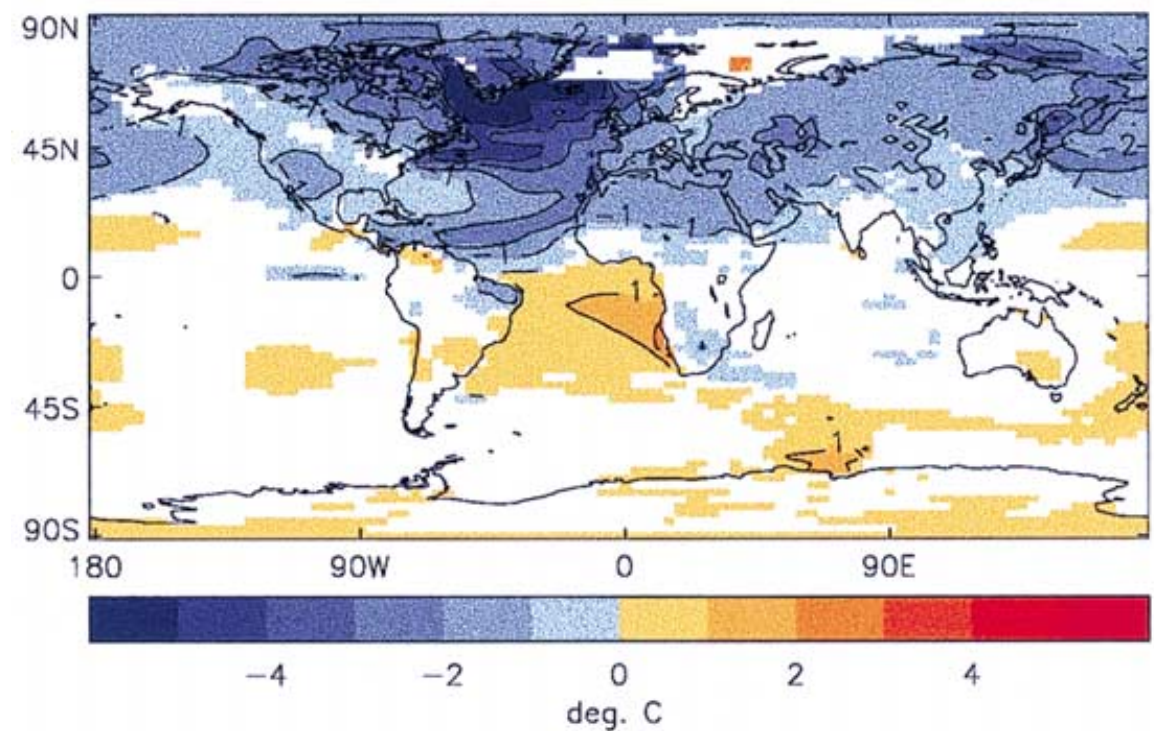
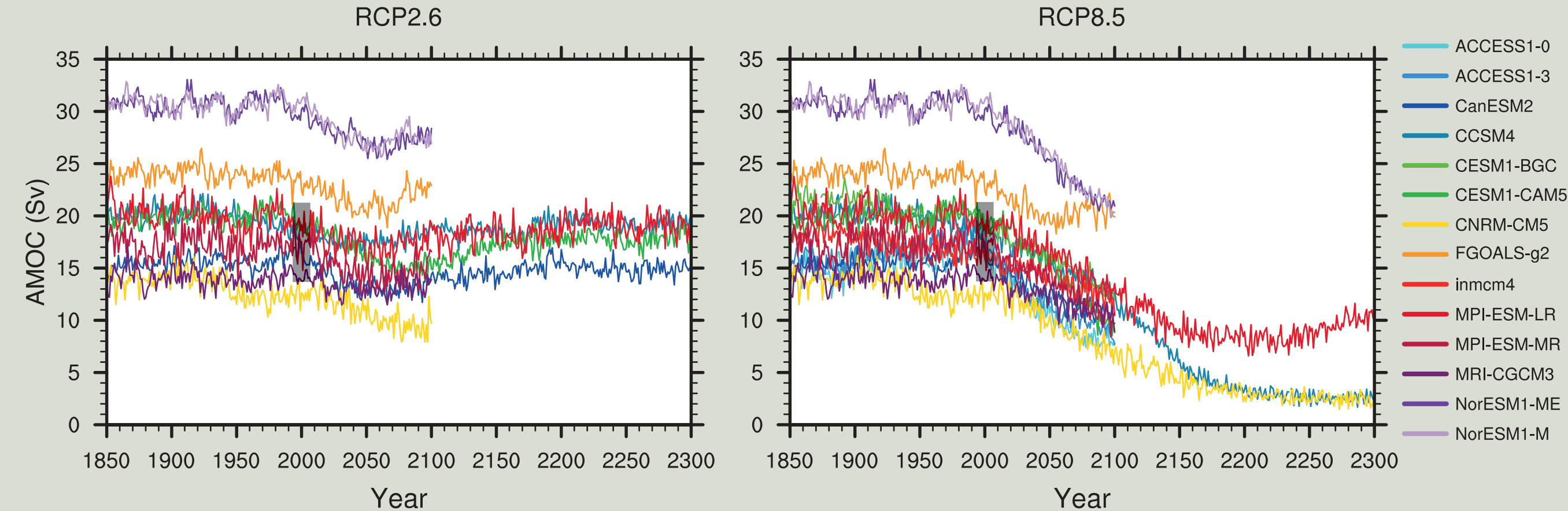


Figure 3. Change in surface air temperature during years 20–30 after the collapse of the THC. Areas where the anomaly is not significant have been masked.

# Collapse of the Atlantic Meridional Overturning Circulation (AMOC) in a global warming scenario

**IPCC AR5, 2013**



**TFE.5, Figure 1 |** Atlantic Meridional Overturning Circulation (AMOC) strength at 30°N (Sv) as a function of year, from 1850 to 2300 as simulated by different Atmosphere–Ocean General Circulation Models in response to scenario RCP2.6 (left) and RCP8.5 (right). The vertical black bar shows the range of AMOC strength measured at 26°N, from 2004 to 2011 {Figures 3.11, 12.35}

# The Atlantic Meridional Overturning Circulation (AMOC) in the IPCC report

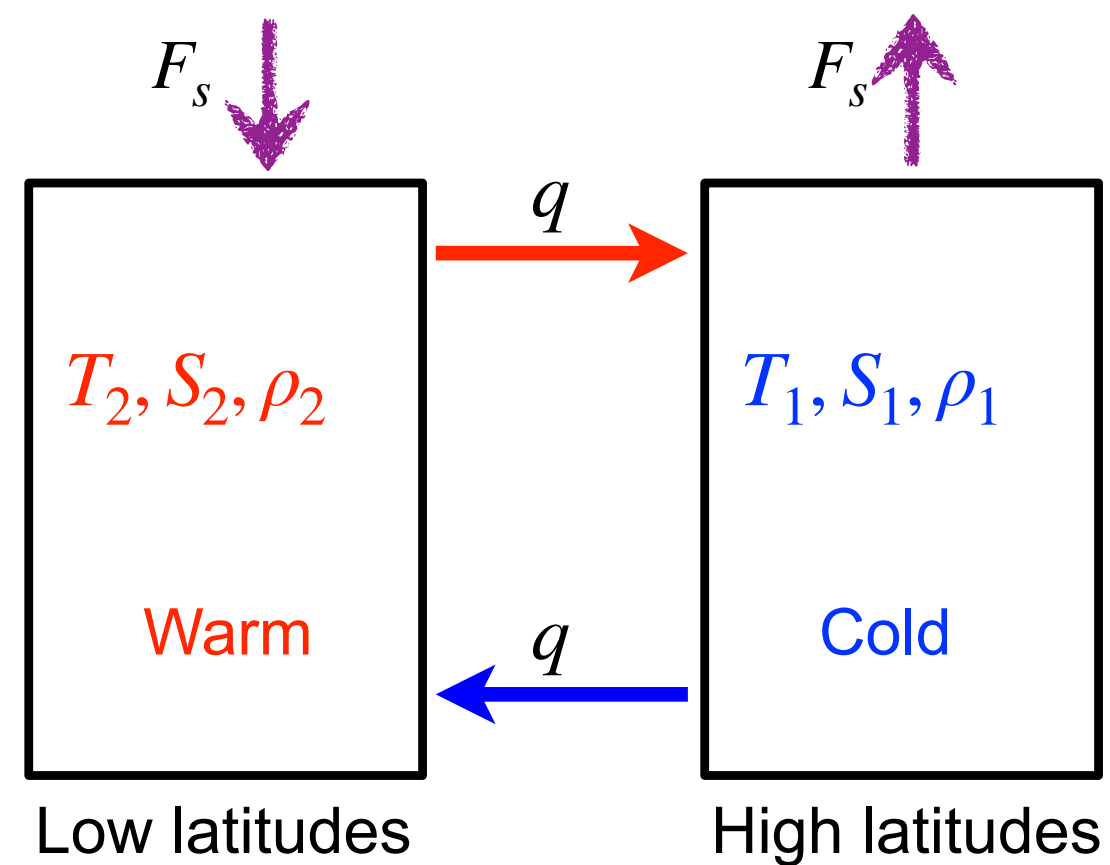
- “There is no observational evidence of a trend in the Atlantic Meridional Overturning Circulation (AMOC), based on the decade-long record of the complete AMOC and longer records of individual AMOC components. {3.6}”

# The Atlantic Meridional Overturning Circulation (AMOC) in the IPCC report

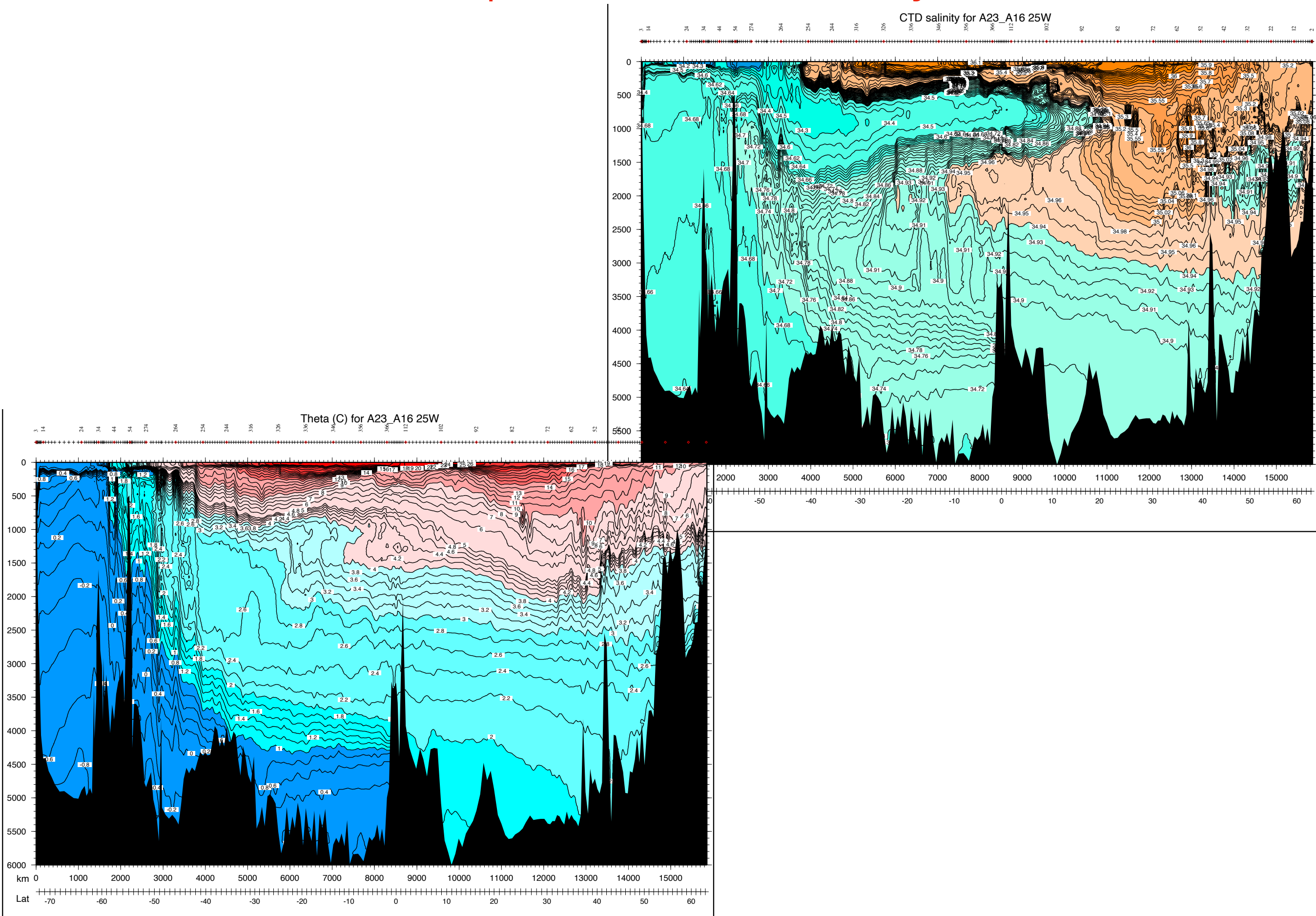
- “There is no observational evidence of a trend in the Atlantic Meridional Overturning Circulation (AMOC), based on the decade-long record of the complete AMOC and longer records of individual AMOC components. {3.6}”
- “It is very likely that the Atlantic Meridional Overturning Circulation (AMOC) will weaken over the 21st century. Best estimates and ranges for the reduction are 11% (1 to 24%) in RCP2.6 and 34% (12 to 54%) in RCP8.5. It is likely that there will be some decline in the AMOC by about 2050, but there may be some decades when the AMOC increases due to large natural internal variability. {11.3, 12.4}”

notes section 6.2:

The Stommel model, understanding AMOC tipping points  
(use next slides)



# Atlantic temperature and salinity, WOCE



# Multiple equilibria and hysteresis of the Atlantic Meridional Overturning Circulation (AMOC)

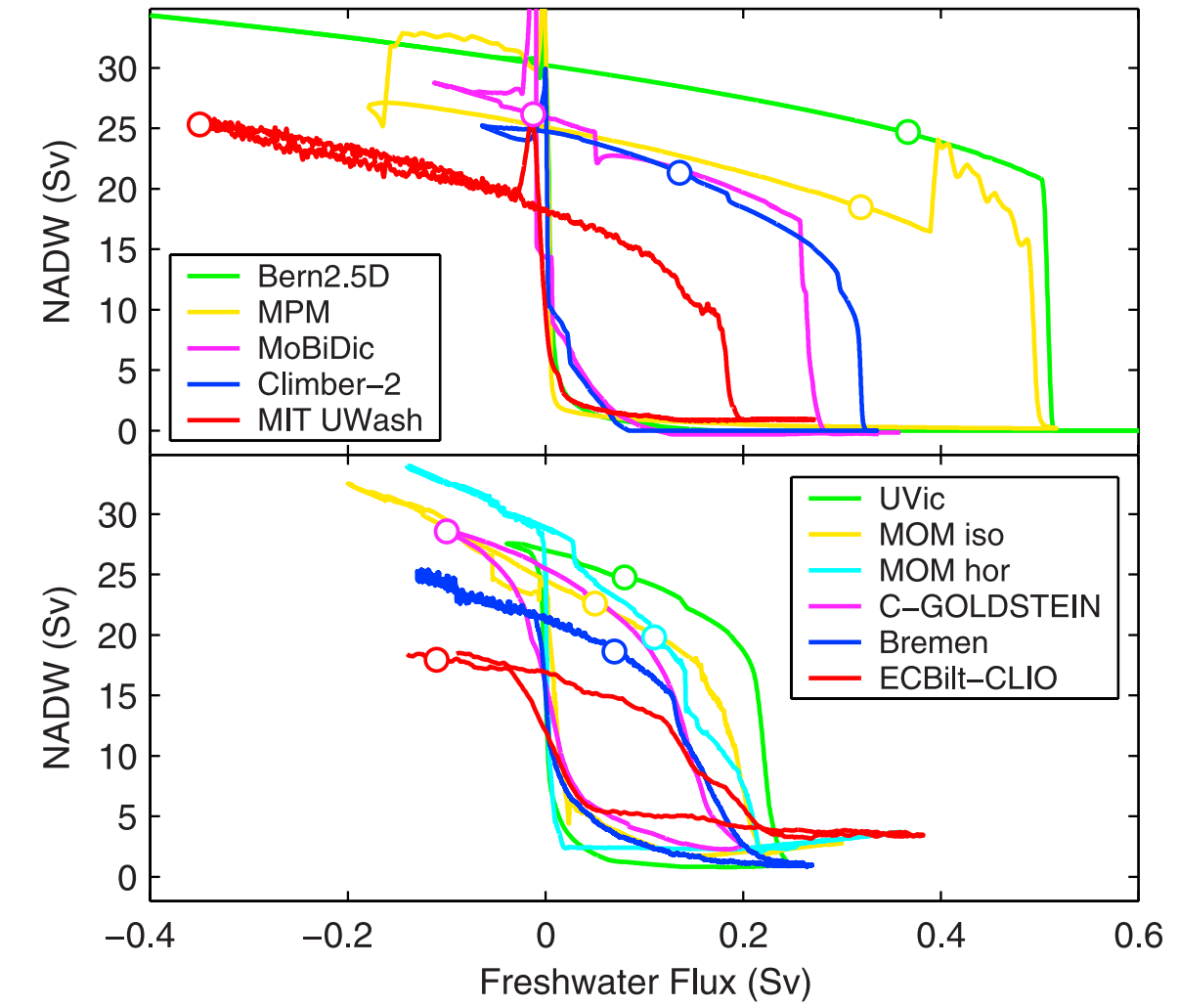
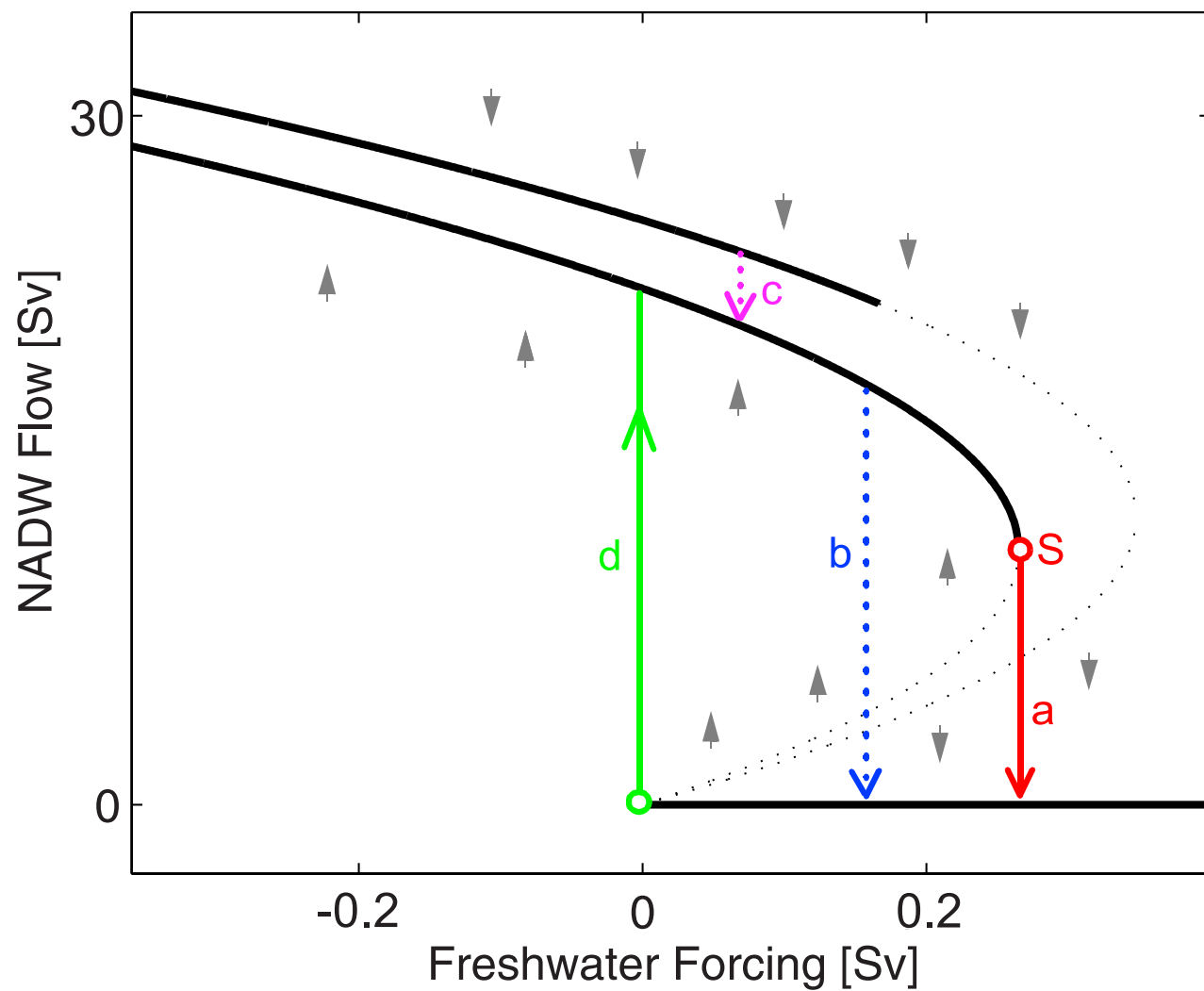


Figure 2. Hysteresis curves found in the model inter-comparison. The bottom panel shows coupled models with 3-D global ocean models, the top panel those with simplified ocean models (zonally averaged or, in case of the MIT\_UWash model, rectangular basins). Curves were slightly smoothed to remove the effect of short-term variability. Circles show the present-day climate state of each model.

# Multiple equilibria and hysteresis of the Atlantic Meridional Overturning Circulation (AMOC)

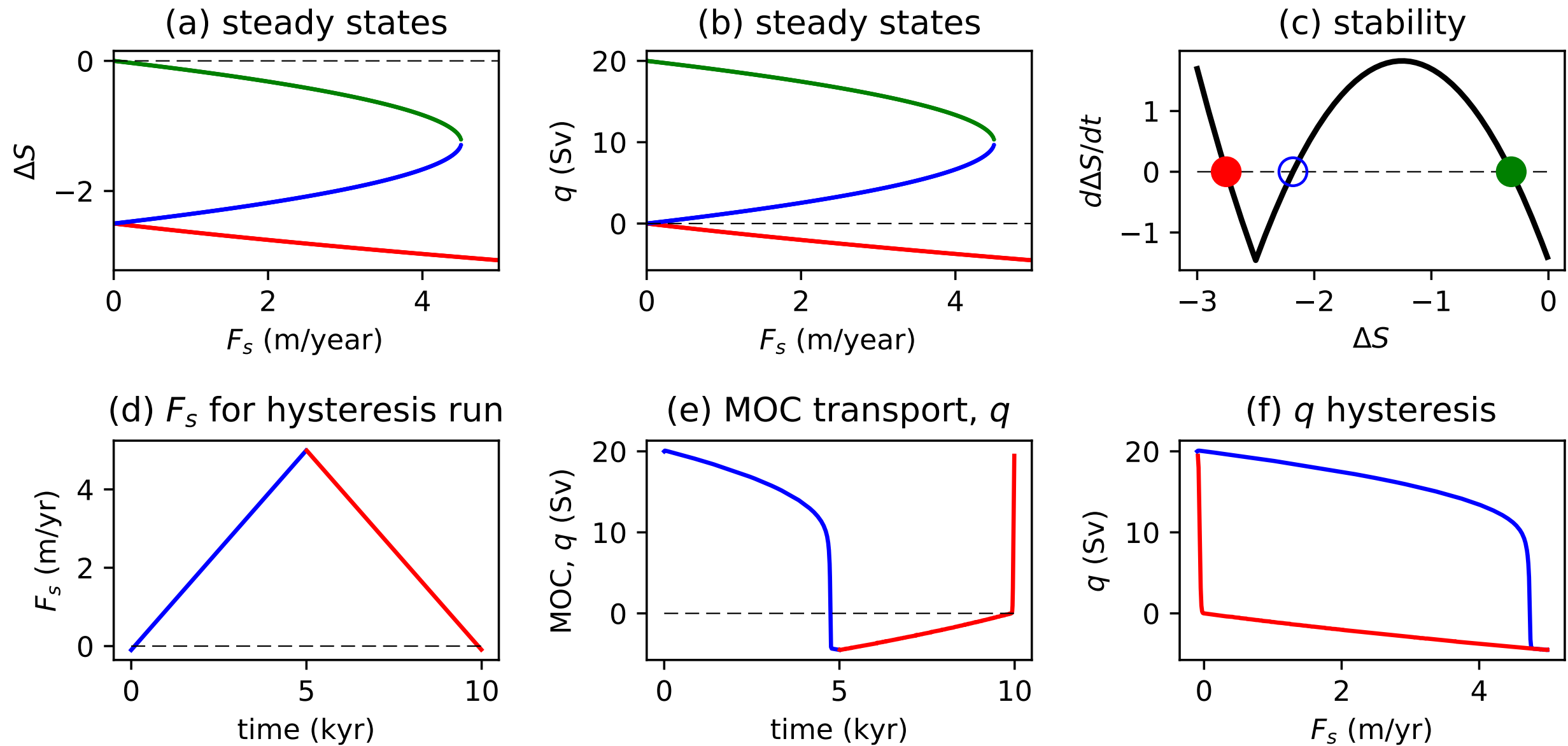
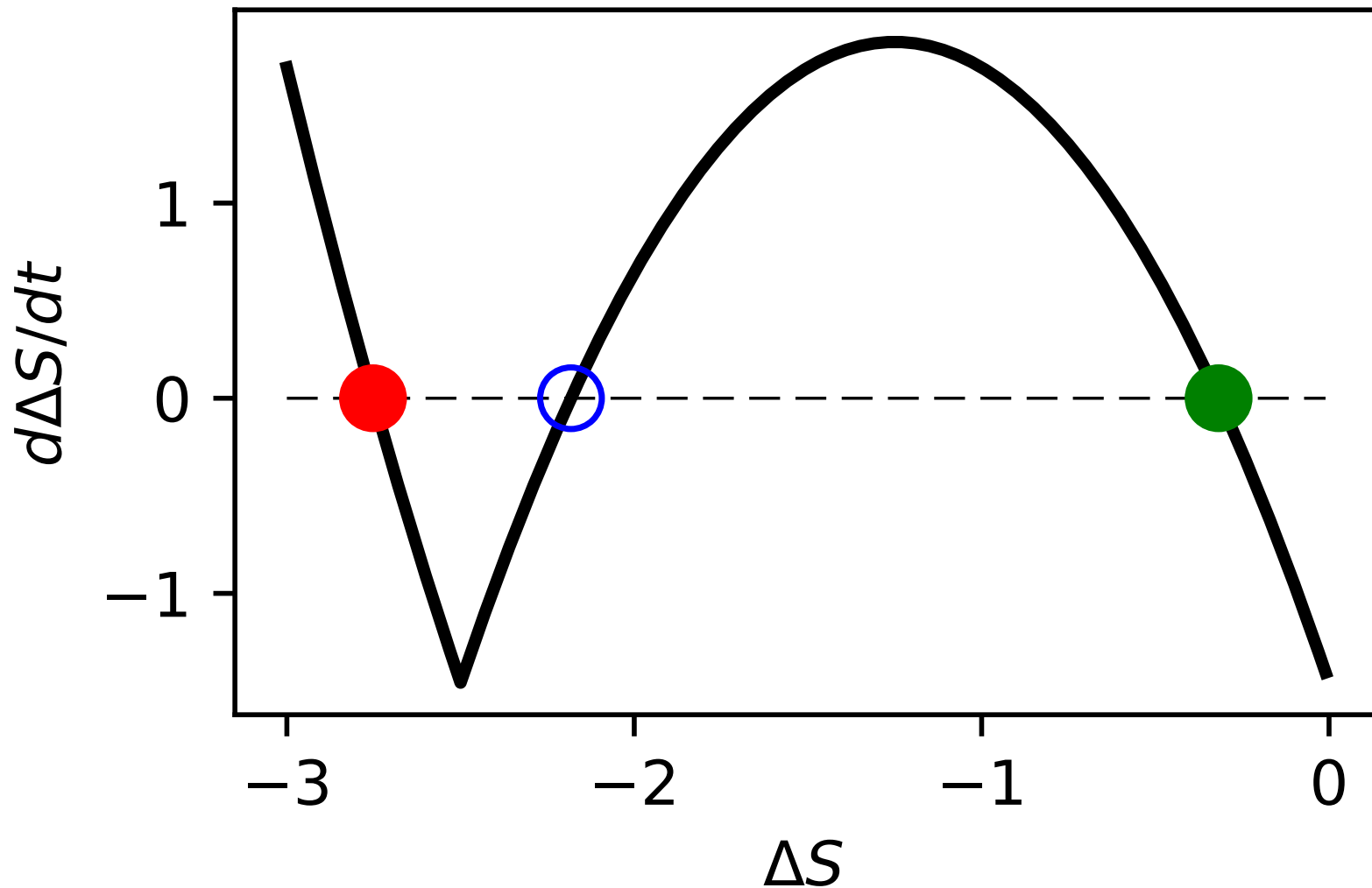


Figure 6.5: Solution of the 2-box model: (a, b) Steady states of salinity difference and MOC as function of fresh water forcing. (c) Stability analysis. (d) Fresh water forcing for hysteresis run. (e, f) Hysteresis results.

# Multiple equilibria and hysteresis of the Atlantic Meridional Overturning Circulation (AMOC)



Analyzing stability of a nonlinear dynamical system: Stommel-Taylor box model example

# Consequences of collapse of Atlantic Meridional Overturning Circulation (AMOC)

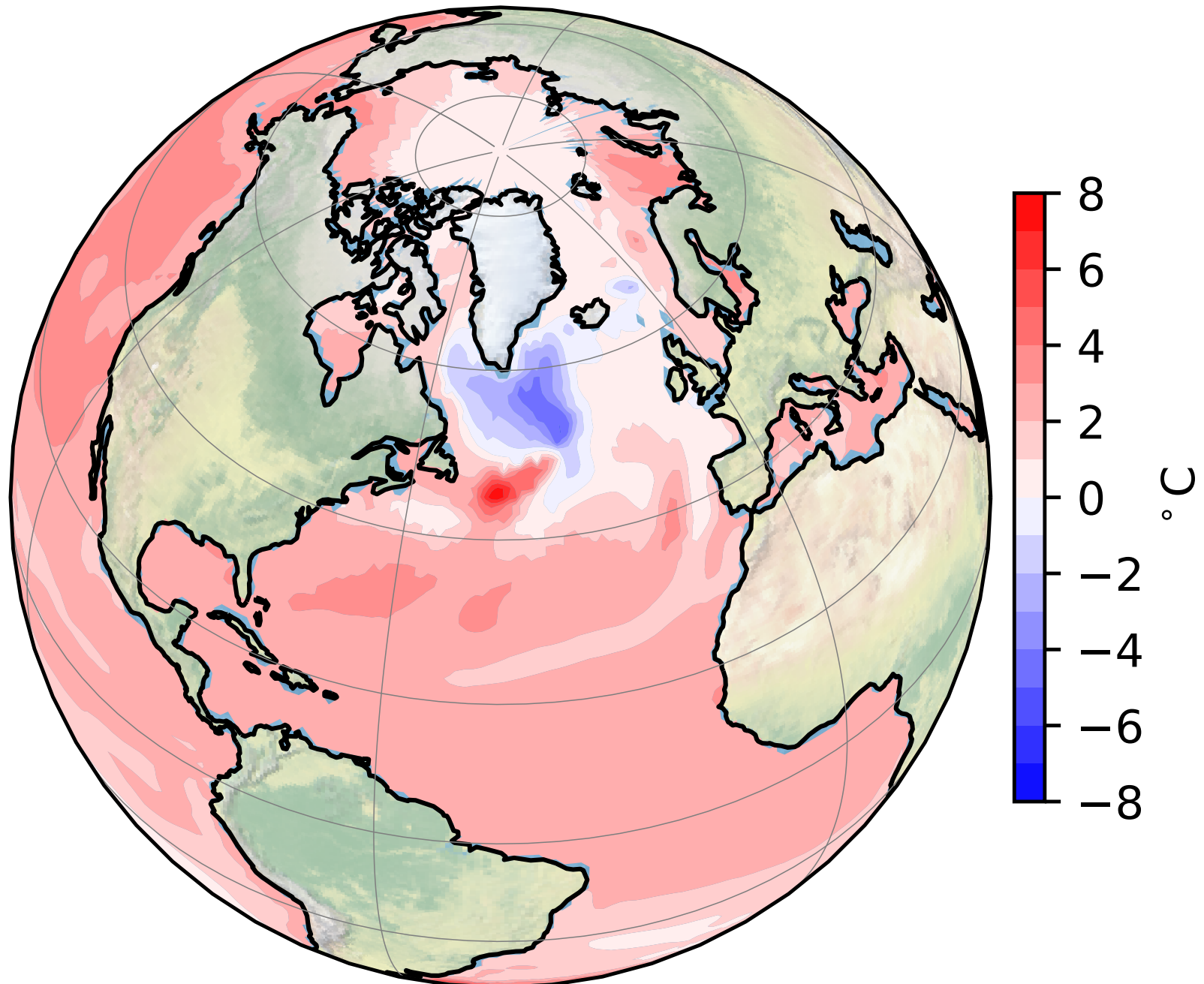
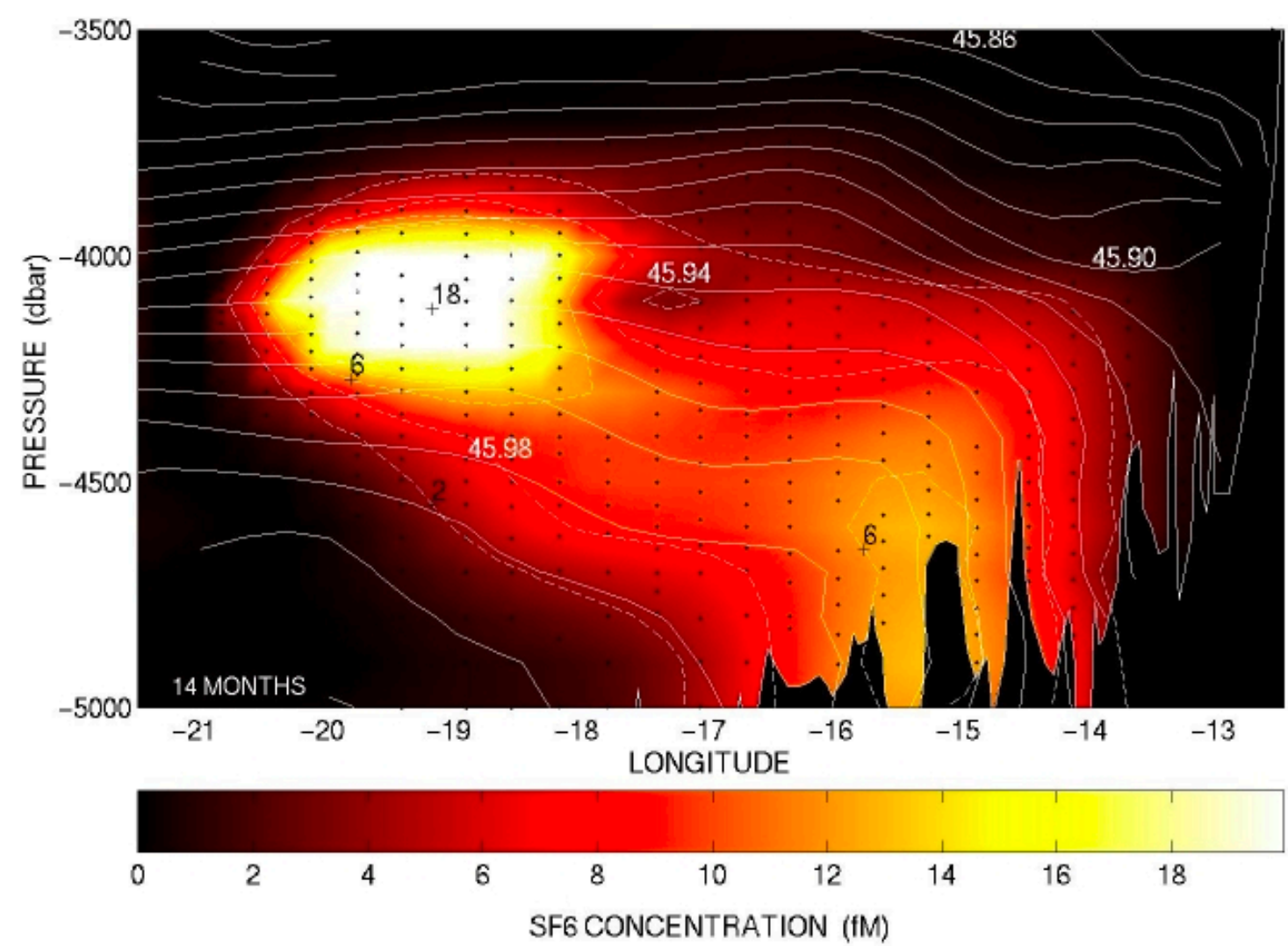


Figure 6.6: SST at 2100 minus that at 2006 in an RCP8.5 scenario.

THC scaling from Vallis showing that the THC/MOC amplitude depends on the vertical mixing

# Ocean diapycnal mixing & rough topography: Brazil basin tracer release experiment



tracer concentration & sigma\_4 from valley where tracer was released obtained in 1997, 14 months after release. dots show sample locations, blue bar labelled 'INJ' shows the location and size of the initial patch. The valley is enclosed by ridges to the north and south whose depths are roughly where the white density contours bend sharply down.

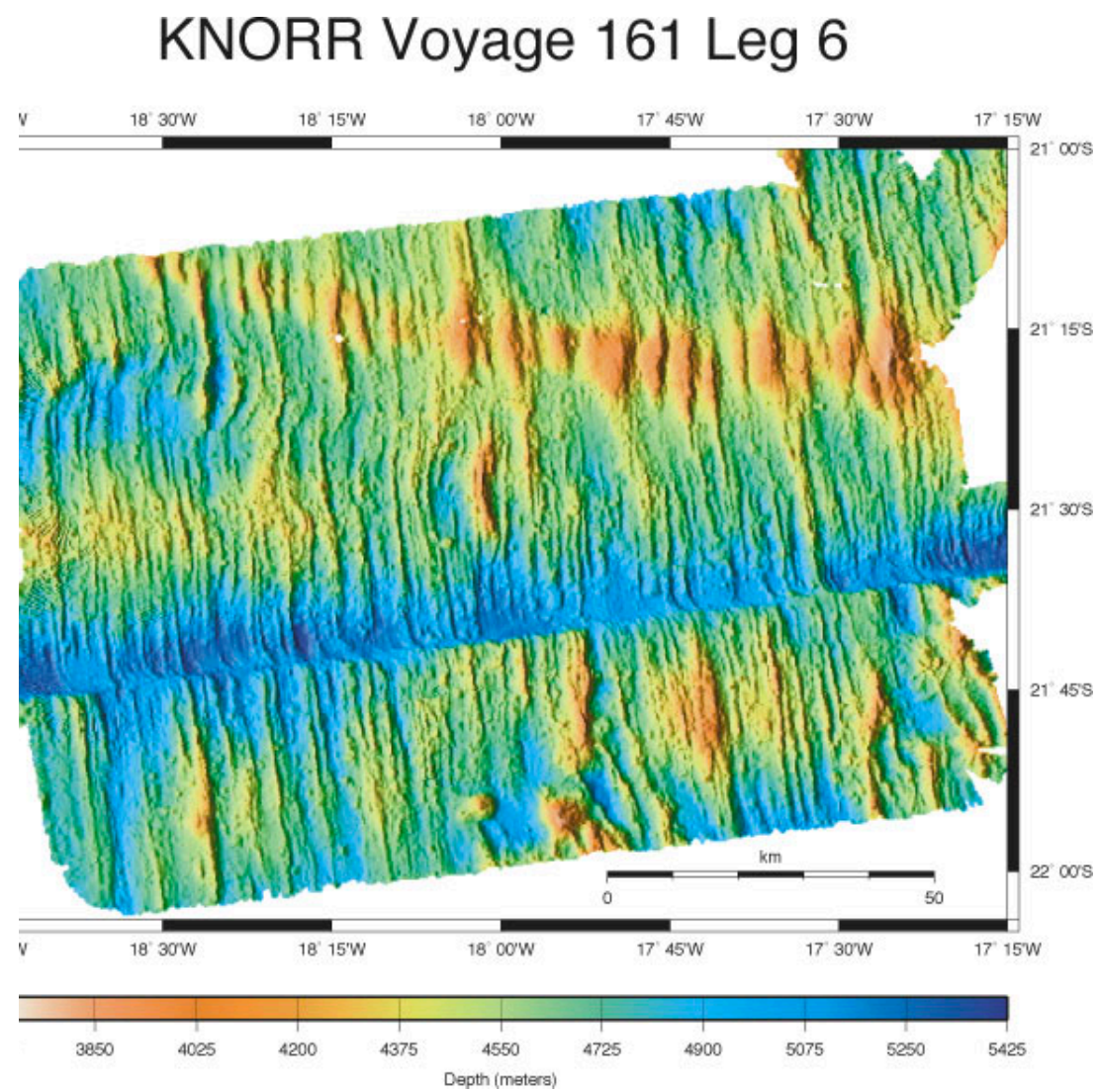


Figure 2. SeaBeam box survey. The shift in the bathymetry on the southern edge of the valley is real, and not an artifact. The tracer was released over this valley at 21.7 S, 18.4 W. The current meter mooring was in the valley to the east of this point at 21.6 S, 17.8 W.

# Ocean diapycnal mixing and tides

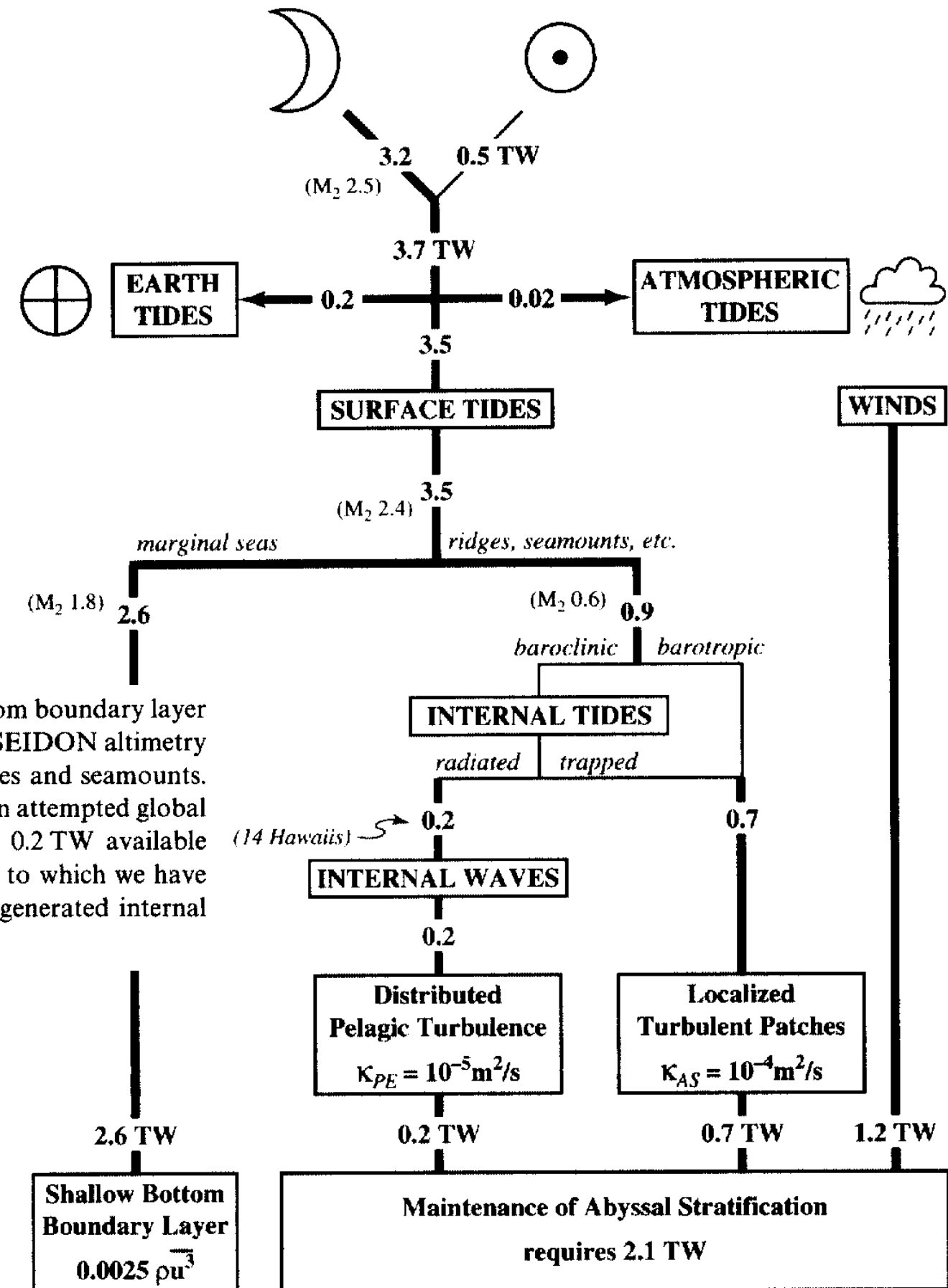
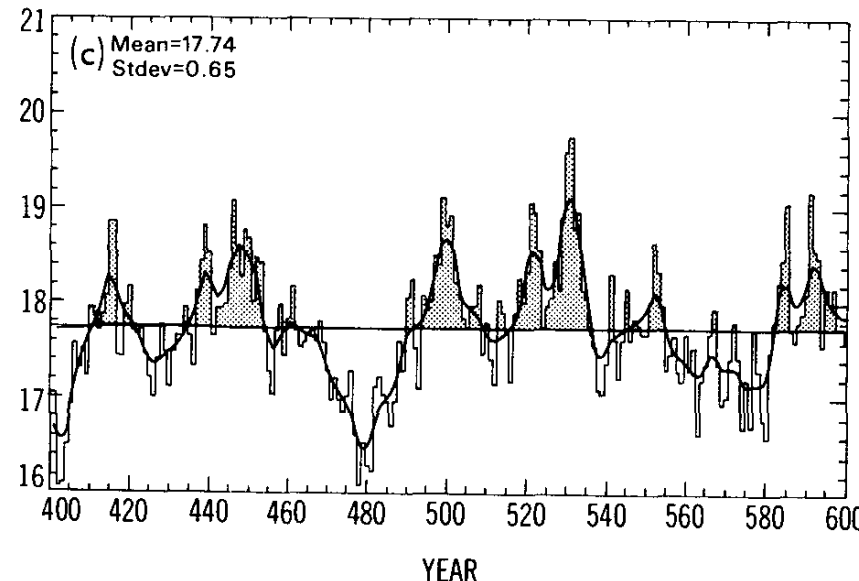
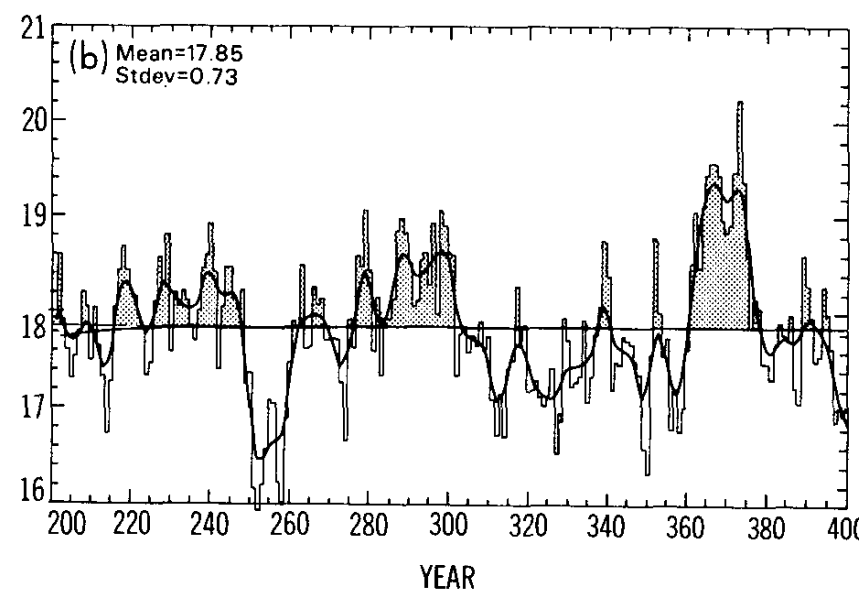
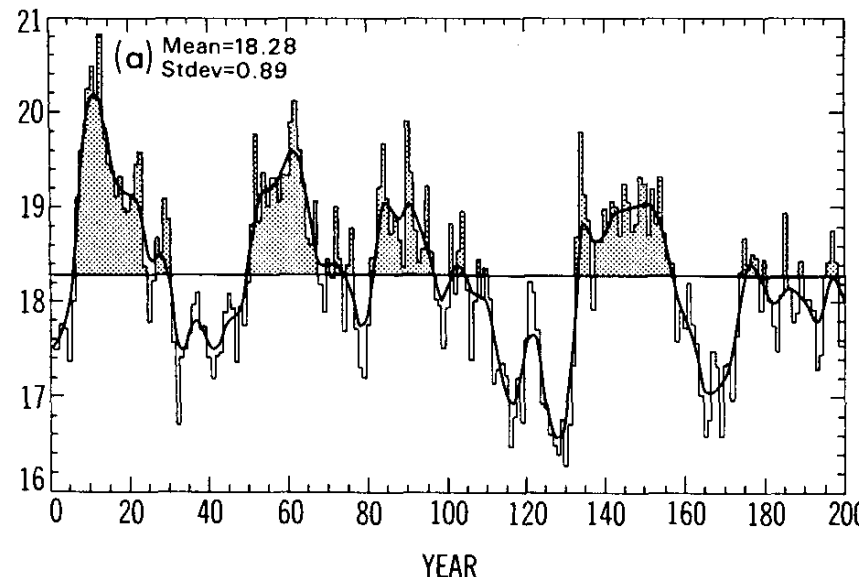


Fig. 4. An impressionistic budget of tidal energy flux. The traditional sink is in the bottom boundary layer (BBL) of marginal seas. Preliminary results from Egbert (1997) based on TOPEX/-POSEIDON altimetry suggest that 0.9 TW (including 0.6 TW of  $M_2$  energy) are scattered at open ocean ridges and seamounts. Light lines represent speculation with no observational support. "14 Hawaiis" refers to an attempted global extrapolation of surface to internal tide scattering measured at Hawaii, resulting in 0.2 TW available for internal wave generation. The wind energy input is estimated from Wunsch (1998), to which we have added 0.2 TW to balance the energy budget. This extra energy is identified as wind-generated internal waves — radiating into the abyss and contributing to mixing processes.

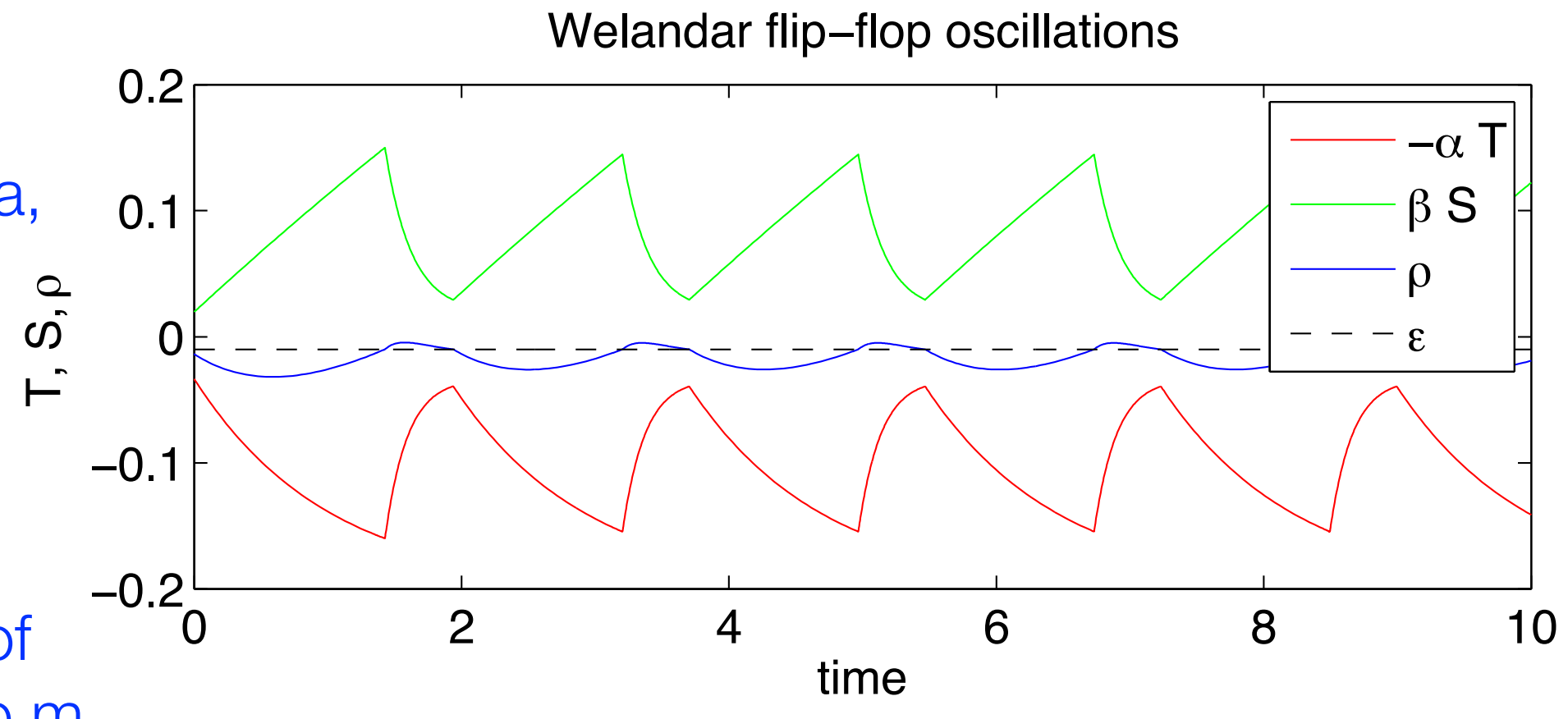
# AMOC variability



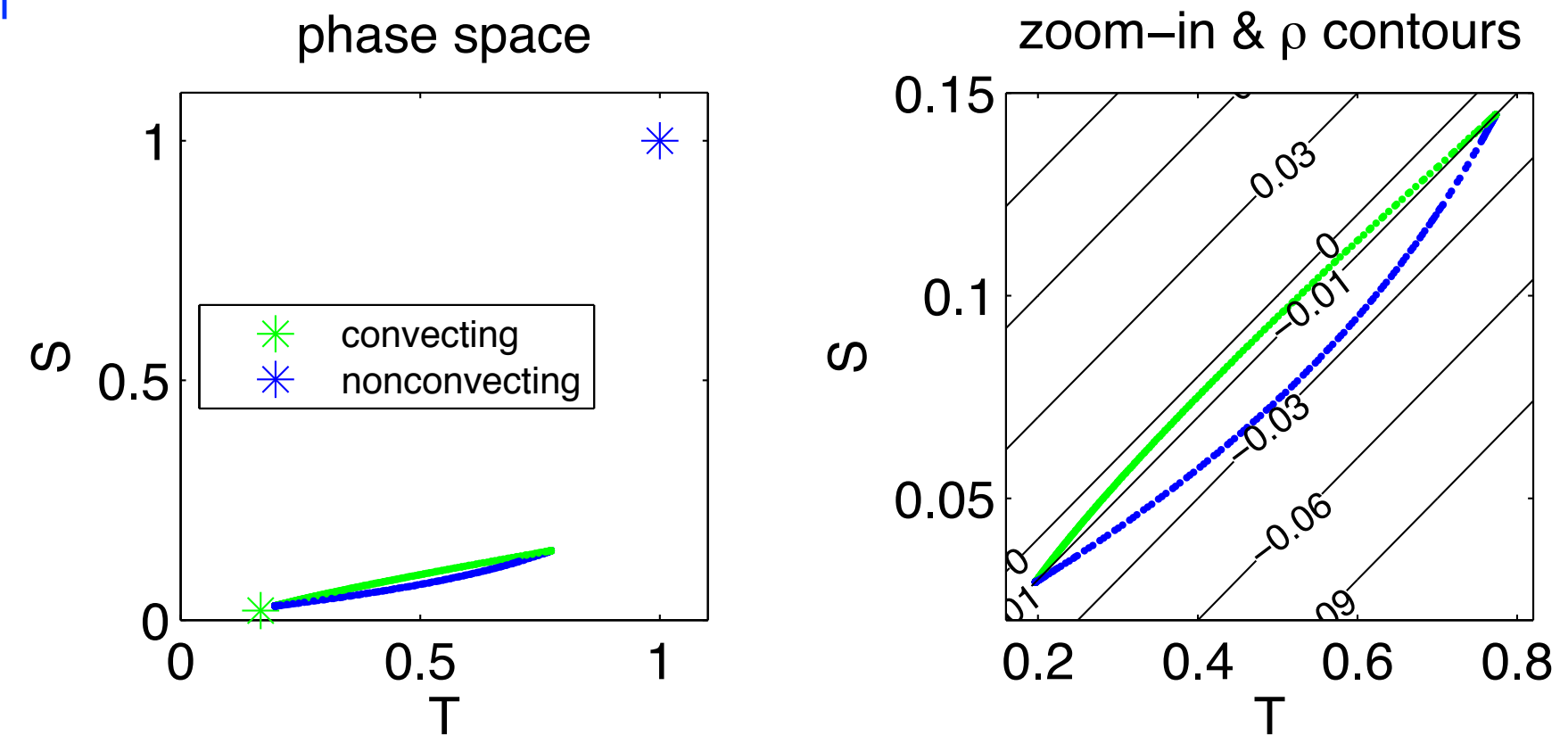
A winter scene in Europe's Little Ice Age, 14th Century  
Pieter Breugel the Elder.

# AMOC: self-sustained variability

1. Flip-flop oscillations  
 (Welander1982; Dijkstra, 2000, section 6.2.3);

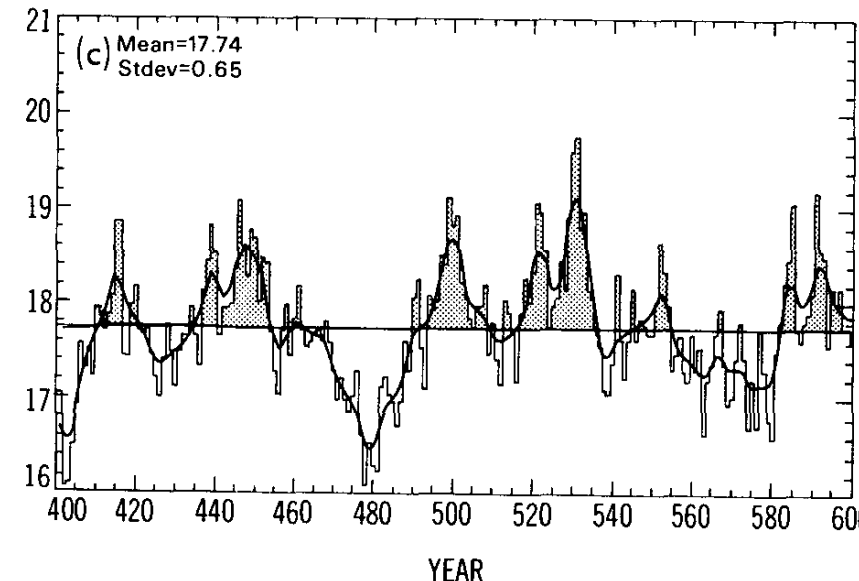
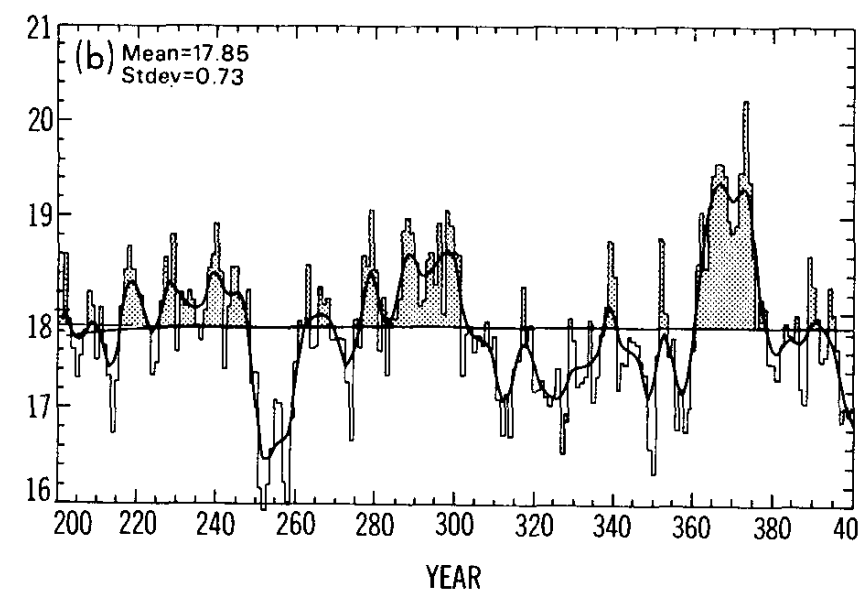
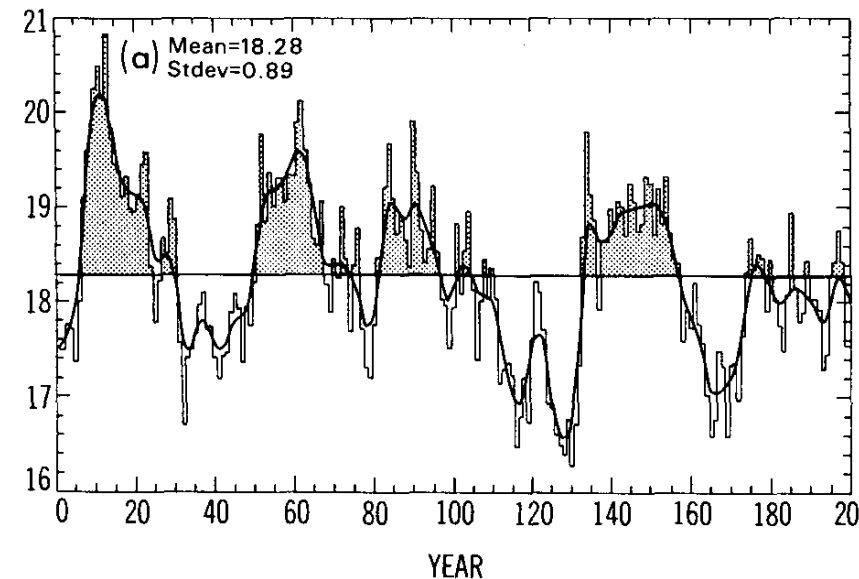


2. Figure here: results of  
 Welander1982\_flip\_flop.m



3. Relaxation  
 oscillations, Strogatz  
 (1994) example 7.5.1  
 pp 212-213.

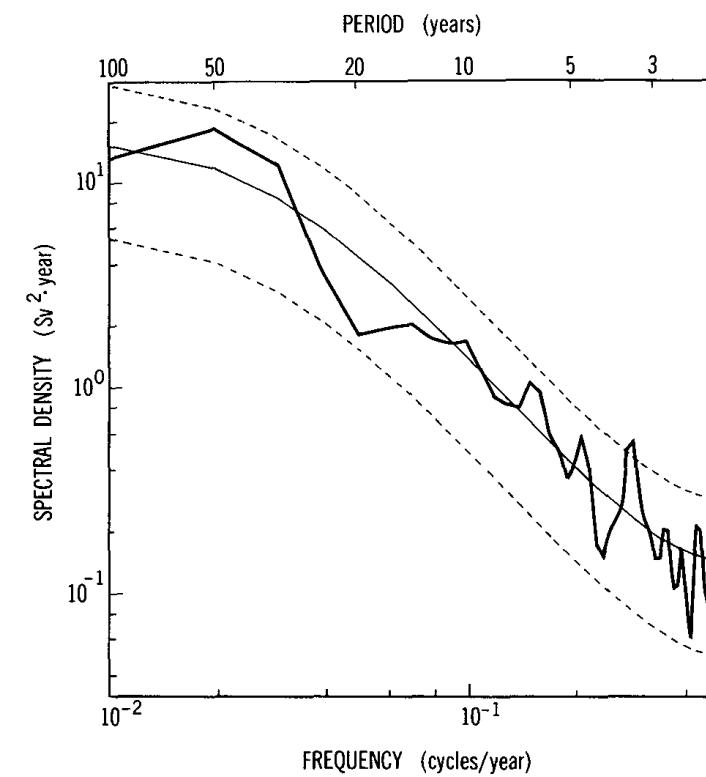
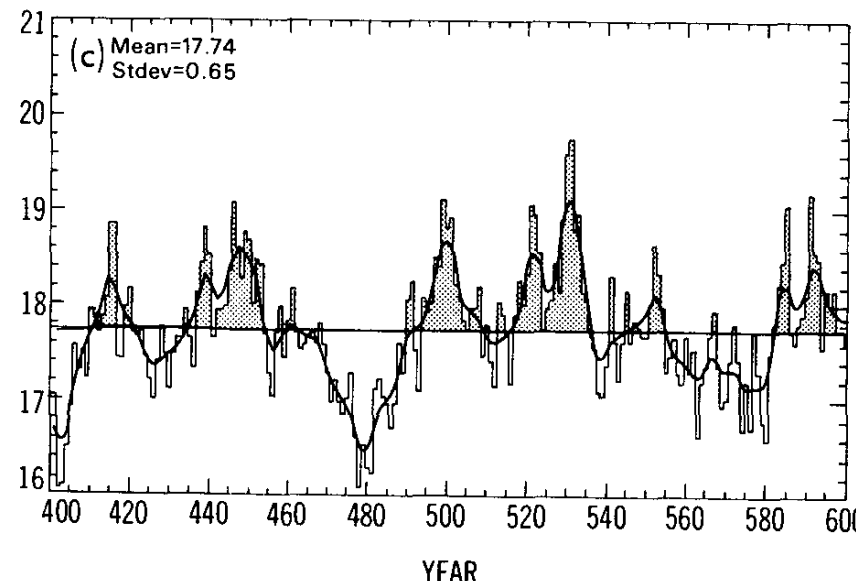
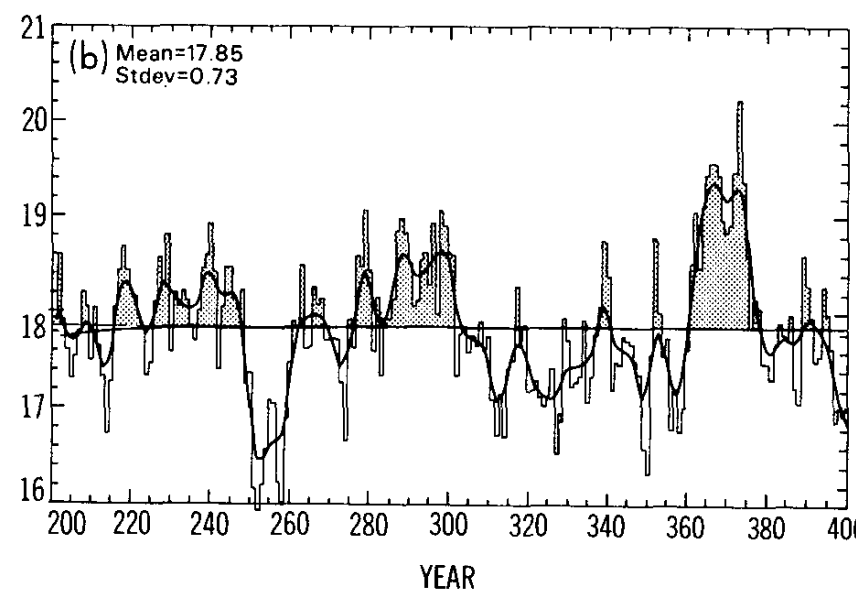
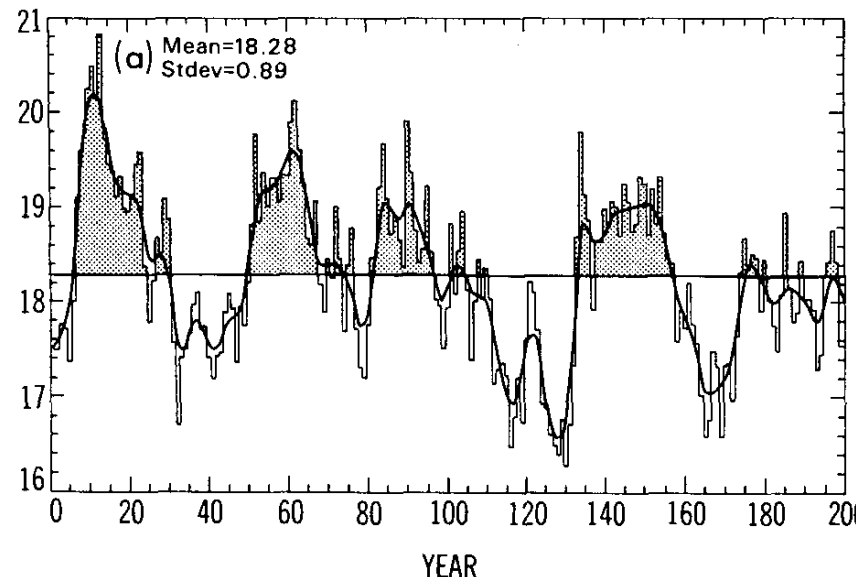
# AMOC: stochastic variability



Proposed mechanism: feedback between SST and wind...

Delworth, Manabe and Stouffer 19933

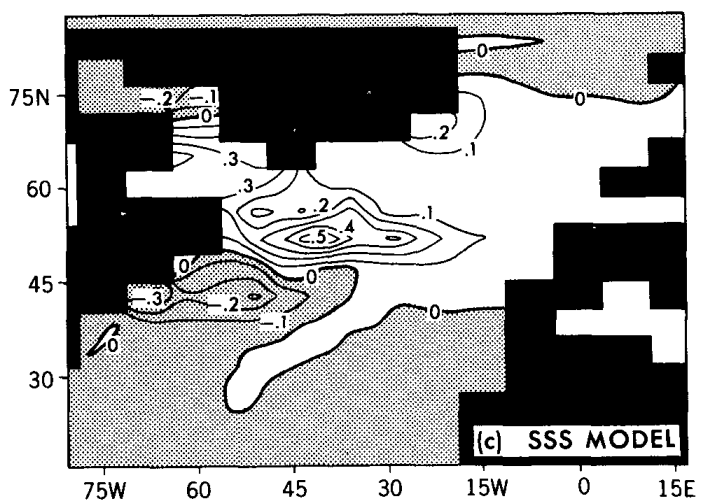
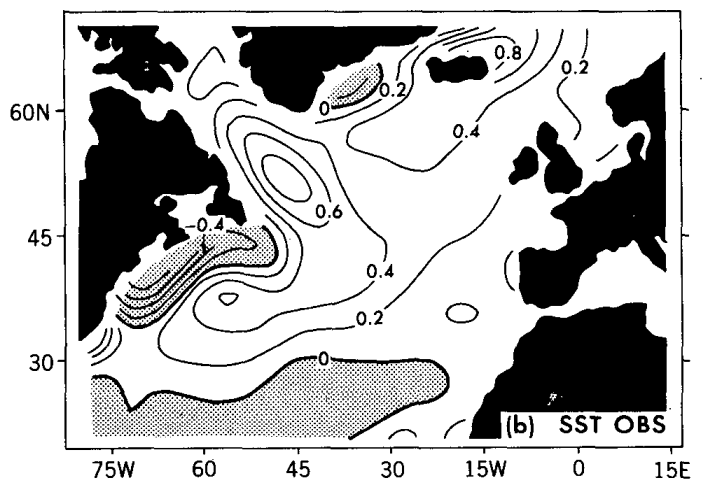
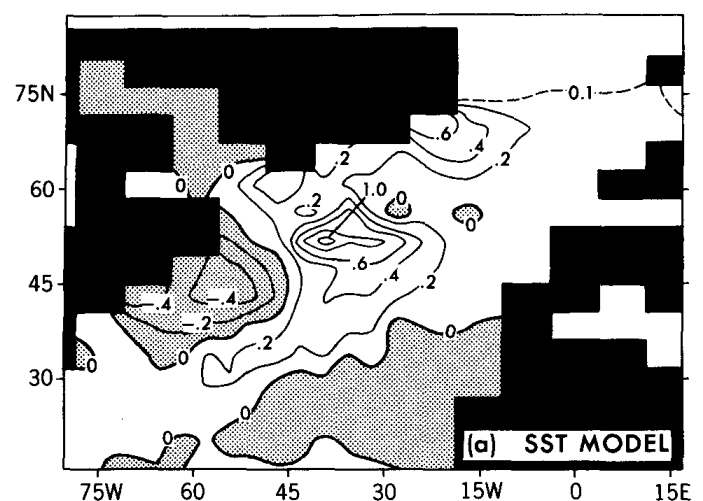
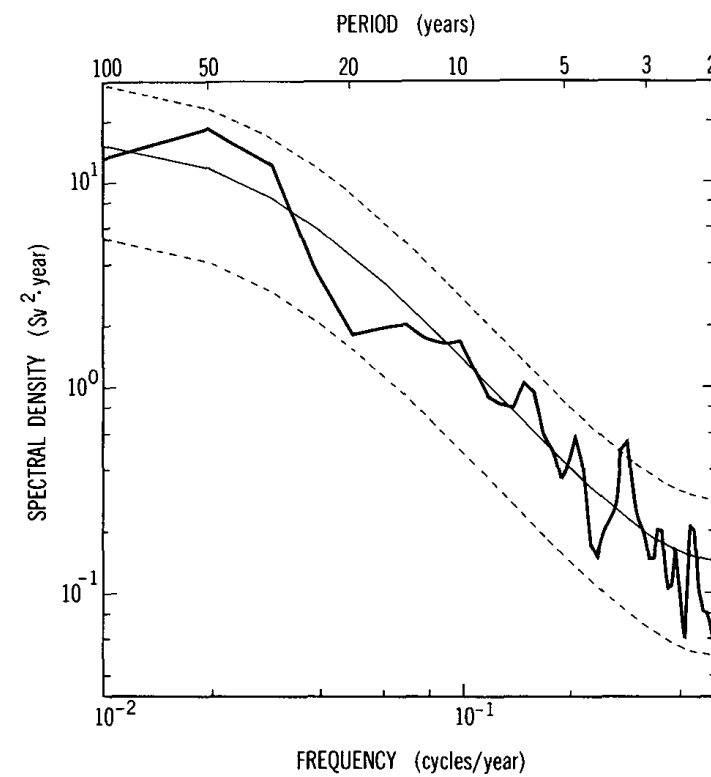
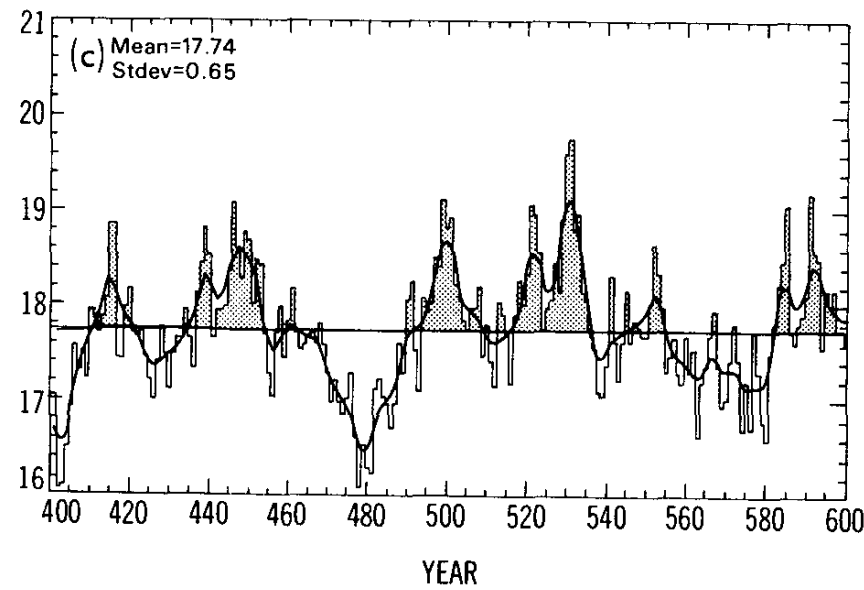
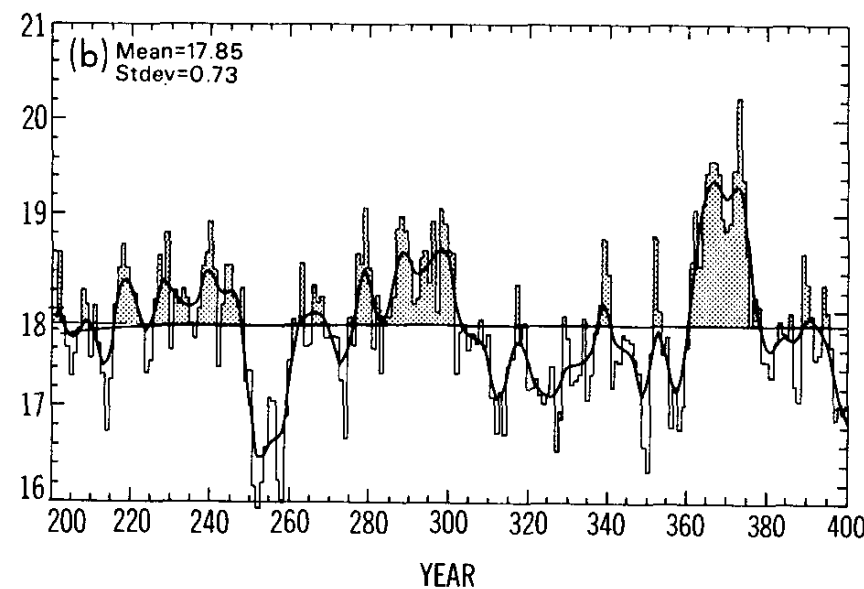
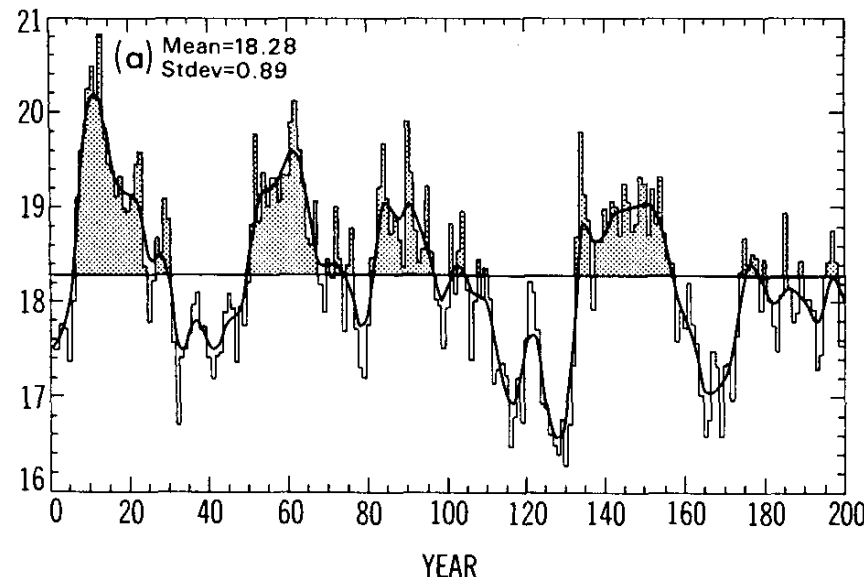
# AMOC: stochastic variability



Proposed mechanism: feedback between SST and wind...

Delworth, Manabe and Stouffer 19933

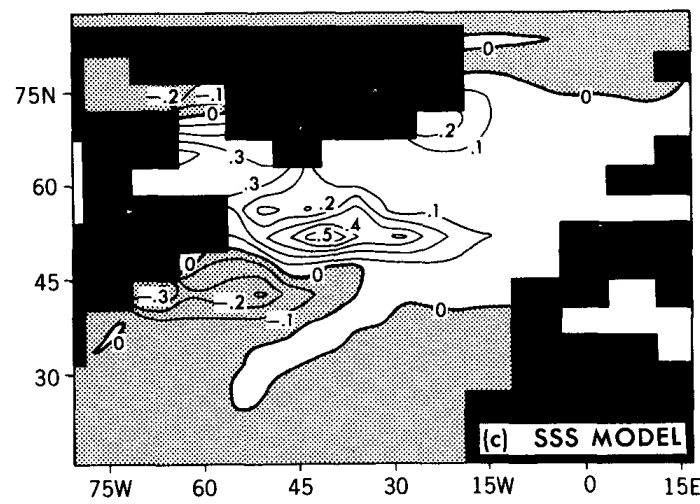
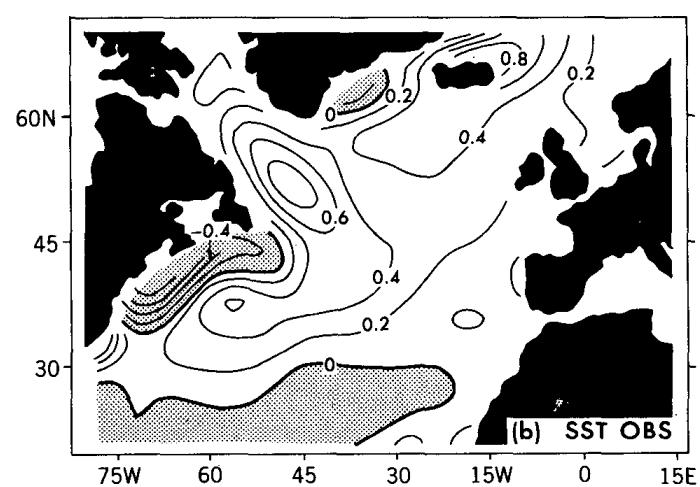
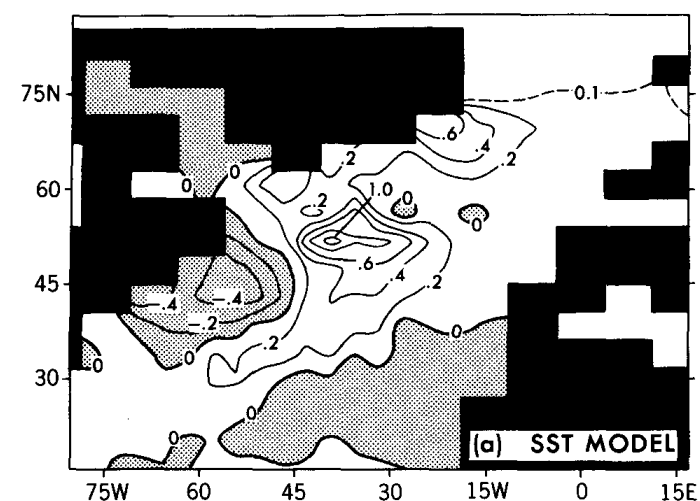
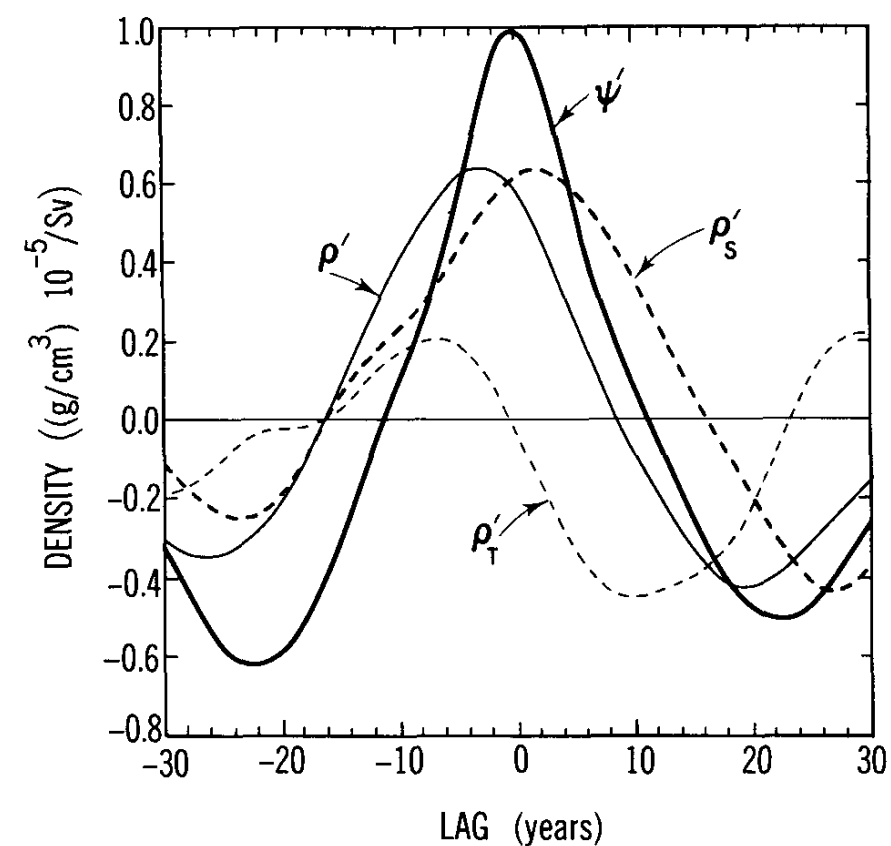
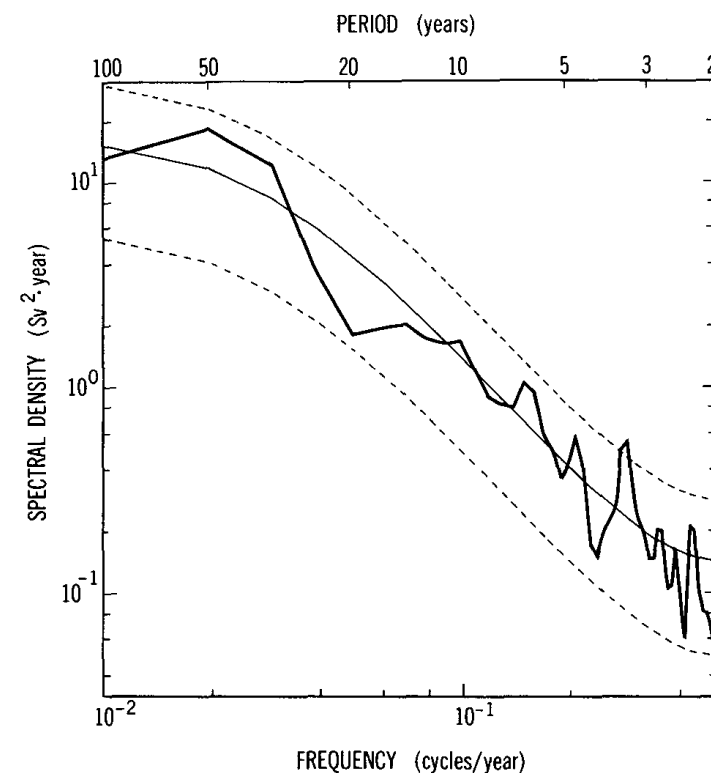
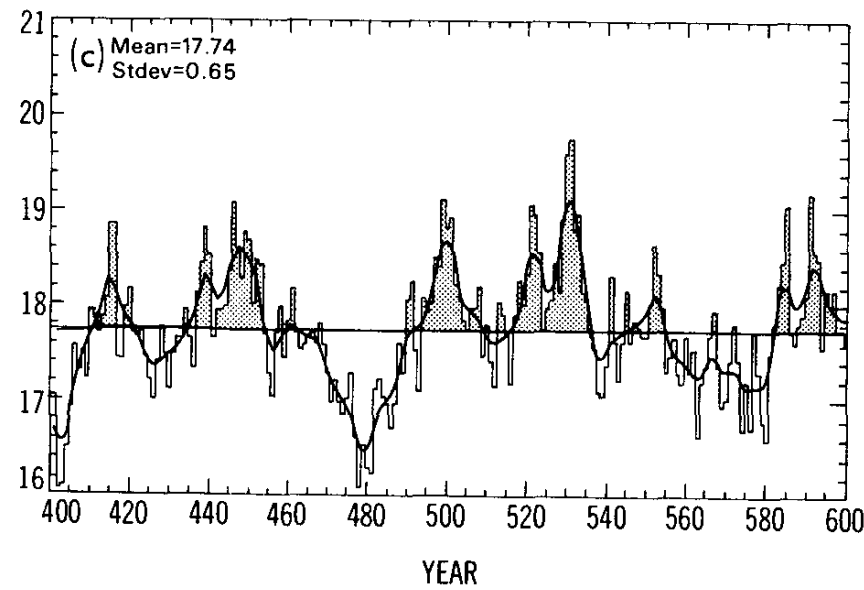
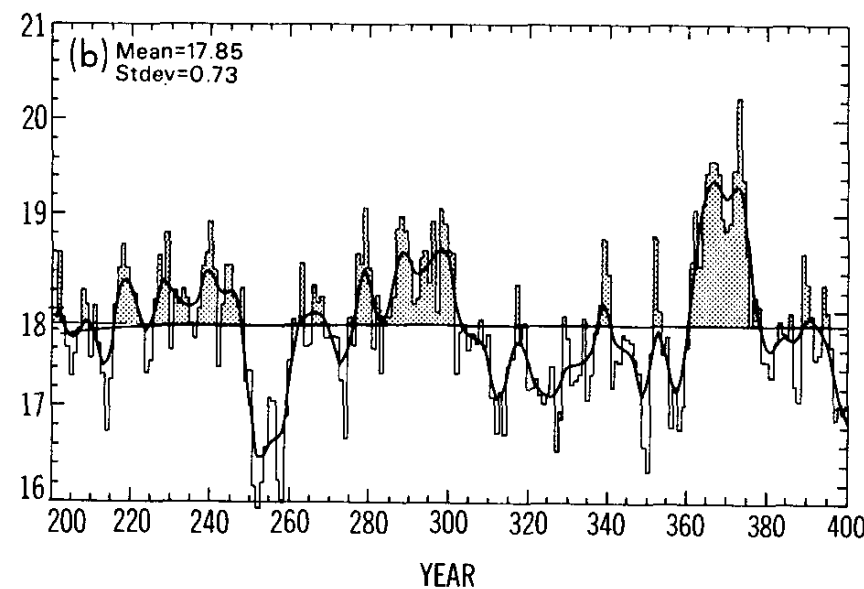
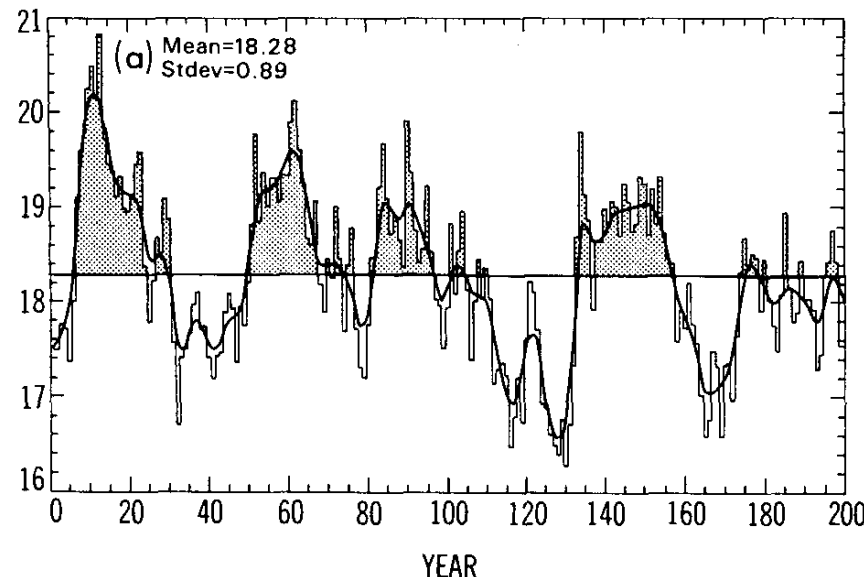
# AMOC: stochastic variability



Proposed mechanism: feedback between SST and wind...

Delworth, Manabe and Stouffer 19933

# AMOC: stochastic variability



Proposed mechanism: feedback between SST and wind...

Delworth, Manabe and Stouffer 19933

# AMOC: stochastic variability

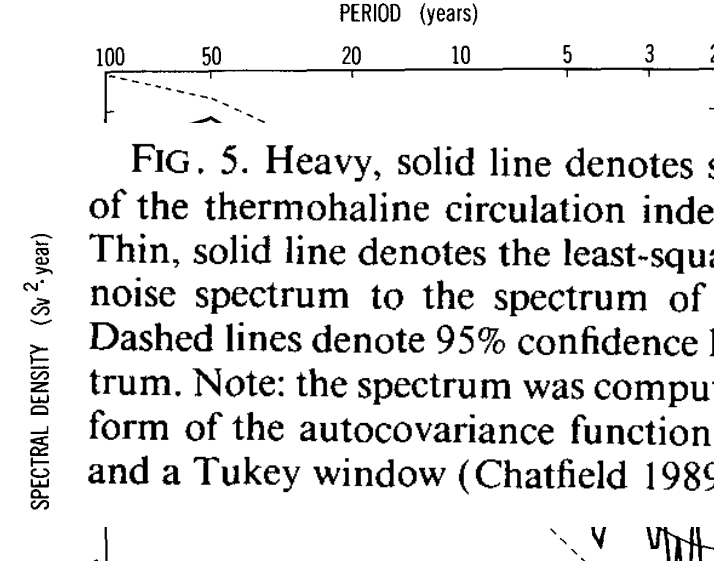
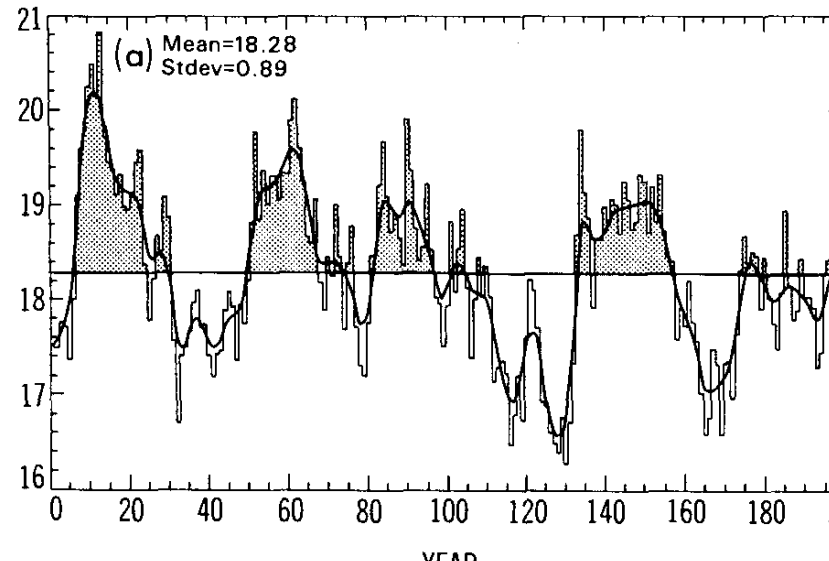


FIG. 4. Time series of the annual-mean intensity of the index of the meridional overturning in the North Atlantic. Units are Sverdrups ( $10^6 \text{ m}^3 \text{ s}^{-1}$ ). Heavy, solid line is a smoothed time series computed by applying a 13-point binomial filter to the annual-mean data (approximately a 10-year low-pass filter). (a) Years 1–200, (b) years 201–400, (c) years 401–600.

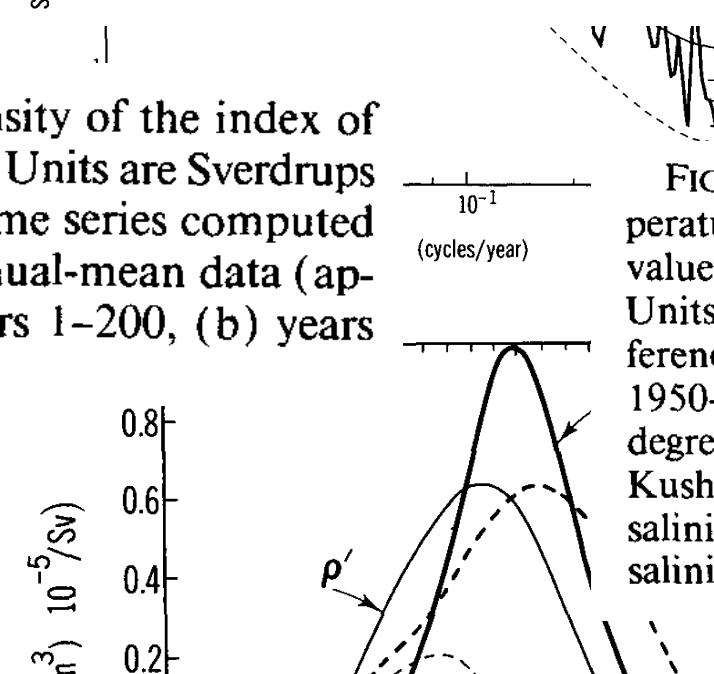
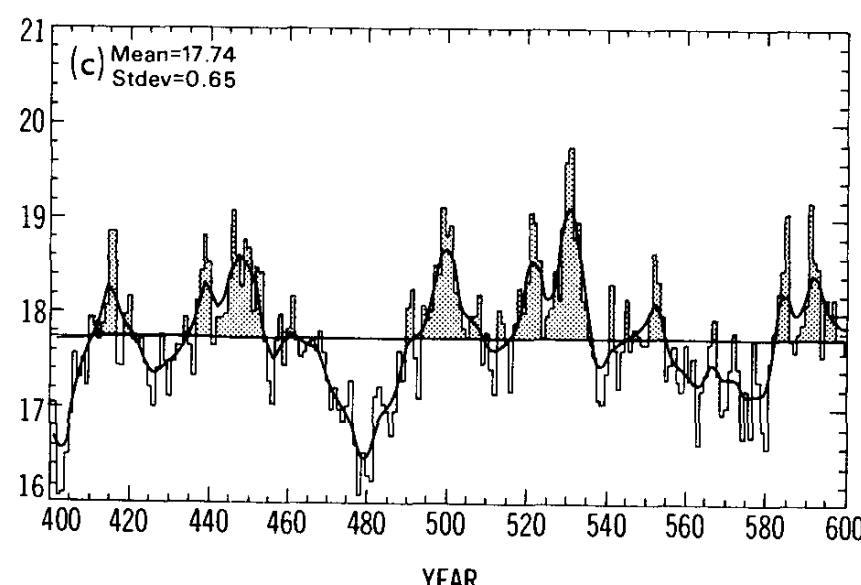
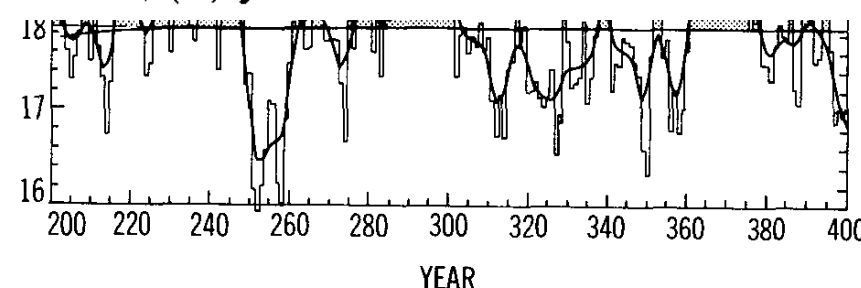


FIG. 6. (a) Differences in annual-mean model sea surface temperature between four decades with anomalously large THC index values and four decades with anomalously small THC index values. Units are degrees Celsius. Values less than zero are stippled. (b) Differences in observed sea surface temperature between the periods 1950–1964 (warm period) and 1970–1984 (cold period). Units are degrees Celsius. Values less than zero are stippled (adapted from Kushnir 1993). (c) Differences in annual-mean model sea surface salinity, computed in the same manner as (a). Units are practical salinity units.

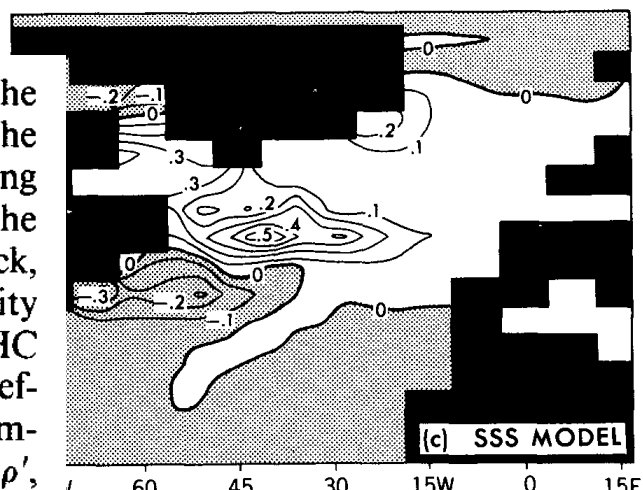
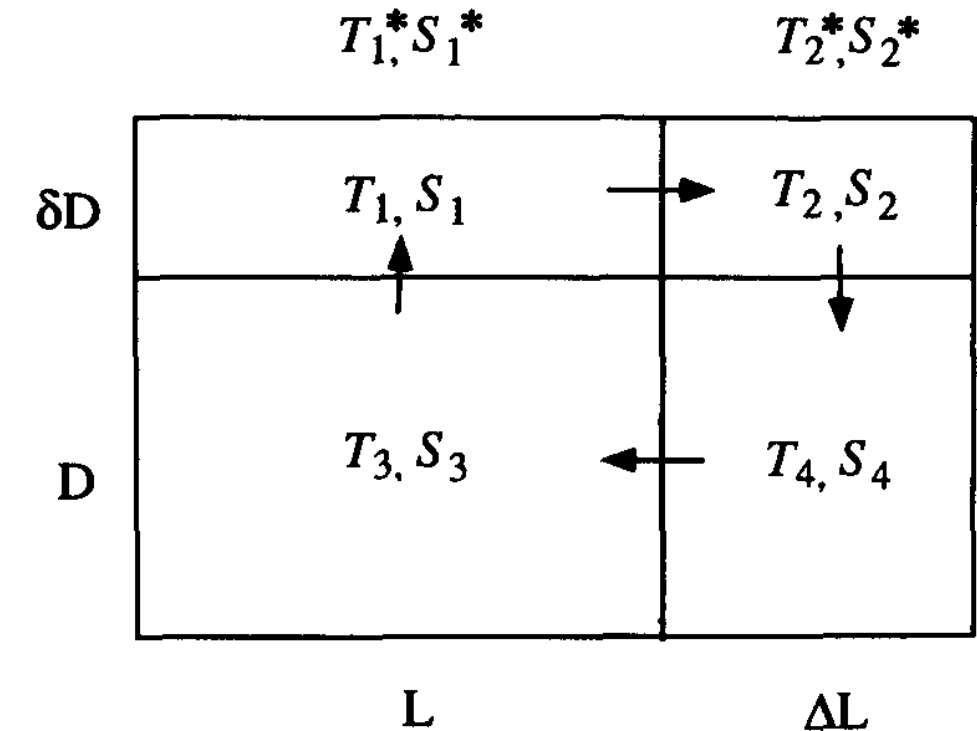


FIG. 8. Regression coefficients between various quantities and the time series of the THC index. The heavy, solid line ( $\psi'$ ) denotes the regression coefficients of the THC index with itself (thus representing a “typical” fluctuation). The thin, solid line ( $\rho'$ ) represents the regression coefficients between density and the THC index. The thick, dashed line ( $\rho'_S$ ) denotes the regression coefficients for the density changes attributable solely to changes in salinity versus the THC index, while the thin, dashed line ( $\rho'_T$ ) represents the regression coefficients for the density changes attributable solely to changes in temperature versus the THC index. The regression coefficients for  $\rho'$ ,  $\rho'_S$ , and  $\rho'_T$  were averaged vertically and horizontally over the sinking region.

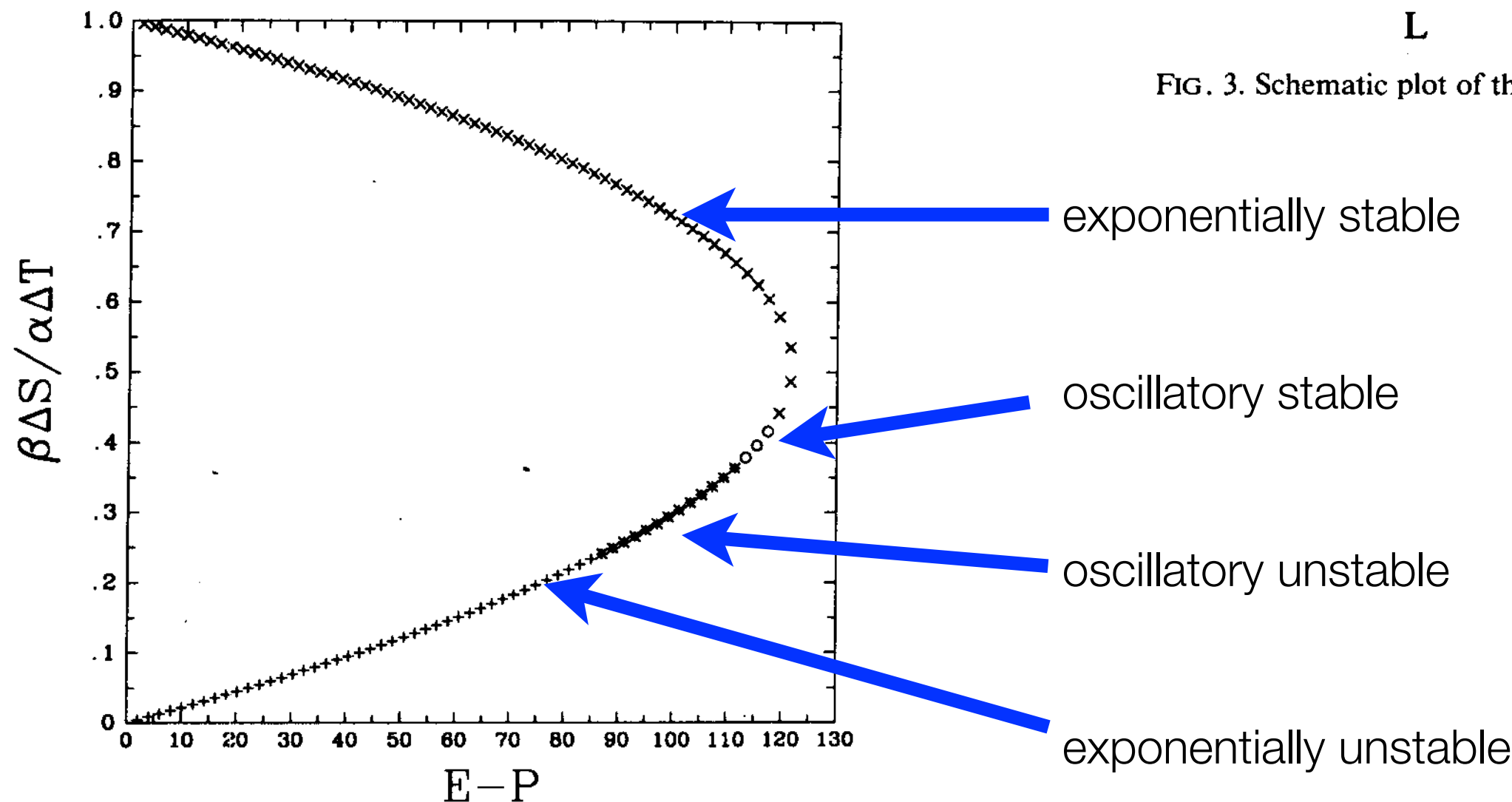
Proposed mechanism: feedback between SST and wind...

Delworth, Manabe and Stouffer 19933

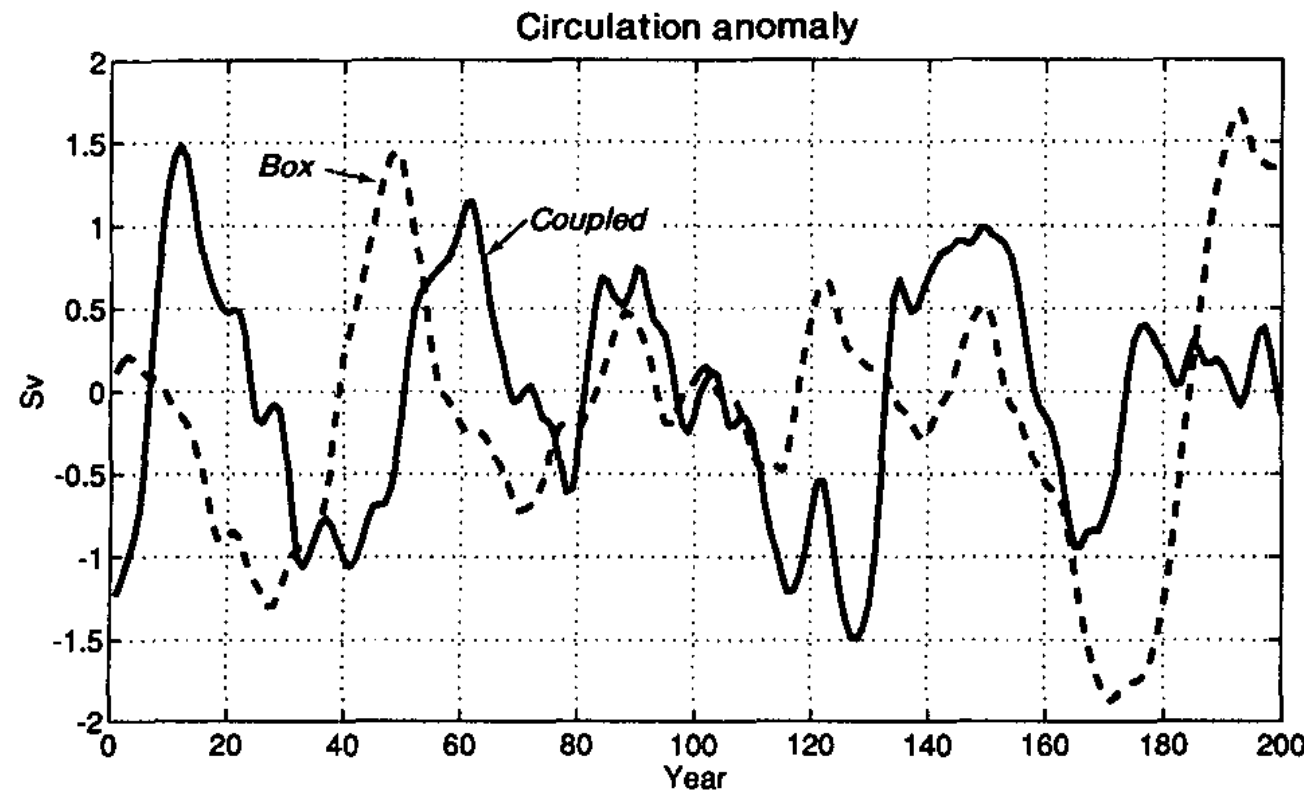
# AMOC: stochastic variability, stability regimes of box model



(a) Stability regimes under mixed b.c.

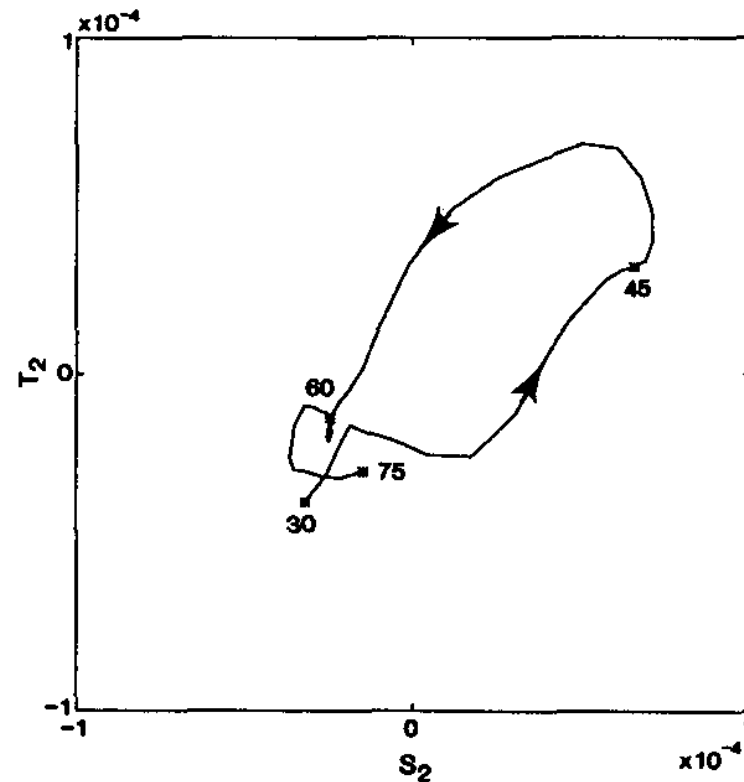
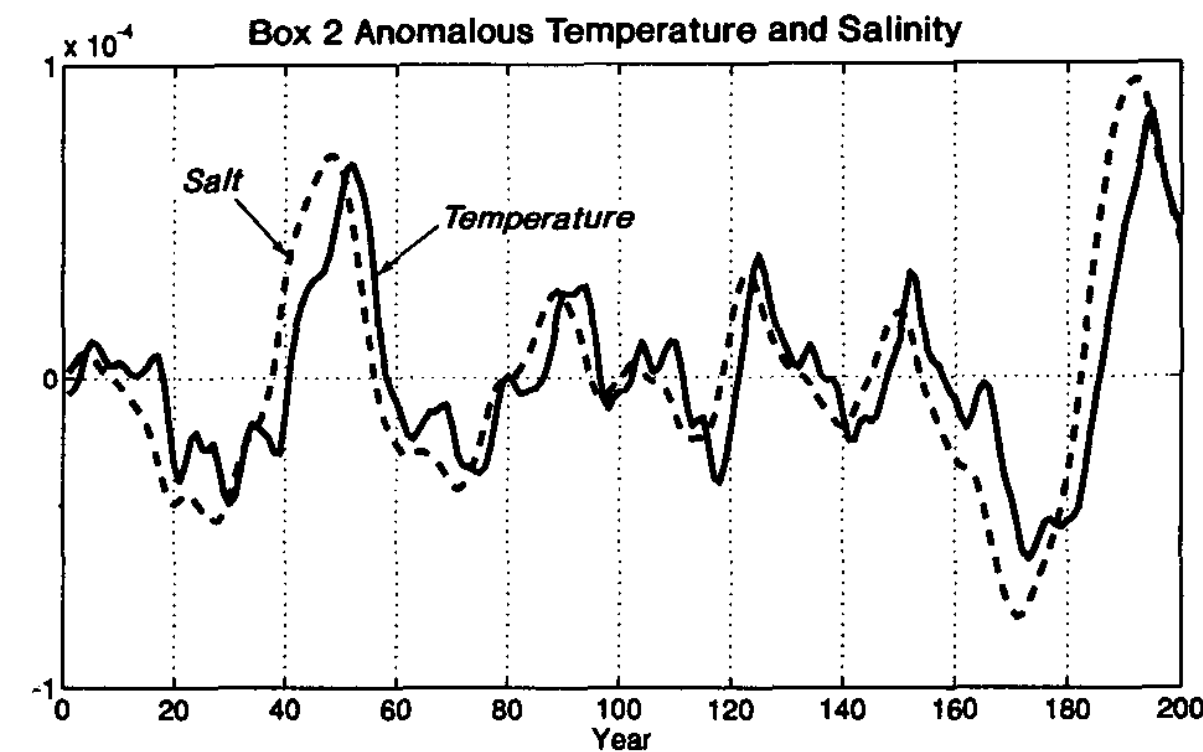
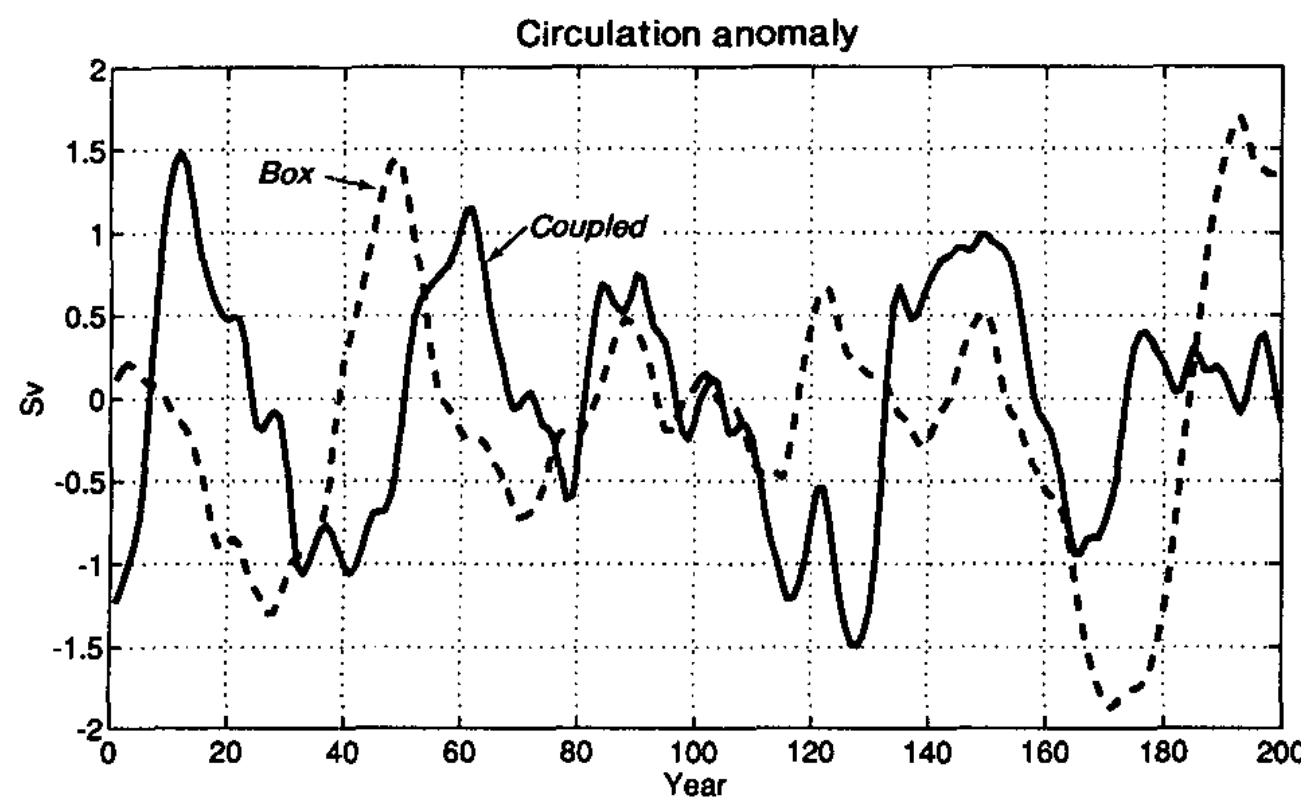


# AMOC: stochastic excitation of damped oscillatory mode



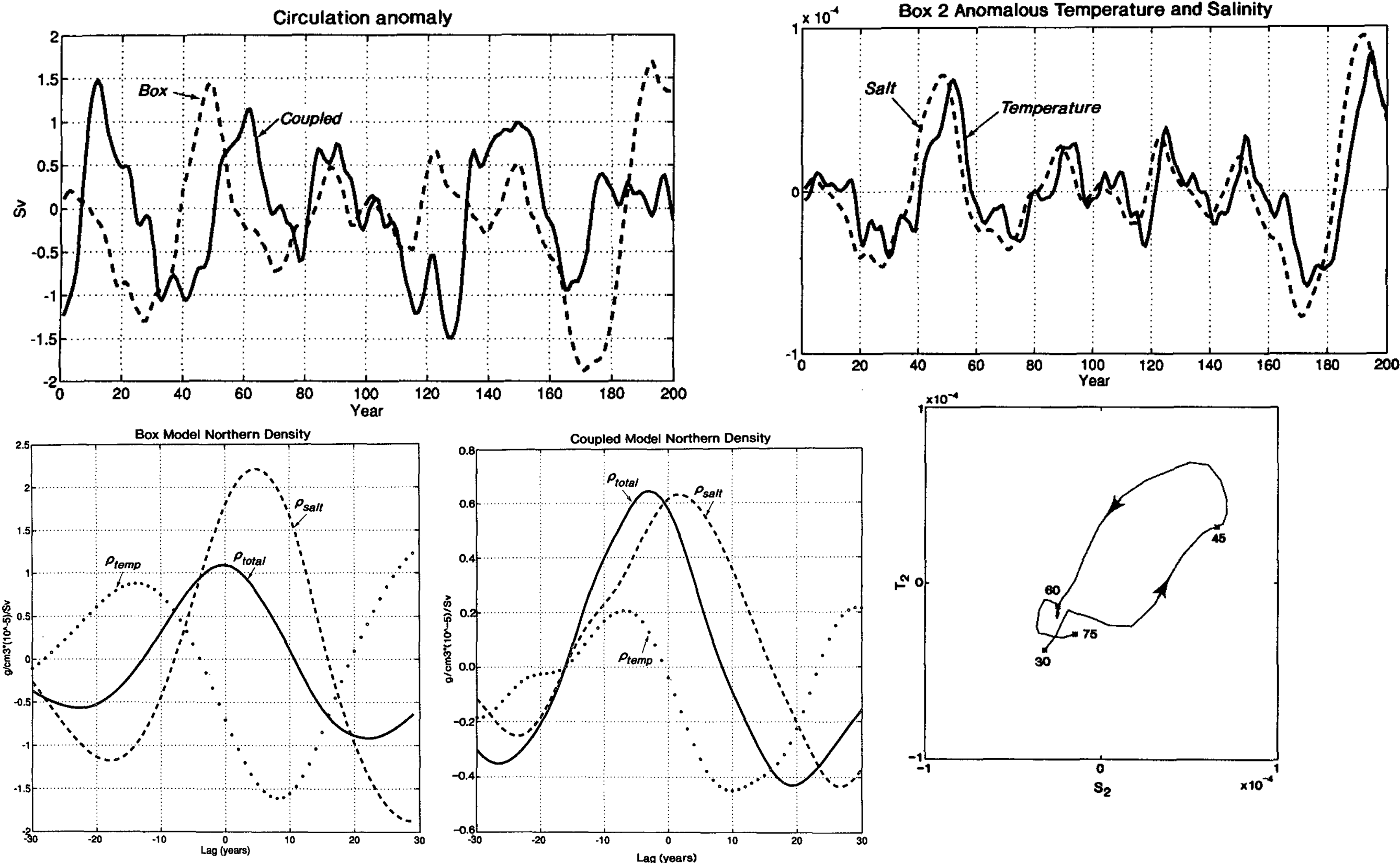
Purely stochastic forcing of a damped oscillatory mode fits GCM results

# AMOC: stochastic excitation of damped oscillatory mode



Purely stochastic forcing of a damped oscillatory mode fits GCM results

# AMOC: stochastic excitation of damped oscillatory mode



Purely stochastic forcing of a damped oscillatory mode fits GCM results

# AMOC: stochastic excitation of damped oscillatory mode

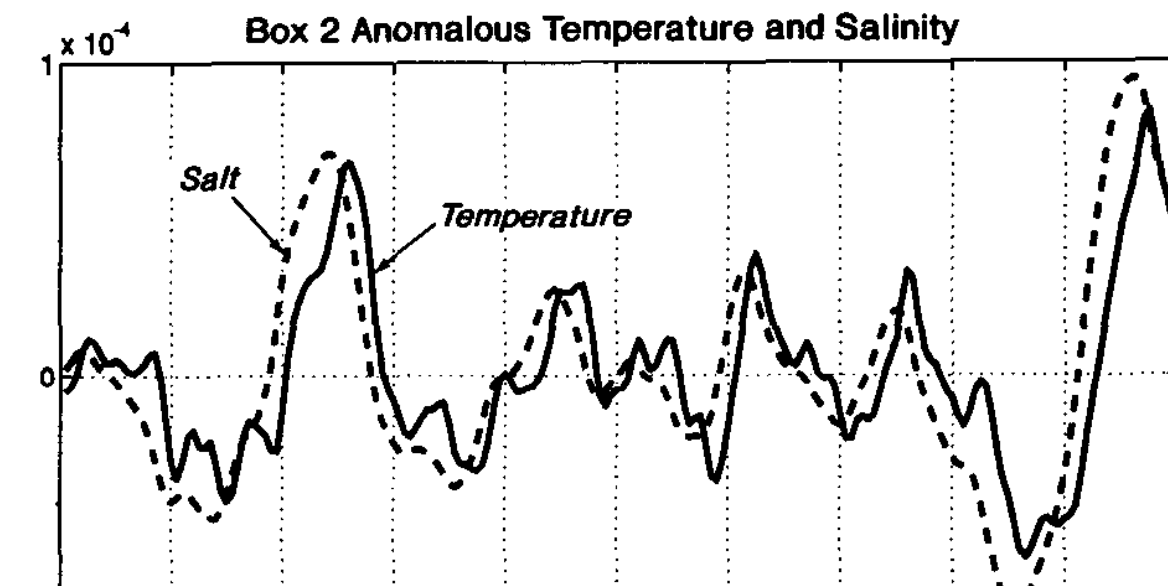
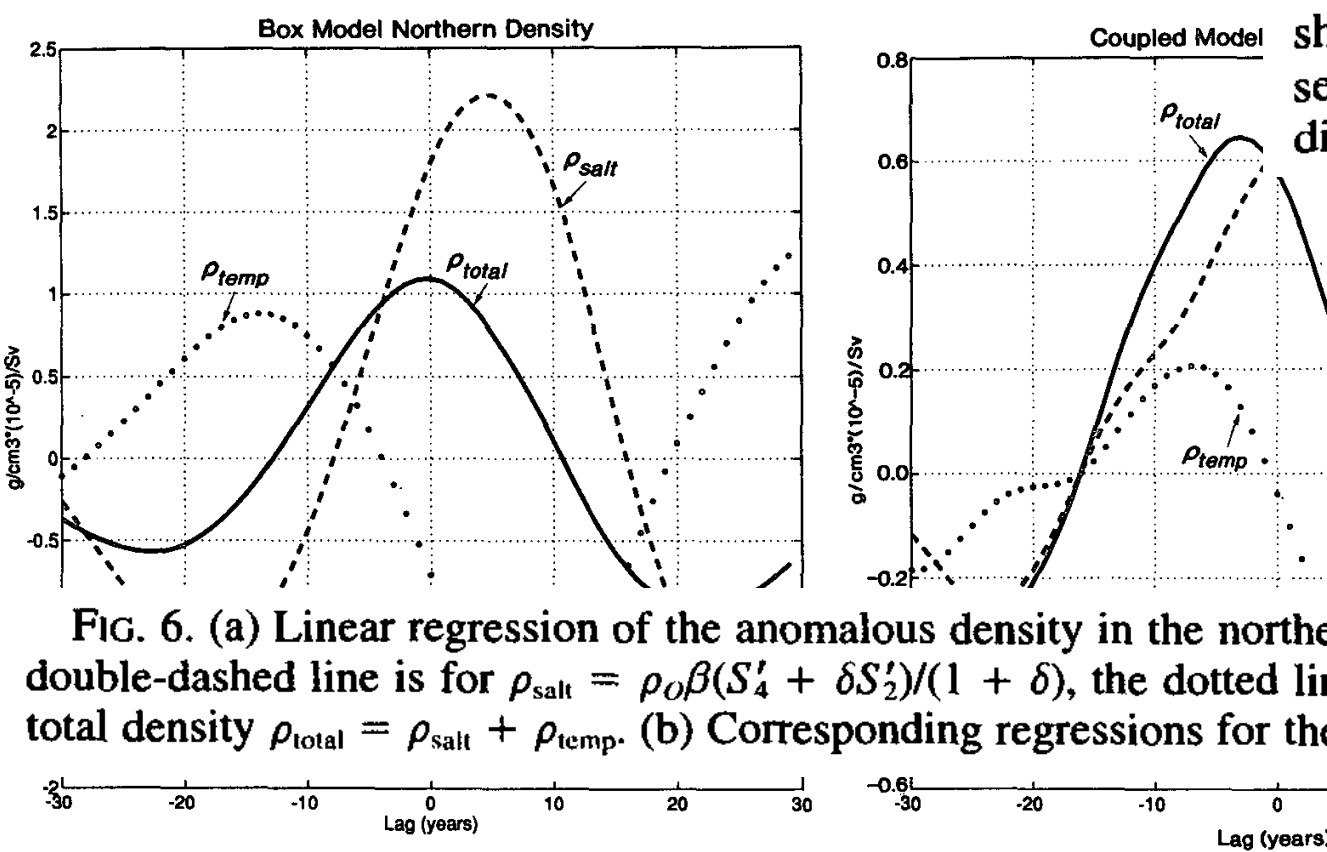
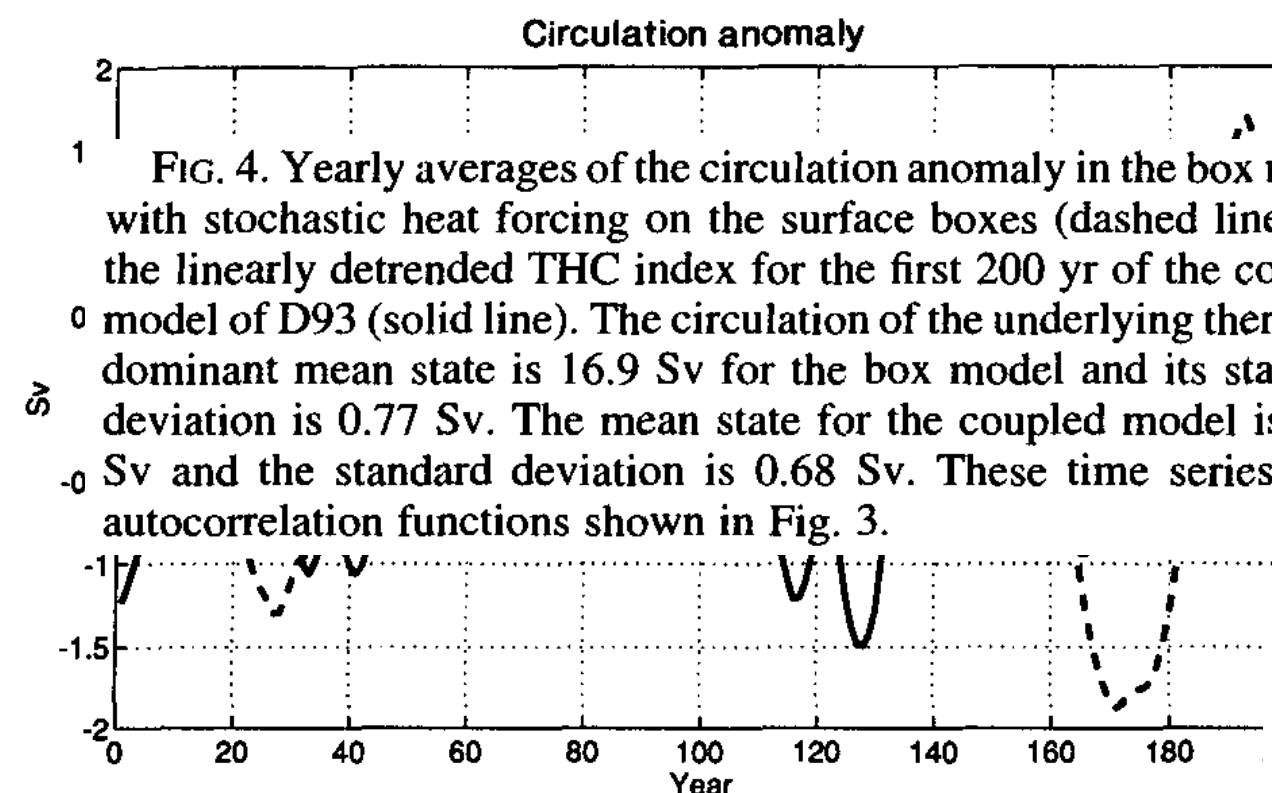
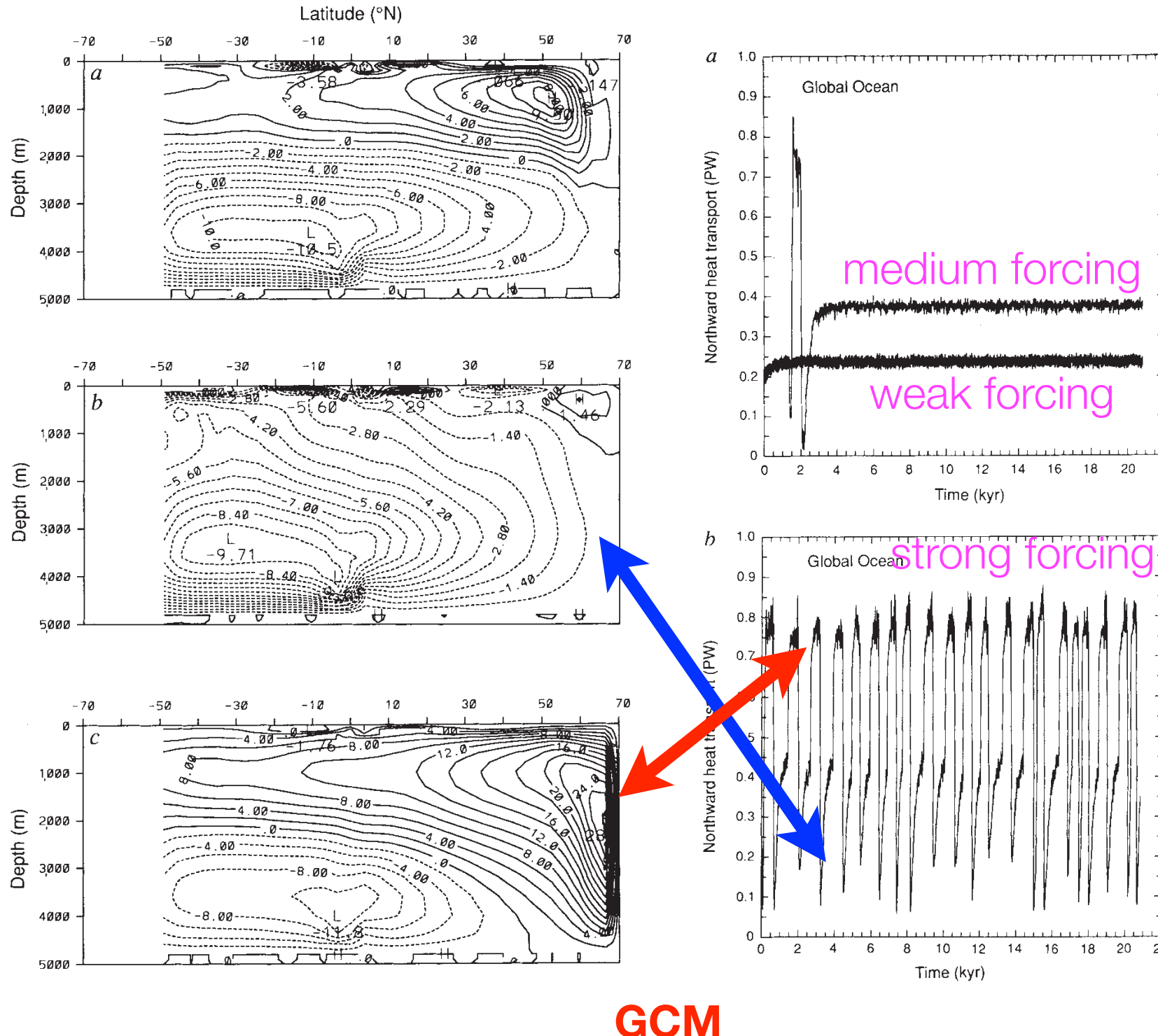


FIG. 5. (a) Dimensionless temperature anomaly  $\alpha T'_2$  (solid line) and salinity anomaly  $\beta S'_2$  (dashed line) for the northern surface box (box 2) in the box model with surface stochastic forcing. Note the phase relation (salt leads temperature) indicative of the oscillating mode shown in Fig. 2. (b) The  $(\beta S'_2, \alpha T'_2)$  plane for years 30–70 of (a) with selected years indicated. The trajectory is in the counterclockwise direction since salt leads temperature.

Purely stochastic forcing of a damped oscillatory mode fits GCM results

notes: Hasselmann and then a second order oscillator  
driven by noise, see course notes

# AMOC: stochastic forcing of jumps between steady states

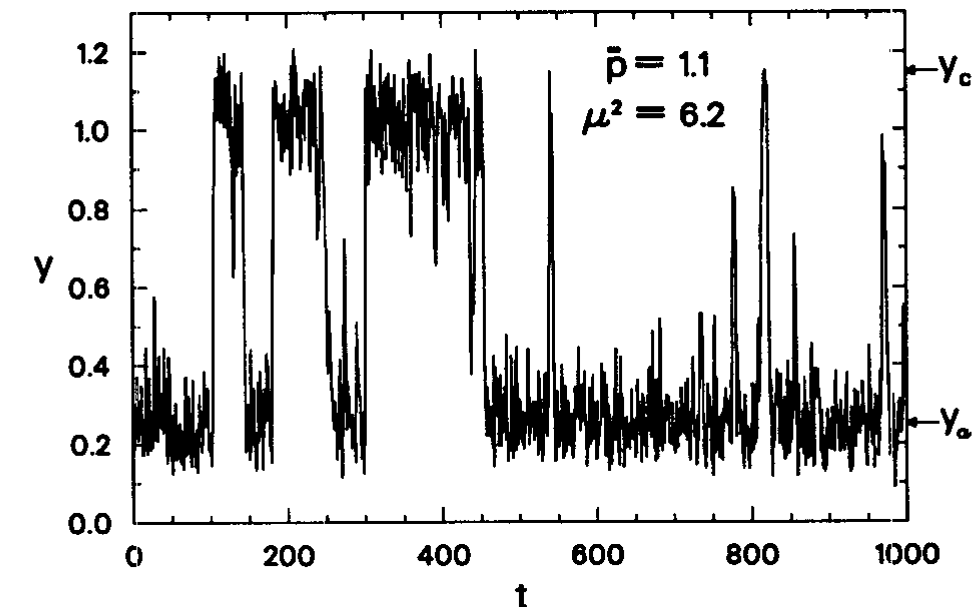
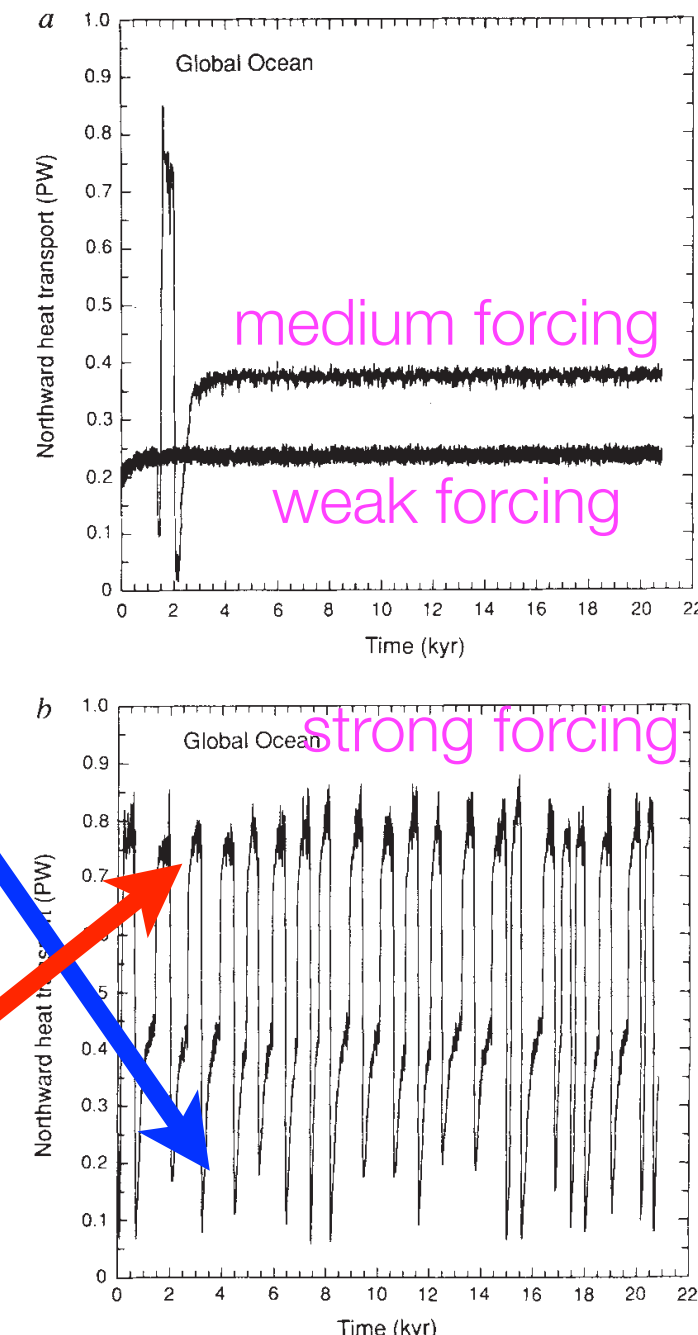
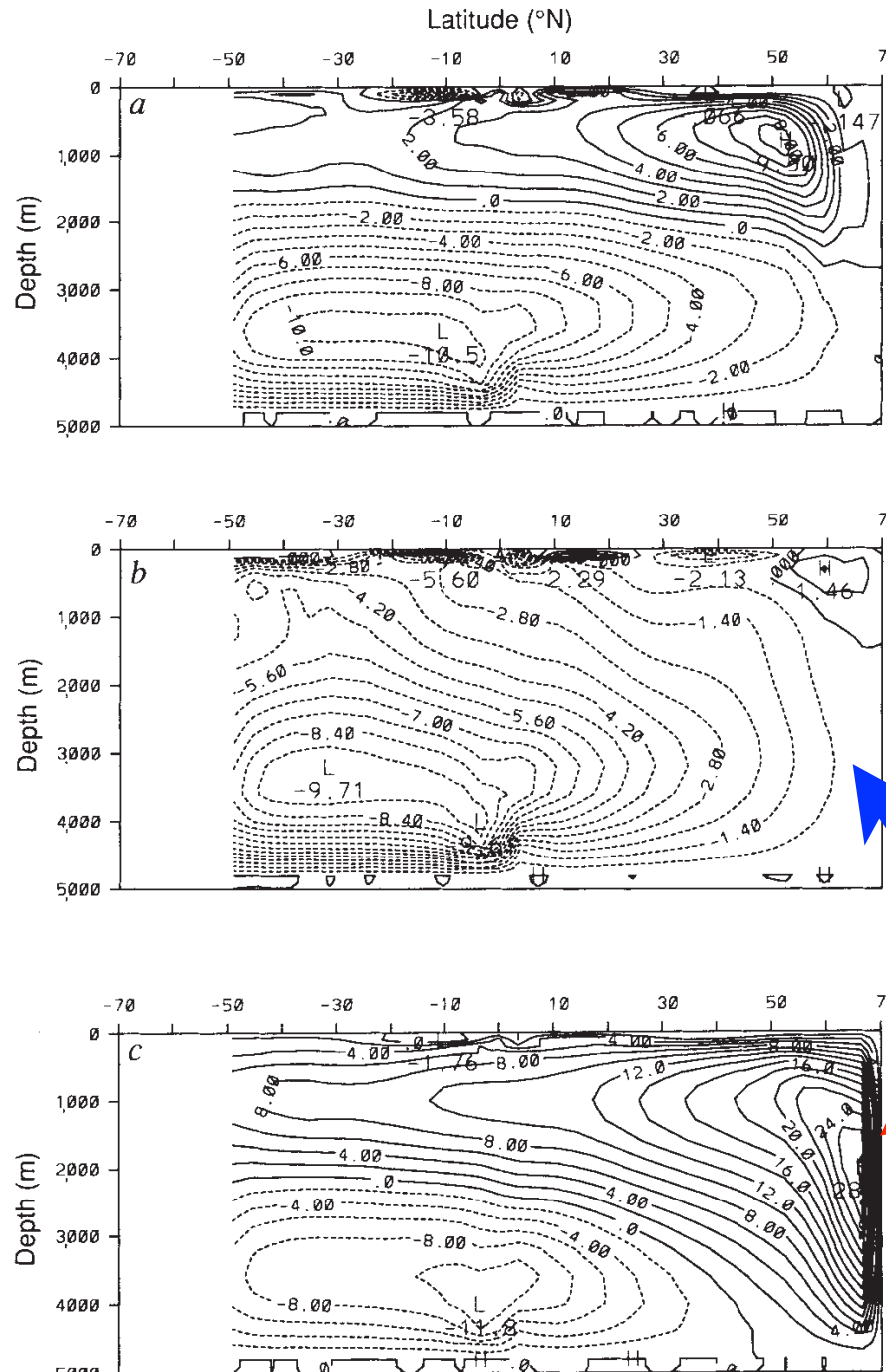


GCM

Weaver and Hughes 1994, Cessi 1994

Strong stochastic forcing of Stommel model and of GCM

# AMOC: stochastic forcing of jumps between steady states



**Stommel model**

**GCM**

Weaver and Hughes 1994, Cessi 1994

Strong stochastic forcing of Stommel model and of GCM

# AMOC: stochastic forcing of jumps between steady states

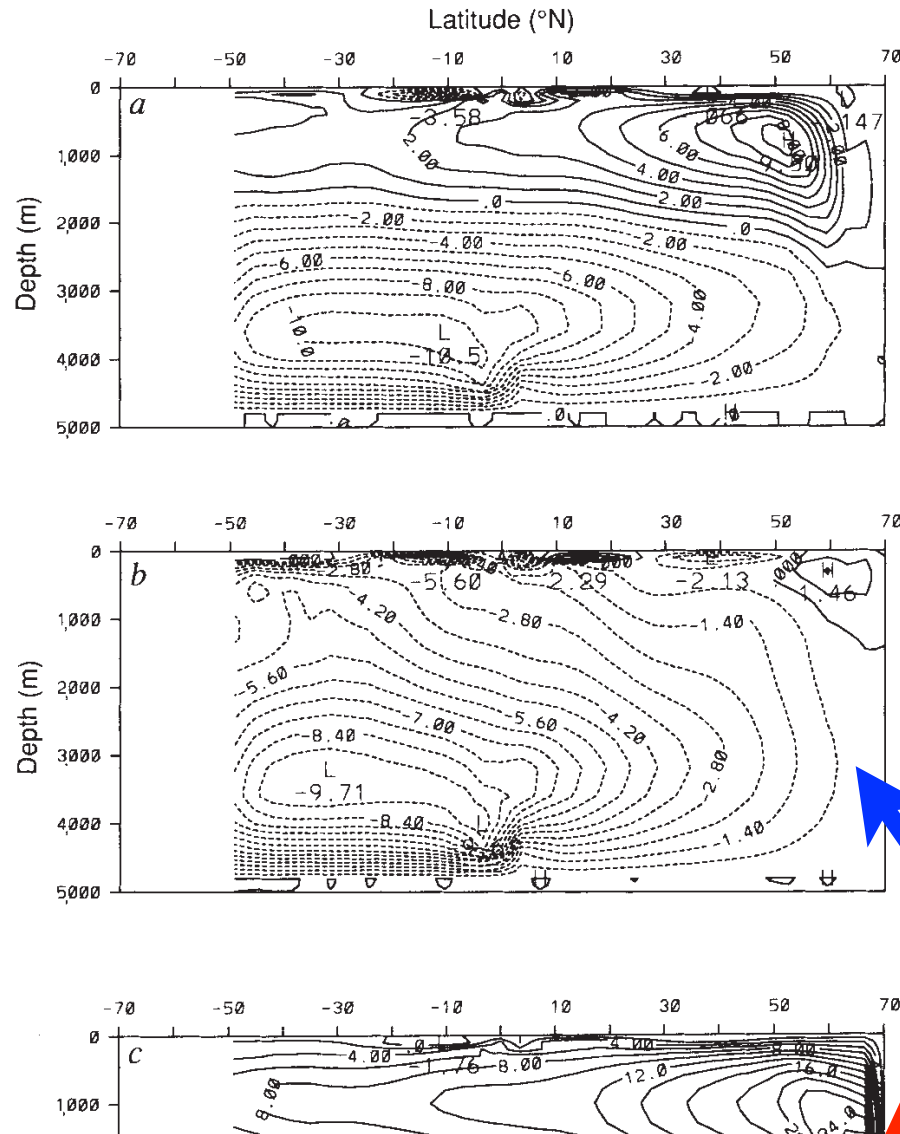


FIG. 2 The Atlantic Ocean meridional overturning streamfunction in Sv (1 Sv is  $10^6 \text{ m}^3 \text{ s}^{-1}$ ) for the three equilibria. a, The normal ‘present-day’ conveyor. b, The weak ‘colder’ conveyor. c, The strong ‘warmer’ conveyor. The x-axis is the latitude with positive and negative values indicating  ${}^{\circ}\text{N}$  and  ${}^{\circ}\text{S}$ , respectively. Positive and negative contours indicate clockwise and counterclockwise circulations, respectively, with H and L indicating local maxima and minima, respectively.

FIG. 4 The global ocean poleward heat transport at  $28^{\circ}$  N over the 20,800 yr of integration. a, The weak stochastic experiment (standard deviation, s.d. = 16 mm per month, lower curve) and the medium stochastic experiment (s.d. = 32 mm per month, upper curve). b, The strong stochastic experiment (s.d. = 48 mm per month).

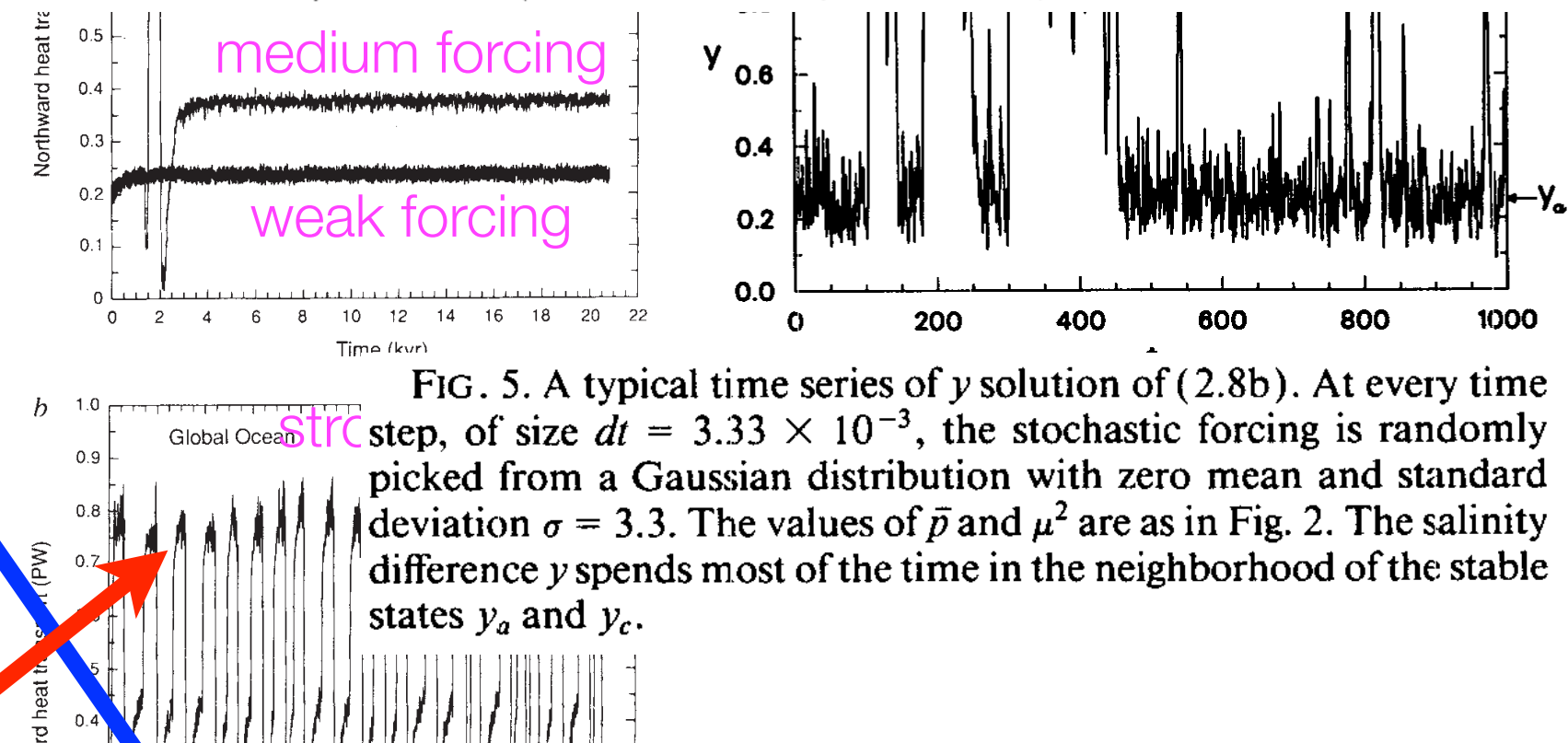
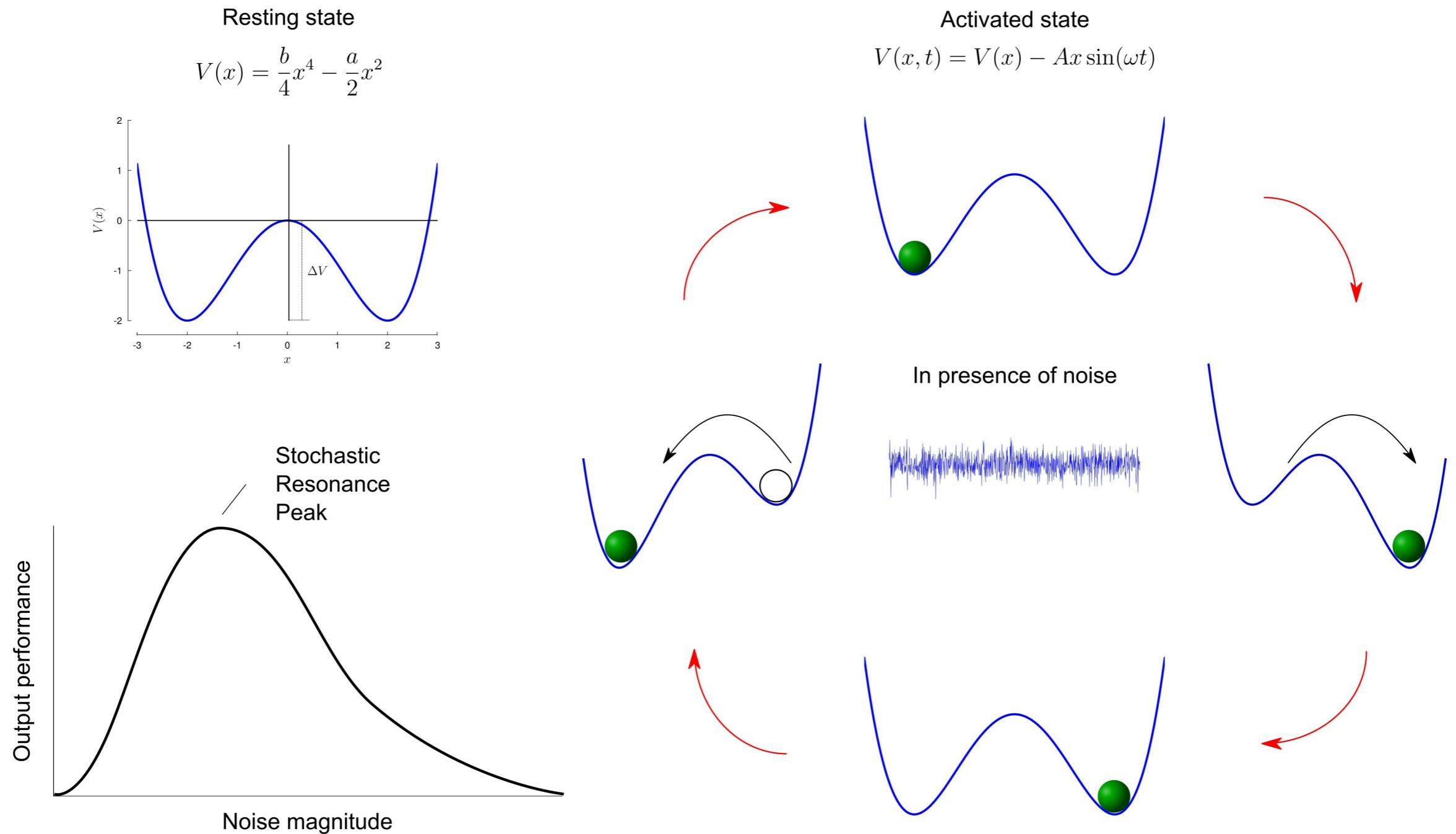


FIG. 5. A typical time series of  $y$  solution of (2.8b). At every time step, of size  $dt = 3.33 \times 10^{-3}$ , the stochastic forcing is randomly picked from a Gaussian distribution with zero mean and standard deviation  $\sigma = 3.3$ . The values of  $\bar{p}$  and  $\mu^2$  are as in Fig. 2. The salinity difference  $y$  spends most of the time in the neighborhood of the stable states  $y_a$  and  $y_c$ .

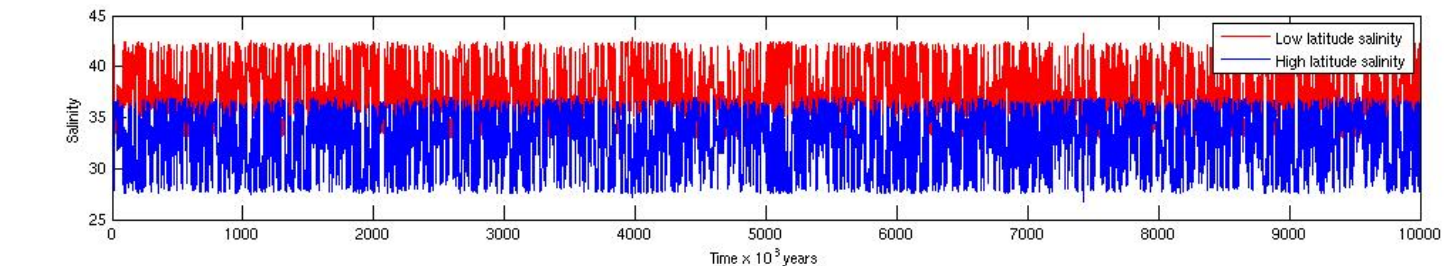
Weaver and Hughes 1994, Cessi 1994

# AMOC variability: stochastic resonance

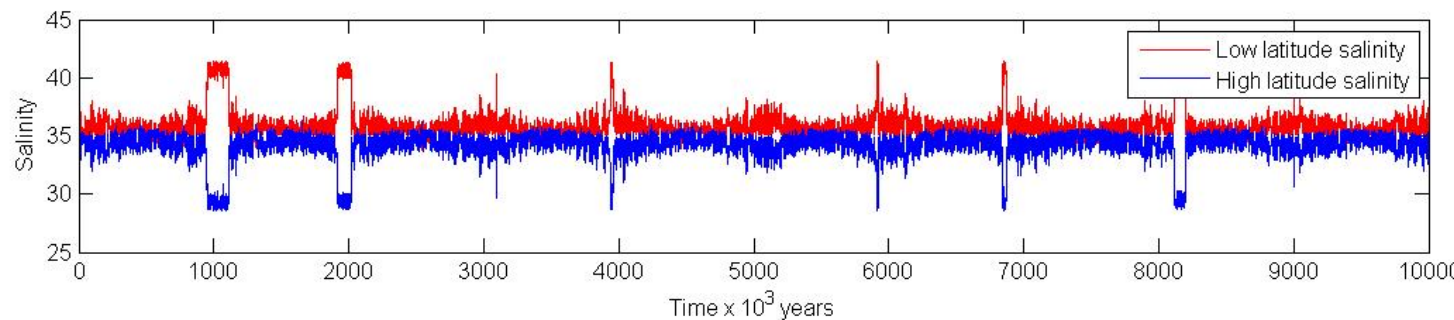
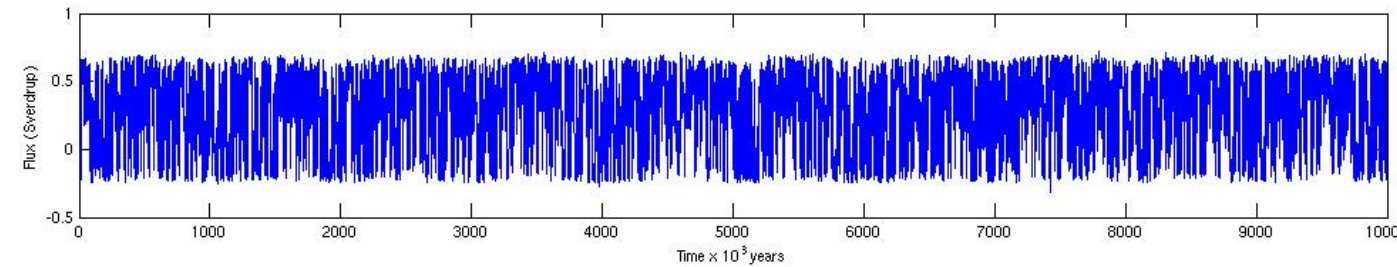


**FIGURE 1 |** Mechanism of stochastic resonance. **(A)** Sketch of a double well potential  $V(x)$ . In this example, the values  $a$  and  $b$  are set to 2 and 0.5, respectively. The minima are located at  $x = \pm\sqrt{\frac{a}{b}}$  and are separated by a barrier potential  $\Delta V = \frac{a^2}{4b}$ . **(B)** In the presence of periodic driving, the height of the potential barrier oscillates through an antiphase lowering and raising of the wells. The cyclic variations are depicted in the cartoon. A suitable dose of noise (represented by the central white noise plot) will allow the marble to hop to the globally stable state. **(C)** Typical curve of output performance versus input noise magnitude, for systems capable of stochastic resonance. For small and large noise, the performance metric is very small, while some intermediate non-zero noise level provides optimal performance. Panels **A,B** adapted from Gammaitoni et al. (1998).

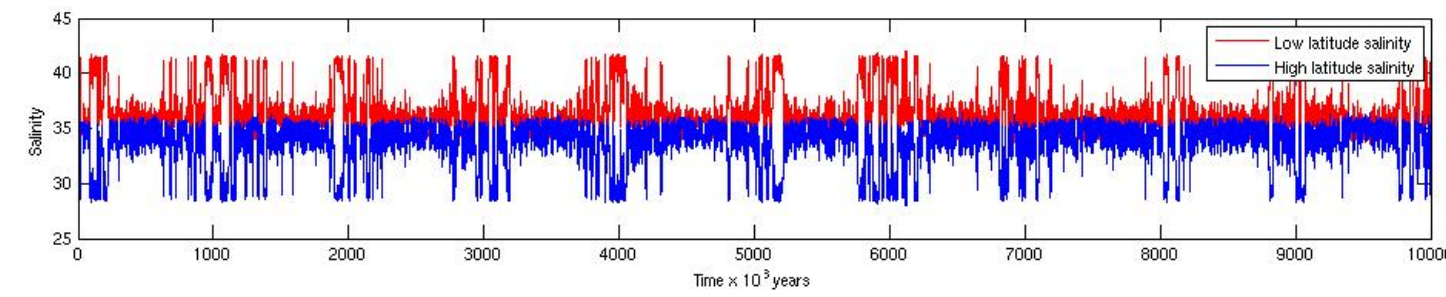
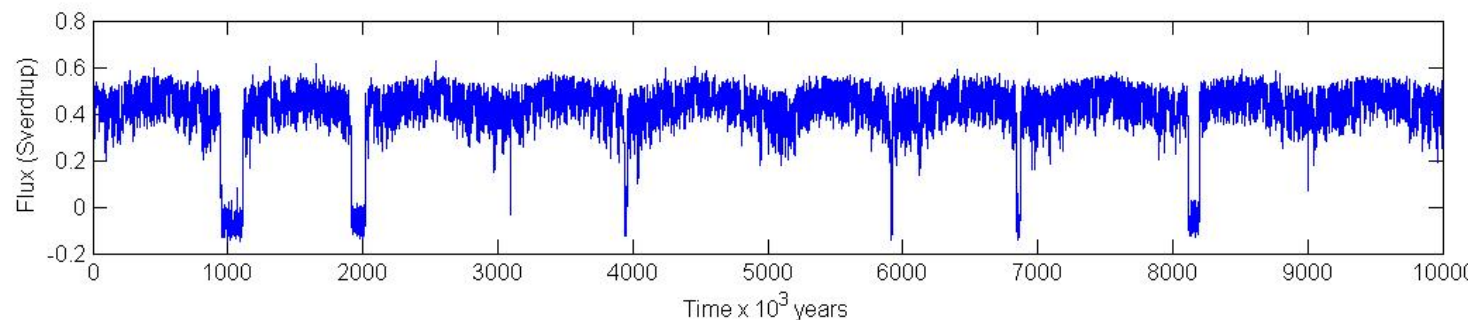
# AMOC variability: stochastic resonance



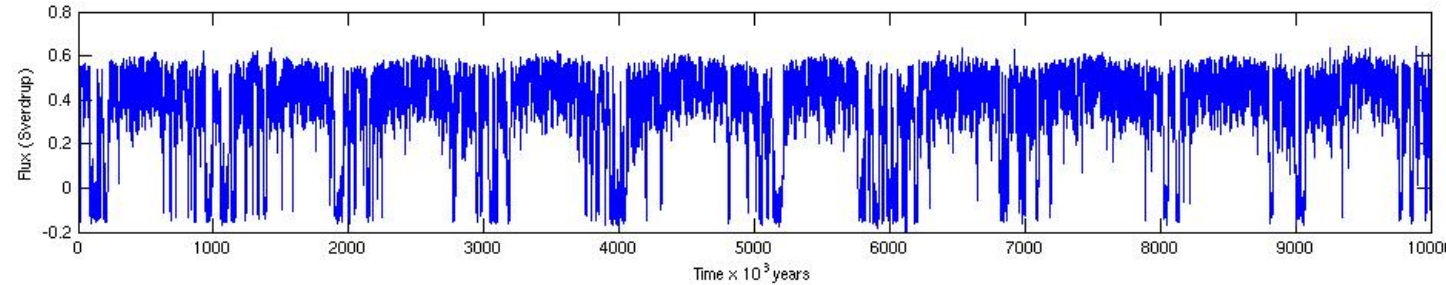
strong forcing,  
frequent  
transitions



weak forcing,  
rare transitions



'optimal' forcing,  
periodic  
transitions

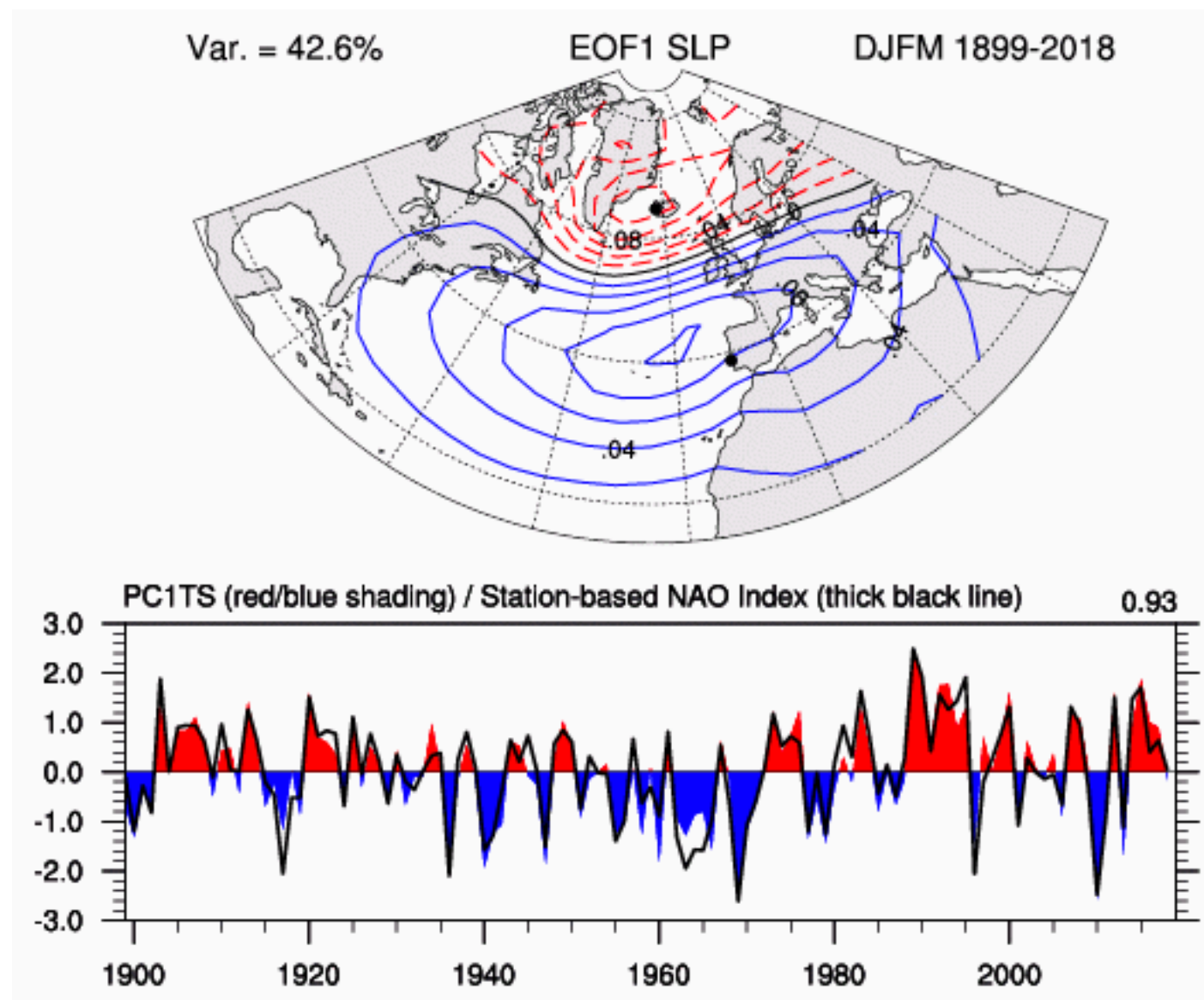


notes: stochastic AMOC variability:

1. Hasselmann
2. stochastically forced damped oscillator
3. reminder: transient non-normal growth
4. stochastic optimals

what is this stochastic forcing? e.g. NAO, next 2 slides

# Stochastic forcing of AMOC variability by NAO



NAO index time series:  
Sea Level Pressure (SLP) at Lisbon, Portugal, minus Reykjavik, Iceland, Dec–Mar mean

# Stochastic forcing of AMOC variability by NAO

1. NAO index time series: SLP from Lisbon, Portugal, minus Reykjavik, Iceland, Dec–Mar mean
2. calculate composite air-sea fluxes for +/- NAO phases
3. create anomalous fluxes w/NAO spatial pattern & sine amplitude, periods 2, 5, 10, 20, 50, 100 yrs.

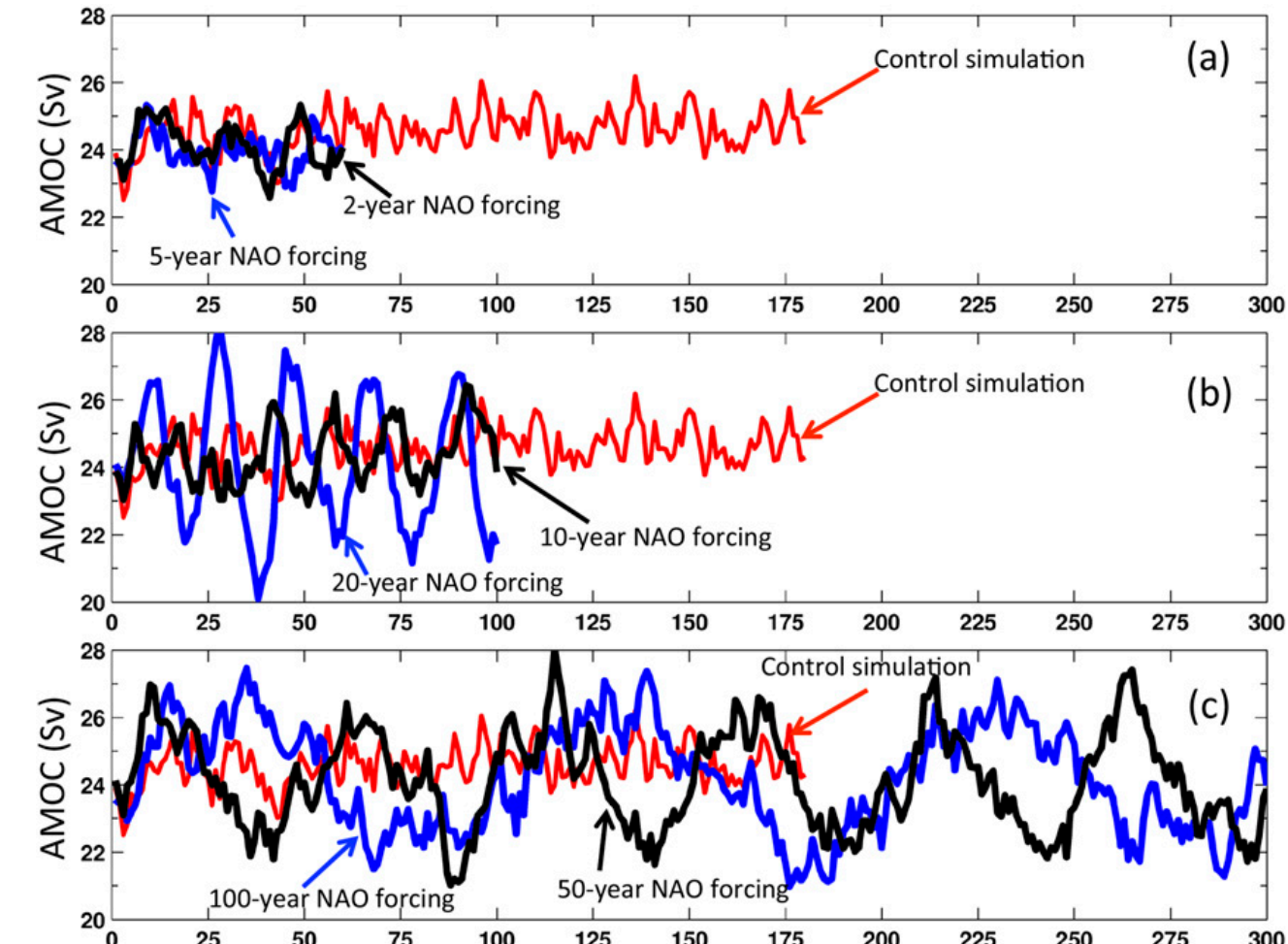
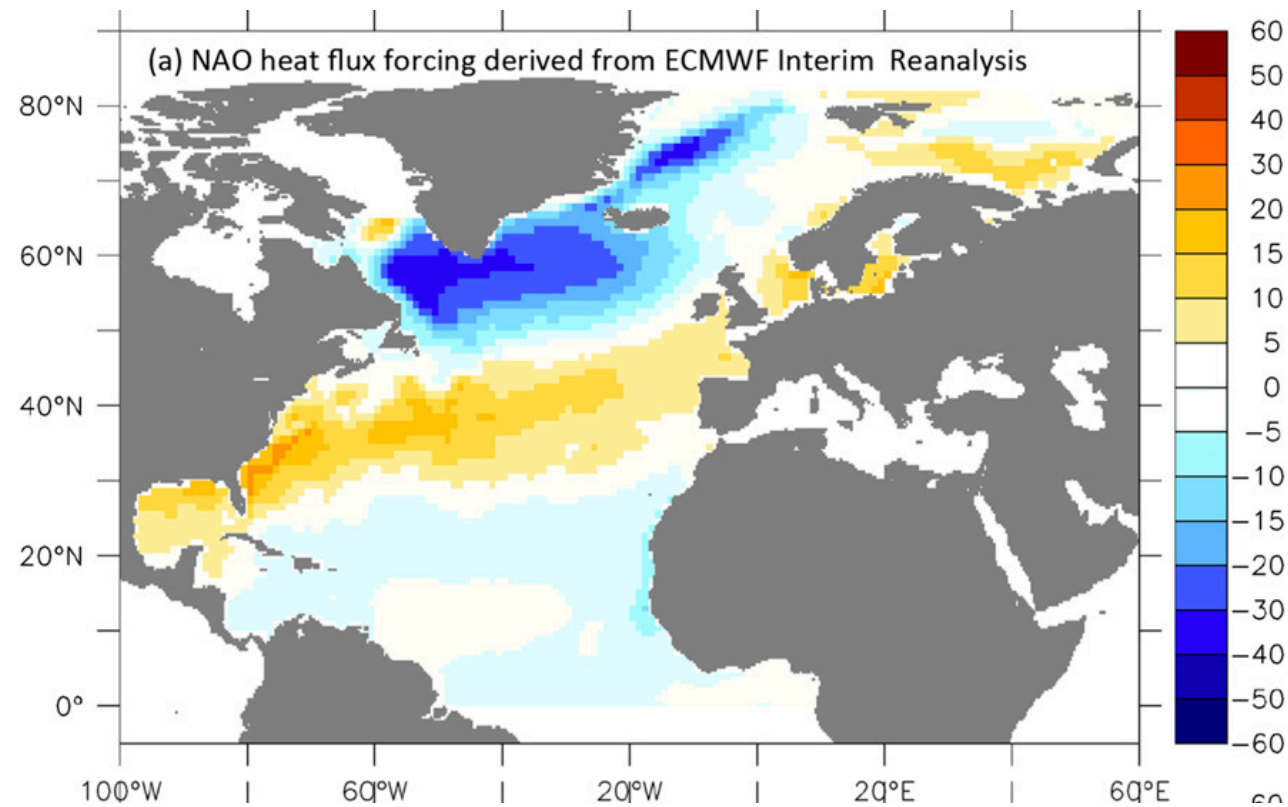


FIG. 1. Spatial pattern of heat flux anomalies ( $\text{W}/\text{m}^2$ ) used as model forcing. Negative = ocean cooling. From ERA-Interim, avg over Dec–Mar, corresponding to a 1-std of NAO.

FIG. 5. AMOC response to periodic forcing. 10-member ensemble averages.

→ Longer NAO time scale leads to a larger amplitude AMOC response, up to a limit.

Stochastic response not explored yet

The End